

Fishery Data Series No. 11-52

**Estimates of Chinook Salmon Passage in the Kenai
River Using Split-Beam Sonar, 2007**

by

James D. Miller

Debby L. Burwen

and

Steve J. Fleischman

November 2011

Alaska Department of Fish and Game

Divisions of Sport Fish and Commercial Fisheries



Symbols and Abbreviations

The following symbols and abbreviations, and others approved for the Système International d'Unités (SI), are used without definition in the following reports by the Divisions of Sport Fish and of Commercial Fisheries: Fishery Manuscripts, Fishery Data Series Reports, Fishery Management Reports, and Special Publications. All others, including deviations from definitions listed below, are noted in the text at first mention, as well as in the titles or footnotes of tables, and in figure or figure captions.

Weights and measures (metric)		General		Mathematics, statistics	
centimeter	cm	Alaska Administrative Code	AAC	<i>all standard mathematical signs, symbols and abbreviations</i>	
deciliter	dL	all commonly accepted abbreviations	e.g., Mr., Mrs., AM, PM, etc.	alternate hypothesis	H_A
gram	g	all commonly accepted professional titles	e.g., Dr., Ph.D., R.N., etc.	base of natural logarithm	e
hectare	ha	at	@	catch per unit effort	CPUE
kilogram	kg	compass directions:		coefficient of variation	CV
kilometer	km	east	E	common test statistics	(F, t, χ^2 , etc.)
liter	L	north	N	confidence interval	CI
meter	m	south	S	correlation coefficient (multiple)	R
milliliter	mL	west	W	correlation coefficient (simple)	r
millimeter	mm	copyright	©	covariance	cov
		corporate suffixes:		degree (angular)	°
Weights and measures (English)		Company	Co.	degrees of freedom	df
cubic feet per second	ft ³ /s	Corporation	Corp.	expected value	E
foot	ft	Incorporated	Inc.	greater than	>
gallon	gal	Limited	Ltd.	greater than or equal to	≥
inch	in	District of Columbia	D.C.	harvest per unit effort	HPUE
mile	mi	et alii (and others)	et al.	less than	<
nautical mile	nmi	et cetera (and so forth)	etc.	less than or equal to	≤
ounce	oz	exempli gratia (for example)	e.g.	logarithm (natural)	ln
pound	lb	Federal Information Code	FIC	logarithm (base 10)	log
quart	qt	id est (that is)	i.e.	logarithm (specify base)	log ₂ , etc.
yard	yd	latitude or longitude	lat. or long.	minute (angular)	'
		monetary symbols (U.S.)	\$, ¢	not significant	NS
Time and temperature		months (tables and figures): first three letters	Jan,...,Dec	null hypothesis	H_0
day	d	registered trademark	®	percent	%
degrees Celsius	°C	trademark	™	probability	P
degrees Fahrenheit	°F	United States (adjective)	U.S.	probability of a type I error (rejection of the null hypothesis when true)	α
degrees kelvin	K	United States of America (noun)	USA	probability of a type II error (acceptance of the null hypothesis when false)	β
hour	h	U.S.C.	United States Code	second (angular)	"
minute	min	U.S. state	use two-letter abbreviations (e.g., AK, WA)	standard deviation	SD
second	s			standard error	SE
Physics and chemistry				variance	
all atomic symbols				population sample	Var
alternating current	AC			sample	var
ampere	A				
calorie	cal				
direct current	DC				
hertz	Hz				
horsepower	hp				
hydrogen ion activity (negative log of)	pH				
parts per million	ppm				
parts per thousand	ppt, ‰				
volts	V				
watts	W				

FISHERY DATA SERIES NO. 11-52

**ESTIMATES OF CHINOOK SALMON PASSAGE IN THE KENAI RIVER
USING SPLIT-BEAM SONAR, 2007**

By
James D. Miller
Debby L. Burwen
Division of Sport Fish, Anchorage
and
Steve J. Fleischman
Division of Sport Fish, Research and Technical Services, Anchorage

Alaska Department of Fish and Game
Division of Sport Fish, Research and Technical Services
333 Raspberry Road, Anchorage, Alaska, 99518-1565

November 2011

This investigation was partially financed by the Federal Aid in Sport Fish Restoration Act (16 U.S.C. 777-777K) under Project F-10-22, Job No. S-2-5b.

ADF&G Fishery Data Series was established in 1987 for the publication of Division of Sport Fish technically oriented results for a single project or group of closely related projects, and in 2004 became a joint divisional series with the Division of Commercial Fisheries. Fishery Data Series reports are intended for fishery and other technical professionals and are available through the Alaska State Library and on the Internet: <http://www.adfg.alaska.gov/sf/publications/>. This publication has undergone editorial and peer review.

*James D. Miller, Debby L. Burwen,
Alaska Department of Fish and Game, Division of Sport Fish,*

and

*Steve J. Fleischman
Alaska Department of Fish and Game, Division of Sport Fish,
Research and Technical Services
333 Raspberry Road, Anchorage, Alaska 99518-1599, USA*

This document should be cited as:

Miller, J. D., D. L. Burwen, and S. J. Fleischman. 2011. Estimates of Chinook salmon passage in the Kenai River using split-beam sonar, 2007. Alaska Department of Fish and Game, Fishery Data Series No. 11-52, Anchorage.

The Alaska Department of Fish and Game (ADF&G) administers all programs and activities free from discrimination based on race, color, national origin, age, sex, religion, marital status, pregnancy, parenthood, or disability. The department administers all programs and activities in compliance with Title VI of the Civil Rights Act of 1964, Section 504 of the Rehabilitation Act of 1973, Title II of the Americans with Disabilities Act (ADA) of 1990, the Age Discrimination Act of 1975, and Title IX of the Education Amendments of 1972.

If you believe you have been discriminated against in any program, activity, or facility please write:

ADF&G ADA Coordinator, P.O. Box 115526, Juneau, AK 99811-5526

U.S. Fish and Wildlife Service, 4401 N. Fairfax Drive, MS 2042, Arlington, VA 22203

Office of Equal Opportunity, U.S. Department of the Interior, 1849 C Street NW MS 5230, Washington DC 20240

The department's ADA Coordinator can be reached via phone at the following numbers:

(VOICE) 907-465-6077, (Statewide Telecommunication Device for the Deaf) 1-800-478-3648,

(Juneau TDD) 907-465-3646, or (FAX) 907-465-6078

For information on alternative formats and questions on this publication, please contact:

ADF&G, Division of Sport Fish, Research and Technical Services, 333 Raspberry Rd, Anchorage AK 99518 (907) 267-2375

TABLE OF CONTENTS

	Page
LIST OF TABLES.....	ii
LIST OF FIGURES.....	ii
LIST OF APPENDICES.....	iv
ABSTRACT.....	1
INTRODUCTION.....	1
OBJECTIVES.....	6
METHODS.....	7
Study Area.....	7
Site Description.....	7
Split-Beam Sonar Data Collection and Processing.....	9
Acoustic Sampling.....	9
Fish Tracking and Echo Counting.....	16
Data Analysis.....	17
Dual-Frequency Identification Sonar (DIDSON) Testing.....	28
Tethered Fish.....	29
Free-Swimming Fish.....	29
DIDSON-Based Fish Length Measurements.....	29
Data Analysis.....	29
RESULTS.....	31
Split-Beam Sonar.....	31
System Calibration.....	31
Target Tracking.....	31
Tidal Distribution.....	32
Spatial Distribution.....	33
Target Strength.....	42
TS-Based Estimates of Chinook Salmon Passage.....	44
Alternative Estimates of Chinook Salmon Passage.....	49
DIDSON Testing.....	49
Tethered Fish.....	49
Free-Swimming fish.....	49
DISCUSSION.....	52
Accuracy of Passage Estimates.....	52
2007 Early Run.....	52
2007 Late Run.....	55
Summary and Outlook.....	57
ACKNOWLEDGMENTS.....	57
REFERENCES CITED.....	57
APPENDIX A: TARGET STRENGTH ESTIMATION.....	65
APPENDIX B: SYSTEM PARAMETERS.....	67
APPENDIX C: DATA FLOW.....	75
APPENDIX D: EXCLUDED HOURLY SAMPLES.....	77

TABLE OF CONTENTS (Continued)

	Page
APPENDIX E: WINBUGS CODE FOR ECHO-LENGTH STANDARD DEVIATION (ELSD) MIXTURE MODEL ESTIMATES OF SPECIES COMPOSITION	79
APPENDIX F: DIDSON CONFIGURATION FOR KENAI RIVER CHINOOK SONAR STUDY, 2007.....	83
APPENDIX G: DAILY PROPORTION OF UPSTREAM AND DOWNSTREAM MOVING FILTERED TARGETS FOR THE EARLY AND LATE RUNS, KENAI RIVER, 2007	87
APPENDIX H: AVERAGE VERTICAL ANGLE OF FILTERED TARGETS BY TIDE STAGE, RUN, BANK, AND DIRECTION OF TRAVEL (UPSTREAM OR DOWNSTREAM) FOR THE EARLY AND LATE RUNS, KENAI RIVER, 2007	91
APPENDIX I: HISTORIC PASSAGE BY YEAR AND DATE (1987–2007)	95
APPENDIX J: ESTIMATED UPSTREAM FISH PASSAGE IN MID-RIVER (ALL SPECIES), TS-BASED (CHINOOK SALMON ONLY), NET-APPORTIONED (ALTERNATIVE ESTIMATE, CHINOOK SALMON ONLY), AND BEHAVIOR-CENSORED ELSD (ALTERNATIVE ESTIMATE, CHINOOK SALMON ONLY), KENAI RIVER SONAR, EARLY AND LATE RUNS, 2007	101

LIST OF TABLES

Table	Page
1. Main components of the split-beam sonar system used in 2007.	9
2. Hydroacoustics Technology Inc. model 244 digital echo sounder settings used in 2007.....	14
3. Echo acceptance criteria for digital echo processing, 2007.....	14
4. Results of 2007 <i>in situ</i> calibration verifications using a 38.1 mm tungsten carbide standard sphere.....	31
5. Percentage of filtered targets by tide stage and direction of travel for the 2007 early run.	32
6. Percentage of filtered targets by tide stage and direction of travel for the 2007 late run	32
7. Percentage of filtered targets by riverbank and direction of travel for the 2007 early run	33
8. Percentage of filtered targets by riverbank and direction of travel for the 2007 late run	34
9. Mean target strength (dB) for upstream and downstream moving filtered targets by riverbank during the early and late runs, 2007.....	44
10. Daily upstream Chinook salmon passage estimates, early run, 2007.....	45
11. Daily upstream Chinook salmon passage estimates, Kenai River sonar, late run, 2007.	46

LIST OF FIGURES

Figure	Page
1. Cook Inlet showing location of Kenai River.	2
2. Kenai River sonar site locations, 2007.....	8
3. Cross-sectional and aerial diagrams of sonar site illustrating insonified portions of the Kenai River, 2007.....	10
4. Daily right- and left-bank transducer placement and insonified ranges relative to bipod tower located on the right bank, Kenai River, 2007.	11
5. Bottom profiles by bank for the Kenai River Chinook salmon sonar site with approximate transducer placement and sonar beam coverage for 16 May 2007.	13
6. Diagram of 2007 split-beam sonar system configuration and data flow.	15
7. Hypothetical distributions of fish length measurements at the Kenai River sonar site.	22
8. Echo length standard deviation versus fish length for tethered Pacific salmon in the Kenai River, 1995..	23
9. An example of threshold-based discrimination of Chinook and sockeye salmon.	24
10. Flow chart of a mixture model.	27

LIST OF FIGURES (Continued)

Figure	Page
11. Mounting system for a long-range, high resolution DIDSON (left on mount) and split-beam transducer.....	30
12. Percentage of upstream and downstream moving filtered targets by tide stage for the early and late runs, Kenai River, 2007.....	33
13. Standardized distance from transducer (range) of early-run upstream and downstream moving filtered targets by bank, Kenai River, 2007.	34
14. Standardized distance from transducer (range) of late-run upstream and downstream moving filtered targets by bank, Kenai River, 2007.	35
15. Standardized distance from transducer (range) of early-run upstream moving filtered targets by tide stage and bank, Kenai River, 2007.....	36
16. Standardized distance from transducer (range) of late-run upstream moving filtered targets by tide stage and bank, Kenai River, 2007.....	37
17. Vertical distributions above and below the acoustic axis of early-run upstream and downstream moving filtered targets by bank, Kenai River, 2007.....	38
18. Vertical distributions above and below the acoustic axis of early-run upstream moving filtered targets by tide stage and bank, Kenai River, 2007.....	39
19. Vertical distributions above and below the acoustic axis of late-run upstream and downstream moving filtered targets by bank, Kenai River, 2007.....	40
20. Vertical distributions above and below the acoustic axis of late-run upstream moving filtered targets by tide stage and bank, Kenai River, 2007.....	41
21. Early-run target strength (acoustic size) for all upstream and downstream moving targets by bank, Kenai River, 2007.	42
22. Late-run target strength (acoustic size) for all upstream and downstream moving targets by bank, Kenai River, 2007.	43
23. Daily sonar passage estimates by bank (top), total passage (center), and historical cumulative proportions (bottom) for the Chinook salmon early run returning to the Kenai River, 2007.....	47
24. Daily sonar passage estimates by bank (top), total passage (center), and historical cumulative proportions (bottom) for the Chinook salmon late run returning to the Kenai River, 2007.....	48
25. DIDSON-based length (DL) measures with fork length (FL) for tethered fish insonified by the long-range DIDSON fitted with a high-resolution lens.	50
26. Plot of residuals (observed-expected) with range of DIDSON-based length (DL) measures versus fork length (FL).	50
27. Species / age mixture model fitted to observed DIDSON length frequency data, 21 July and 22 July 2007.....	51
28. Estimated upstream fish passage in mid-river (all species), TS-based (Chinook salmon only), net-apportioned (alternative estimate Chinook salmon only) and behavior-censored ELSD-based sonar (alternative estimate, Chinook salmon only), early- and late-run, Kenai River, 2007.	53
29. Daily discharge rates collected at the Soldotna Bridge, Secchi disk readings taken at the sonar site, Chinook salmon TS-based sonar passage estimates, inriver gillnet CPUE, and Chinook salmon sport fish CPUE, early run (20 May–30 June), Kenai River, 2007.....	54
30. Daily Chinook and sockeye salmon inriver gillnetting CPUE, early run (20 May–30 June), Kenai River, 2007.....	55
31. Daily discharge rates collected at the Soldotna Bridge, Secchi disk readings taken at the sonar site, Chinook salmon sonar passage estimates, inriver Chinook salmon gillnet CPUE, river mile-19 sockeye salmon sonar passage estimates and gillnet CPUE, and Chinook salmon sport fish CPUE, late run (1 July–4 August), Kenai River, 2007.....	56

LIST OF APPENDICES

Appendix	Page
A1. The sonar equation used to estimate target strength in decibels with dual- and split-beam applications.....	66
B1. Example of system parameters used for data collection on the right bank (transducer 733).....	68
B2. Example of system parameters used for data collection on the left bank (transducer 738).....	71
C1. Data flow diagram for the Kenai River Chinook salmon sonar project, 2007.....	76
D1. Hourly samples excluded by bank from calculation of early- and late-run Chinook salmon daily passage estimates, Kenai River, 2007.....	78
E1. WinBUGS code for ELSD mixture model fit to 2007 early- and late-run Kenai River Chinook salmon sonar, gillnetting, and tethered fish data.....	80
E2. WinBUGS code for hierarchical age-composition model for development of prior distributions for ELSD mixture model.....	81
F1. DIDSON configuration for Kenai River Chinook Sonar Study, 2007.....	84
F2. Diagram showing the horizontal plane of a DIDSON-LR sonar with a high resolution lens (DIDSON-LR+HRL).....	85
F3. Enlargement of a DIDSON video of a tethered Chinook salmon showing the individual pixels that comprise the image.....	86
G1. Daily proportion of upstream and downstream moving filtered targets for the early run, Kenai River, 2007.....	88
G2. Daily proportion of upstream and downstream moving filtered targets for the late run, Kenai River, 2007.....	89
H1. Average vertical angle of filtered targets by tide stage and direction of travel (upstream or downstream) for the early run, Kenai River, 2007.....	92
H2. Average vertical angle of filtered targets by tide stage and direction of travel (upstream or downstream) for the late run, Kenai River, 2007.....	93
I1. Kenai River early-run Chinook salmon sonar passage estimates, 1987–2007.....	96
I2. Kenai River late-run Chinook salmon sonar passage estimates, 1987–2007.....	98
J1. Estimated upstream fish passage in mid-river (all species), TS-based (Chinook salmon only), net-apportioned (alternative estimate, Chinook salmon only), and behavior-censored ELSD-based (alternative estimate, Chinook salmon only), Kenai River, early run, 2007.....	102
J2. Estimated upstream fish passage in mid-river (all species), TS-based (Chinook salmon only), net-apportioned (alternative estimate, Chinook salmon only), and behavior-censored ELSD-based (alternative estimate, Chinook salmon only), Kenai River, late run 2007.....	103

ABSTRACT

Chinook salmon (*Oncorhynchus tshawytscha*) passage in the Kenai River in 2007 was estimated using split-beam sonar technology. Early (16 May–30 June) and late (1 July–10 August) runs of Kenai River Chinook salmon have been monitored acoustically since 1987. A 200 kHz split-beam sonar system has been used since 1995 to estimate numbers of adult Chinook salmon migrating into the Kenai River. From 1987 to 1994, a 420 kHz dual-beam sonar was used to generate similar estimates. In 2007, the sonar project operated 20 May through 4 August. The standard estimate of total upstream passage of Chinook salmon, based on target strength and range thresholds, was 58,883 (SE = 741) fish: 15,904 (SE = 285) during the early run (20 May–30 June 2007) and 42,979 (SE = 684) during the late run (1 July–4 August 2007). Total (expanded for missing days) early-run passage estimated for 16 May to 30 June was 16,217 (SE = 403) fish. The standard errors associated with these estimates reflect only sampling error and no other sources of uncertainty (such as target detection, species composition, direction of travel, and target tracking). Comparisons with alternative estimators of abundance suggest that the standard estimates are too high. Long-range Dual-frequency Identification Sonar (DIDSON) was tested in 2007 and found to provide sufficient resolution to estimate fish length at ranges up to 21 m, and to estimate species composition of passing fish.

Key words: split-beam sonar, DIDSON, Chinook salmon, *Oncorhynchus tshawytscha*, acoustic assessment, Kenai River, riverine sonar, early run, late run.

INTRODUCTION

Chinook salmon (*Oncorhynchus tshawytscha*) returning to the Kenai River (Figure 1) support one of the largest and most intensively managed recreational fisheries in Alaska (Gamblin et al. 2004). Kenai River Chinook salmon are among the largest in the world and have sustained in excess of 100,000 angler-days of fishing effort annually (Howe et al. 1995-1996, 2001a-d; Jennings et al. 2004, 2006a-b, 2007, 2009a-b, 2010; Mills 1979-1980, 1981a-b, 1982-1994; Walker et al. 2003). The Kenai River Chinook salmon fishery has been a source of contention because of competition for a fully allocated resource among sport, commercial, subsistence, and personal use fisheries.

Chinook salmon returning to the Kenai River are managed as 2 distinct runs (Burger et al. 1985): early (16 May–30 June) and late (1 July–10 August). Early-run Chinook salmon are harvested primarily by sport anglers, and late-run Chinook salmon are harvested by commercial, sport, subsistence, and personal use fisheries. These fisheries may be restricted if the projected run size falls below escapement goals adopted by the Alaska Board of Fisheries (BOF). From 1989 to 1998, these runs were managed for spawning escapement goals of 9,000 early-run Chinook salmon and 22,300 late-run Chinook salmon (McBride et al. 1989). In February 1999, BOF adopted revised escapement goals based on Chinook salmon passage estimated by sonar and our understanding of biases associated with the sonar (Bosch and Burwen 1999; Hammarstrom and Hasbrouck 1998, 1999). The revised escapement goals defined a range of escapement levels: 7,200 to 14,400 early-run Chinook salmon and 17,800 to 35,700 late-run Chinook salmon. In January 2005, based on additional brood year information, BOF lowered the early-run escapement goal range to 5,000–9,000 Chinook salmon. Escapement goal ranges (as defined by the Alaska Administrative Codes 5 AAC 56.070 [*Kenai River and Kasilof River Early-Run King Salmon Conservation Management Plan*] and 5 AAC 21.359 [*Kenai River Late-Run King Salmon Management Plan*]) are expected to provide a stable fishing season without compromising sustainability.

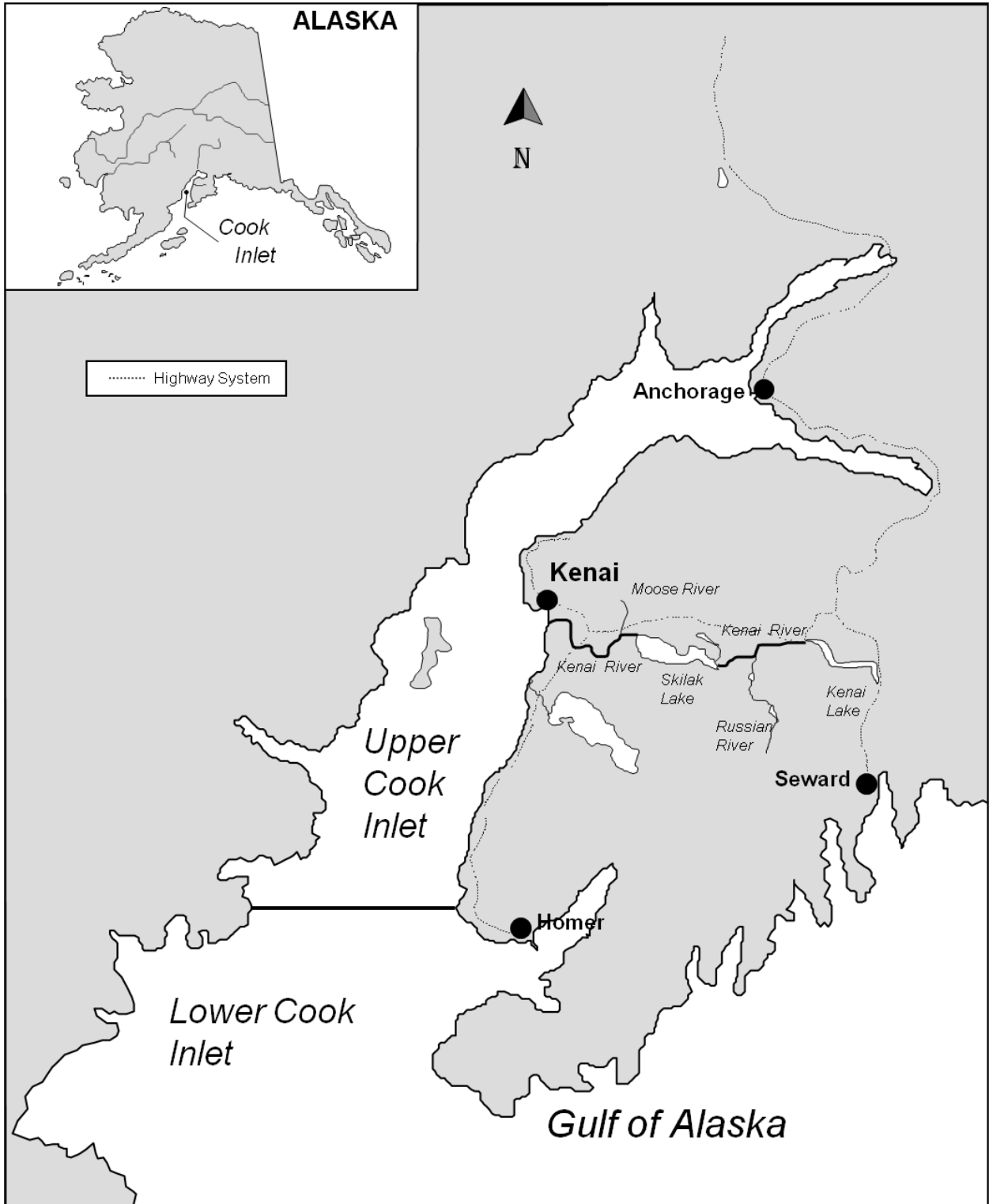


Figure 1.-Cook Inlet showing location of Kenai River.

Sonar estimates of inriver Chinook salmon passage provide the basis for estimating spawning escapement and implementing management plans that regulate harvest in competing sport and commercial fisheries for this stock. Implementation of these management plans has been contentious and attracts public scrutiny. Restrictions were imposed on the sport fishery to meet escapement goals during the early run in 1990 through 1992, 1997, 1998, 2000, and 2002, and during the late run in 1990, 1992, and 1998.

The first estimates of Kenai River Chinook salmon abundance were generated in 1984 for the late run using a mark–recapture project (Hammarstrom et al. 1985). From 1985 through 1990, the mark–recapture project produced estimates for both early- and late-run riverine abundances (Alexandersdottir and Marsh 1990; Carlon and Alexandersdottir 1989; Conrad 1988; Conrad and Larson 1987; Hammarstrom and Larson 1986). These estimates had low precision and appeared to be positively biased, particularly during the late run (Bernard and Hansen 1992).

The Alaska Department of Fish and Game (ADF&G) initiated studies in 1984 to determine whether an acoustic assessment program could provide timely and accurate daily estimates of Chinook salmon passage in the Kenai River (Eggers et al. 1995). Acoustic assessment of Chinook salmon in the Kenai River is complicated by the presence of more abundant sockeye salmon (*O. nerka*), which migrate concurrently with Chinook salmon. From 1987 to 2007, sockeye salmon escapement estimates generated by the river mile-19 sockeye salmon sonar project ranged from 625,000 to 1,600,000 fish (Westerman and Willette 2010) while late-run Chinook salmon passage estimates generated by the Chinook salmon sonar project at river mile 8.5 ranged from 29,000 to 56,000 fish. Dual-beam sonar was initially chosen for the Chinook salmon sonar project because of its ability to estimate acoustic size (target strength), which was to serve as the discriminatory variable to systematically identify and count only Chinook salmon. Because of the considerable size difference between Chinook salmon and other fish species in the Kenai River, it was postulated that dual-beam sonar could be used to distinguish Chinook salmon from smaller fish (primarily sockeye salmon) and estimate their numbers returning to the river.

Early Kenai River sonar and gillnetting studies indicated that Chinook salmon could be distinguished from sockeye salmon based on target strength and spatial separation in the river (Eggers et al. 1995). Target strength (TS) is a measure of the loudness of the echo returning from a fish, corrected for position of the fish in the beam. Sockeye salmon are smaller, on average, than Chinook salmon, and were assumed to have smaller target strength. A target strength threshold was established to censor (remove from count data) small fish. Sockeye salmon also were thought to migrate primarily near the bank, therefore a range or distance threshold was also imposed. These two criteria have been the primary basis for generating estimates of the number of Chinook salmon returning to the Kenai River, and for comparison with established escapement goals.

“TS-based” estimates of Chinook salmon passage have been generated since 1987. Estimates of passage made with dual-beam sonar were consistently lower than the 1987–1990 mark–recapture estimates (Eggers et al. 1995). The inconsistencies between sonar and mark–recapture estimates were highest during the late run, presumably due to the mark–recapture biases mentioned above.

A more advanced acoustic technology, known as split-beam sonar, was used to test assumptions and design parameters of the dual-beam configuration in 1994 (Burwen et al. 1995). The split-beam system provided advantages over the dual-beam system in its ability to determine the 3-

dimensional position of an acoustic target in the sonar beam. Consequently, the direction of travel for each target and the 3-dimensional spatial distribution of fish in the acoustic beam could be determined for the first time. The split-beam system also operated at a lower frequency than the dual-beam system, providing a higher (improved) signal-to-noise ratio (SNR; Simmonds and MacLennan 2005). It also interfaced with improved fish-tracking software, which reduced the interference from boat wake, and improved fish-tracking capabilities (Burwen and Bosch 1996). The split-beam system was deployed side-by-side with the dual-beam and was run concurrently for much of the 1994 season (Burwen et al. 1995). Both systems detected comparable numbers of fish. The split-beam data confirmed earlier studies (Eggers et al. 1995) showing that most fish targets were strongly oriented to the river bottom. However, experiments conducted with the split-beam system could not confirm that Chinook salmon could be discriminated from sockeye salmon based on target strength. Modeling exercises performed by Eggers (1994) also questioned the feasibility of discriminating between Chinook and sockeye salmon using target strength. It was hypothesized that discrimination between the two species was primarily accomplished using range thresholds on the acoustic data that exploited the known spatial segregation of the species (sockeye salmon migrate near shore and Chinook salmon migrate mid-river; Burwen et al. 1995; Eggers et al. 1995). In 1995, the dual-beam system was replaced with the split-beam system to take advantage of the additional information on direction of travel and spatial position of targets.

Ancillary drift gillnetting and sonar studies conducted in 1995 (Burwen et al. 1998) were directed at providing definitive answers to remaining questions regarding 1) the degree to which sockeye and Chinook salmon are spatially separated at the river mile-8.5 Chinook salmon sonar site and 2) the utility of using target strength and other acoustic parameters for species separation. These studies confirmed the potential for misclassifying sockeye salmon as Chinook salmon. The drift gillnetting study found that sockeye salmon were present in the middle insonified portion of the river. In the concurrent sonar experiment using live fish tethered in front of the split-beam sonar, most sockeye salmon had mean target strengths exceeding the target strength threshold.

Radiotelemetry projects were implemented in 1996 and 1997 to estimate the magnitude of bias introduced into the Chinook salmon passage estimates during periods of high sockeye salmon passage (Hammarstrom and Hasbrouck 1998, 1999). The radiotelemetry studies were designed to provide an independent and accurate estimate of inriver Chinook salmon passage during the late run when the potential to misclassify sockeye salmon using sonar is greatest. Although the precision between radiotelemetry estimates and previous mark-recapture estimates was similar, the use of radiotelemetry avoided certain biases associated with the earlier mark-recapture studies. Sonar estimates of late-run Chinook salmon abundance were 26% greater in 1996 and 28% greater in 1997 than the telemetry estimates.

An investigation in 1999 (Burwen et al. 2000) attempted to identify alternative sites above tidal influence with stronger bank-orientation of sockeye salmon, where range thresholds would be more effective. The investigation concentrated on a site located at river mile 13.2 that was upstream of tidal influence, but downstream of major spawning areas. Gillnetting data indicated that there were fewer sockeye salmon in the offshore area at the alternative site than at the current site. However, there were still relatively large numbers of sockeye salmon present in the offshore area of the alternative site during peak migration periods as well as high numbers of Chinook salmon present in the nearshore area. The alternate sonar site also had several

disadvantages over the current site including more boat traffic, less acoustically favorable bottom topography, and higher background noise resulting in difficult fish tracking conditions.

The inriver drift gillnetting program, originally designed to collect age, sex, and length (ASL) samples (Marsh 2000), was modified in 1998 to produce standardized estimates of Chinook salmon catch per unit effort (CPUE) for use as an index of Chinook salmon passage (Reimer et al. 2002). A drift zone was established just downstream from the sonar site and crews fished relative to the tide cycles because gillnets could not be effectively fished during parts of the rising and high tide stages due to lack of river current. In addition, the schedule was intensified so that CPUE estimates could be generated daily. During subsequent years, inriver gillnet CPUE was used as a comparison with sonar passage estimates to detect periods when Chinook salmon passage estimates were potentially high because of inclusion of sockeye salmon or other species (Bosch and Burwen 2000; Miller et al. 2002, 2003-2005, 2007a-b; Miller and Burwen 2002).

Analysis of the 1998–2000 standardized CPUE data suggested the gillnetting data were better suited for determining species apportionment of split-beam sonar counts than for passage estimates (Reimer et al. 2002). In 2002, the inriver gillnetting program was modified further. A 5-in mesh gillnet was introduced, alternating with the existing 7.5-in mesh to reduce size selectivity; nets were constructed of multi-monofilament (formerly cable-lay braided nylon); the color of the mesh was changed to more closely match that of the river; and drifts were shortened and constrained to more closely match the portion of the channel sampled by the sonar. These changes increased netting efficiency and decreased the effect of water clarity on gillnet catches (Reimer 2004).

In 2002, we refined the species discrimination algorithm for TS-based estimates, censoring selected hourly samples based on fish behavior. During samples when sockeye salmon were abundant, as evidenced by aggregation of migrating fish into groups, the data were censored, and Chinook salmon passage was estimated from the remaining hourly samples.

Also in 2002, two experimental methods of estimating Chinook salmon passage were initiated. The first alternative estimate, referred to as the net-apportioned estimate, uses the product of Chinook salmon catch proportions from the netting program (Eskelin 2010) and sonar upstream midriver fish passage estimates (see Methods). Net-apportioned estimates have been published annually since 2002 (Miller et al. 2004, 2005, 2007a-b, 2010), and have proven useful for tracking short term trends in Chinook salmon abundance.

The second alternative estimate is based on split-beam measures of echo envelope length, which is a far better predictor of fish length than target strength (Burwen and Fleischman 1998; Burwen et al. 2003). Statistical methods were developed that enable robust estimates of species composition even when species overlap in size (Fleischman and Burwen 2003). Echo length standard deviation (ELSD) information from the sonar is combined with fish length data from the netting program to estimate the species composition of fish passing the sonar site. The resulting estimated proportion of Chinook salmon is then multiplied by upstream fish passage estimates from the sonar. For the early run, ELSD mixture model estimates have been published since 2002, and we consider them to be more accurate than the official TS-based estimates. For the late run, these estimates were not published because we suspected that they overestimated the number of Chinook salmon when fish densities were very high. Echo length measurements can be corrupted when 2 or more fish swim very close to one another, resulting in higher values of ELSD.

In 2007, we modified the ELSD mixture model method in an attempt to reduce the bias at high fish densities. Using split-beam measurements of 3-dimensional fish location, we began monitoring the distance between fish in the beam and censoring those within 1 meter of any other fish¹ before fitting the mixture model.

ADF&G also began testing dual-frequency identification sonar (DIDSON²) in the Kenai River in 2002 (Burwen et al. 2007). DIDSON uses a lens system that provides high resolution images that approach the quality achieved with conventional optics (Simmonds and MacLennan 2005), with the added advantage that images can be obtained in dark or turbid waters. Fish size was immediately evident from DIDSON footage³ of migrating Kenai River salmon, suggesting that DIDSON had promise for improved discrimination of large Chinook salmon from smaller fish in the Kenai River. With ADF&G input, DIDSON developers designed custom software for manually measuring fish size directly from still images.

Initial experiments using live tethered salmon showed that at ranges up to 12 m, precise estimates of fish length could be obtained by manually measuring fish images produced by a standard DIDSON unit (Burwen et al. 2007). High resolution images at ranges up to 30 m are required to adequately insonify the Kenai River at the current sonar location (river mile 8.5).

Subsequent advancements in DIDSON technology resulted in improved long-range image resolution, and in 2007, additional experiments were conducted to determine if the improvements were sufficient to enable DIDSON estimates of Chinook salmon passage in the Kenai River.

In this report, we present daily and seasonal TS-based, net-apportioned, and ELSD-based estimates of Kenai River Chinook salmon inriver abundance for 2007. We also summarize the results of continued testing of DIDSON technology in the Kenai River.

OBJECTIVES

The primary objective of this project was to produce daily and seasonal target-strength-based (TS-based) estimates of the inriver run of Chinook salmon to the Kenai River such that the upper and lower bounds of the 95% confidence interval were within 5% of the seasonal (early run or late run) point estimate. This estimate was based on target strength and range thresholds, with hourly samples subject to censoring based on fish behavior. The precision criterion addressed only the sampling error of the estimates. In keeping with previous practice, errors due to species classification, tracking, and detection that may cause biases in the primary objective were not included in the criteria for the secondary objective (echo length standard deviation [ELSD]-based estimates).

Inseason advancements enabled us to add a second objective in 2007, which was to produce weekly and seasonal ELSD-based estimates of the inriver run of Chinook salmon to the Kenai River such that the seasonal estimate was within 10% of the true value 95% of the time. This estimate was based on mixture modeling of ELSD measurements subject to censoring based on fish behavior. The precision criterion for ELSD-based estimates was intended to address sampling error and species classification, but not target tracking or detection.

¹ Fish swimming close to other fish are assumed not to be Chinook salmon.

² DIDSON was designed by the University of Washington Applied Physics Laboratory, originally for military applications.

³ DIDSON imagery resembles video footage taken from above the river's surface.

Objectives related to DIDSON testing were 1) to estimate the error standard deviation associated with measuring, from DIDSON images, the length of Chinook salmon tethered at distances 15 to 30 m from the transducer; 2) to collect sufficient paired DIDSON vs. split-beam data on free-swimming fish to evaluate the feasibility of modeling DIDSON-estimated fish lengths as a species-age mixture; and 3) to evaluate the ability to detect, track, and measure fish at densities that occur during periods of high fish passage.

METHODS

STUDY AREA

The Kenai River drainage is approximately 2,150 square miles. It is glacially influenced, with discharge rates lowest during winter, increasing throughout the summer, and peaking in August (USDA 1992). The Kenai River has 10 major tributaries, many of which provide important spawning and/or rearing habitat for salmon. Tributaries include the Russian River, Skilak River, Killey River, Moose River, and Funny River.

The Kenai River drainage is located in a transitional zone between a maritime climate and a continental climate (USDA 1992). The geographic position and local topography influence both rainfall and temperature throughout the drainage. For the City of Kenai, located at the mouth of the Kenai River, the average annual precipitation (1971–2006) is 48 cm (WRCC 2008). Average summer (June, July, and August) temperature for the City of Kenai is 12°C (WRCC 2008).

SITE DESCRIPTION

The 2007 sonar site was located 14 km (8.5 miles) from the mouth of the Kenai River (Figure 2). This site has been used since 1985 and was selected for its acoustic characteristics and its location downstream of the sport fishery and known Chinook salmon spawning habitat.

The river bottom in this area has remained stable for the past 22 years (Bosch and Burwen 1999). The slope from both banks is gradual and uniform, which allows a large proportion of the water column to be insonified without acoustic shadowing effects. On the right bank, the bottom is composed primarily of mud, providing an acoustically absorptive surface. This absorptive property improves the signal-to-noise ratio (SNR) when the beam is aimed along the river bottom. The left-bank bottom gradient is steeper and consists of more acoustically reflective small rounded cobble and gravel.

The sonar site is located downstream of the lowest suspected Chinook salmon spawning sites, yet far enough from the mouth that most of the fish counted are probably committed to the Kenai River (Alexandersdottir and Marsh 1990). Most sport fishing activity occurs upstream of the site⁴.

⁴ In 2005, approximately 98% of the early-run Chinook salmon sport fishing effort and 86% of the late-run effort occurred upstream of the Chinook salmon sonar site (Eskelin 2007).

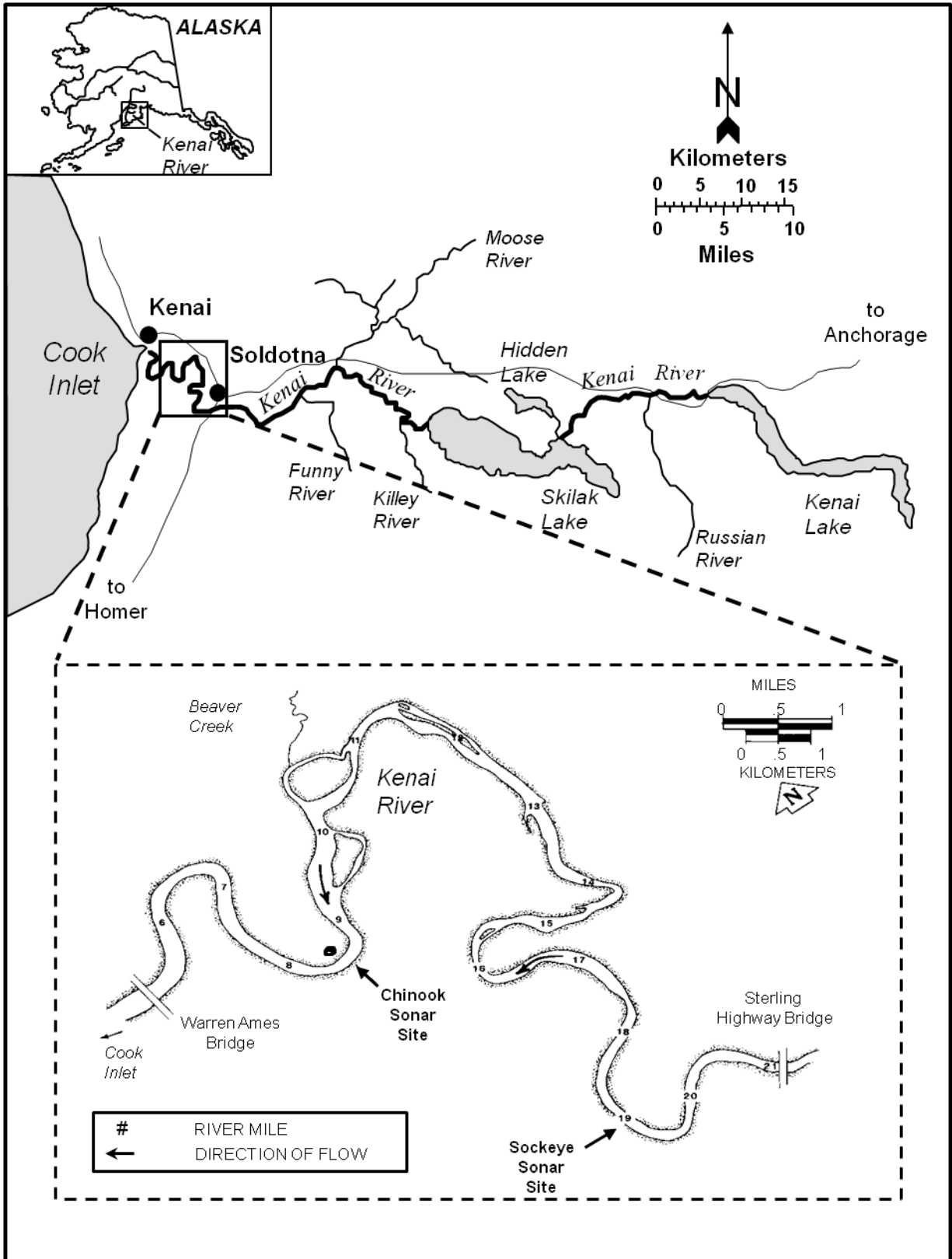


Figure 2.—Kenai River sonar site locations, 2007.

SPLIT-BEAM SONAR DATA COLLECTION AND PROCESSING

Acoustic Sampling

A Hydroacoustic Technology Inc. (HTI)⁵ split-beam sonar system was operated from 20⁶ May to 4⁷ August 2007. Components of the system are listed in Table 1 and are further described in HTI manuals (HTI 1996, 1997). A brief explanation of the theory of split-beam sonar and its use in estimating target strength can be found in Appendix A1. A more detailed explanation can be found in Ehrenberg (1983).

Table 1.–Main components of the split-beam sonar system used in 2007.

System Component	Description
Sounder	Hydroacoustics Technology Inc. (HTI) Model 244 Split-Beam Echo sounder operating at 200 kHz
Data Processing Computer	Dell Dimension 2350 personal computer
Transducers	(2) HTI Split-Beam transducers: Left Bank: nominal beam widths: 2.9°x10.2° Right Bank: nominal beam widths: 2.8°x10.0°
Chart Recorder	HTI model 403 digital dual-channel chart recorder
Oscilloscope	Nicolet model 310 digital storage oscilloscope
Video Display	Hydroacoustic Assessments HARP-HC
Remote Pan and Tilt Aiming Controller	Remote Ocean Systems Model PTC-1 Pan and Tilt Controller
Remote Pan and Tilt Aiming Unit	Remote Ocean Systems Model PT-25 Remote Pan and Tilt Unit
Heading and Angular Measurement Device	JASCO Research Ltd. Uwinstru Underwater Measurement Device.

Note: product names used in this publication are included for completeness but do not constitute product endorsement.

Sonar System Configuration

Sonar sampling on both banks was controlled by electronics housed in a tent located on the right (north) bank of the river. Communication cables were connected to the sonar equipment on both banks. Cables leading to the left-bank equipment were suspended above the river at a height that did not impede boat traffic (Figure 3).

⁵ Product names used in this publication are included for completeness but do not constitute product endorsement.

⁶ Sampling commenced 4 days late (20 May) due to high water and floating debris.

⁷ Sampling was terminated prior to 10 August due to numerous fish holding in the sonar beam, making it difficult to accurately track fish targets. Chinook salmon passage was estimated through 4 August.

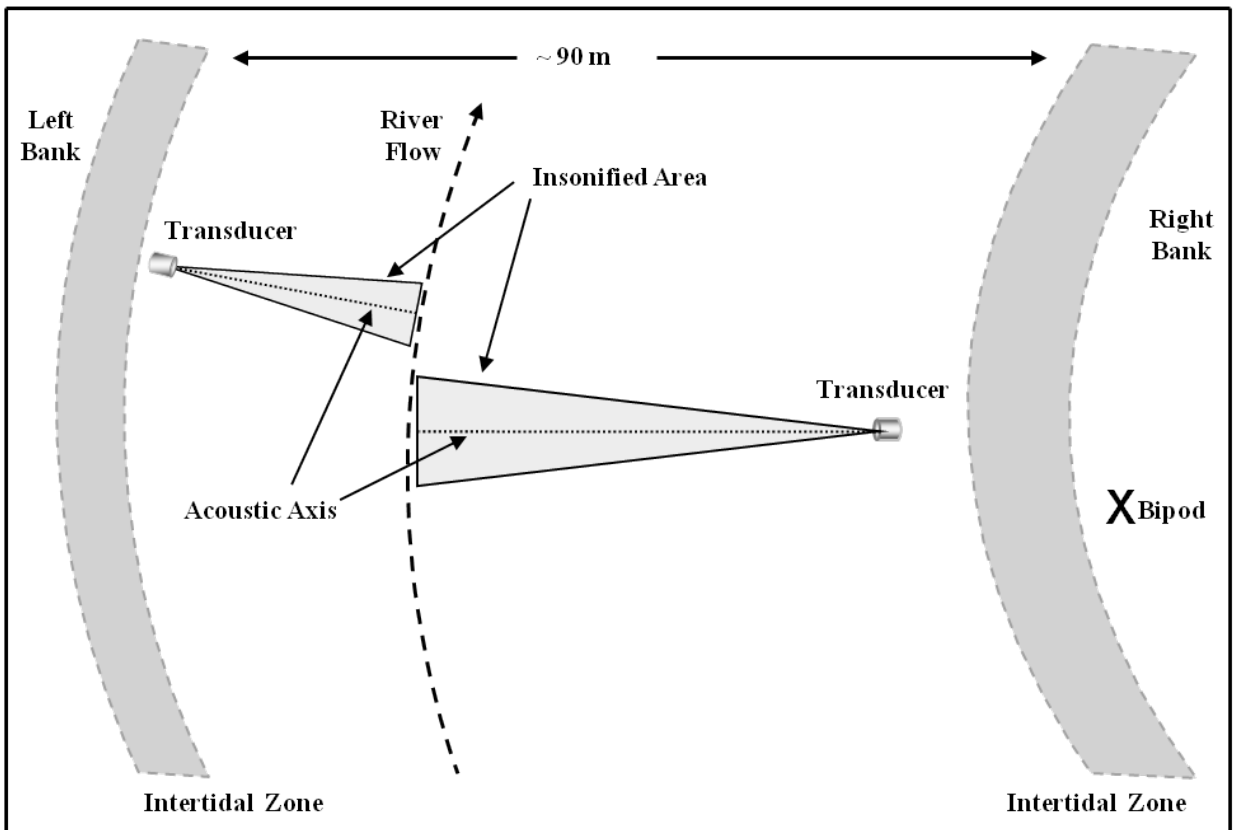
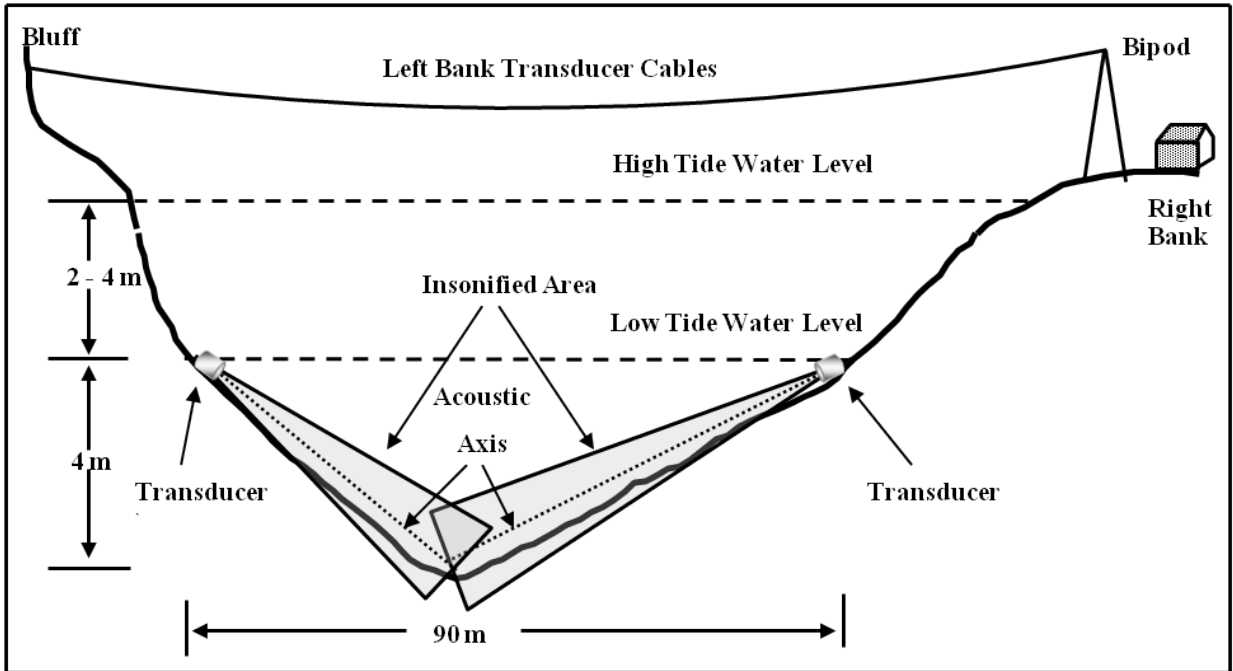


Figure 3.—Cross-sectional (top) and aerial (bottom) diagrams of sonar site illustrating insonified portions of the Kenai River, 2007.

Note: Distance from bipod to thalweg (shown as dashed line depicting the lowest course of the river) is approximately 88 m.

Steel tripods were used to deploy the transducers offshore. One elliptical, split-beam transducer was mounted horizontally (side-looking) on each tripod. At the start of the season, the transducer tripods were placed on each bank in a position close to shore but still submerged at low tide. During sampling from 20 May to 4 August, water levels at low tide increased approximately 1.2 m. Rising water level throughout the season and heavy debris accumulation resulted in occasional relocation of transducer tripods. The total range insonified during the season by both (right and left bank) sonar beams ranged from approximately 57.5 m to 60.4 m (Figure 4).

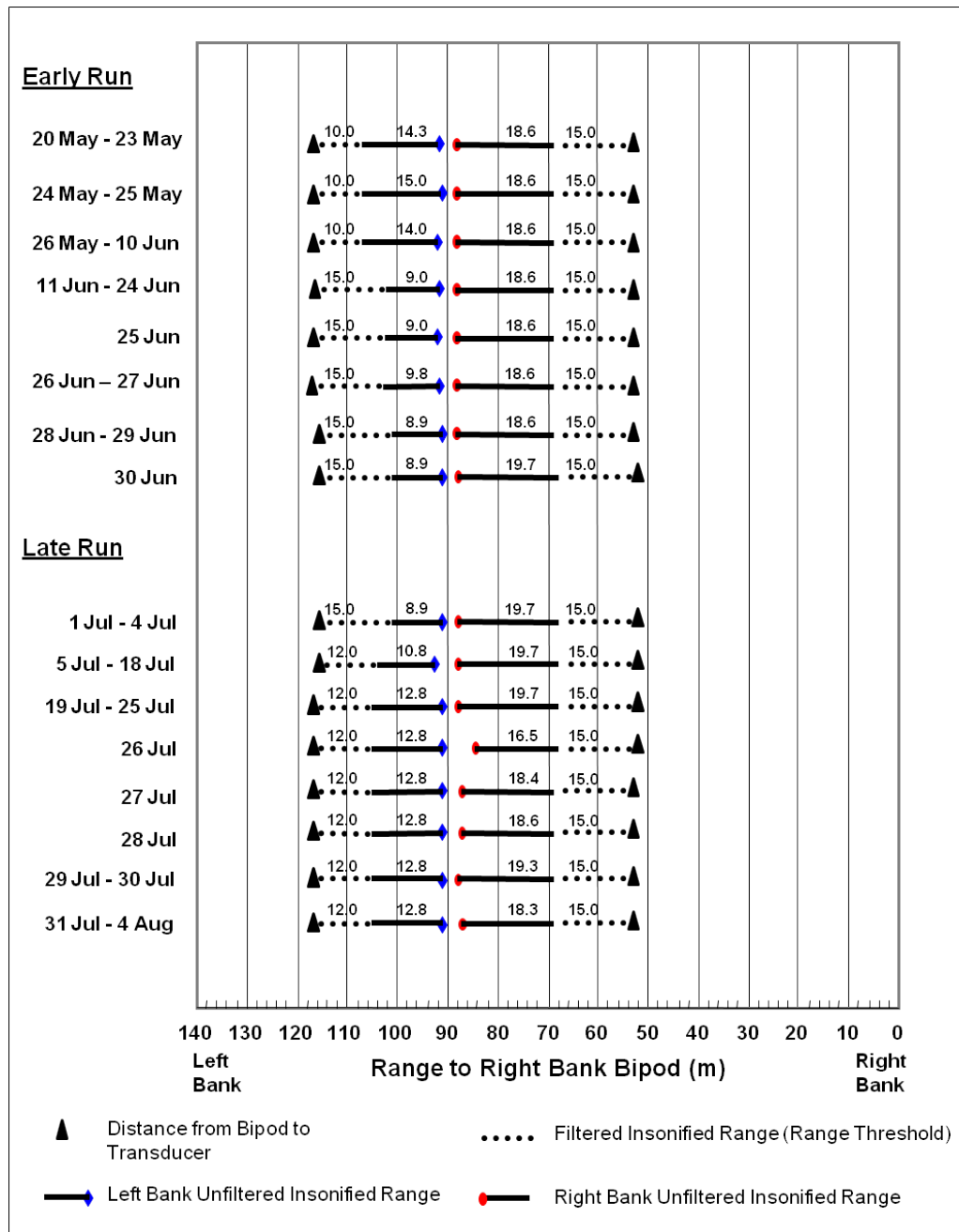


Figure 4.—Daily right- and left-bank transducer placement and insonified ranges relative to bipod tower located on the right bank, Kenai River, 2007.

Vertical and horizontal aiming of each transducer was remotely controlled by a dual-axis electronic pan and tilt system. A digital readout from an angular measurement device (attitude sensor) attached to the transducer indicated the aiming angle in the vertical and horizontal planes. In the vertical plane, the transducer was aimed using an oscilloscope and chart recorder to verify that the sonar beam was aligned along the river bottom. In the horizontal plane, the transducer was aimed perpendicular to the river flow to maximize probability of insonifying fish from a lateral aspect. The range encompassed by each transducer was determined by the river bottom contour and the transducer placement. Transducers were placed to maximize the counting range and to fully insonify the cross section of the river between the right- and left-bank transducers.

River Profile Mapping and Coverage

A detailed profile of the river bottom and the area encompassed by the sonar beams was produced prior to acoustic sampling. Depth readings collected with a Lowrance X-16 were paired with range measurements taken from a Bushnell Laser Ranger (± 1 m accuracy) aimed at a fixed target on shore. When bottom profile information is combined with information from the attitude sensor, a detailed visualization of how the water column above the bottom substrate is insonified by the acoustic beam can be generated (Figure 5). Each time a transducer was moved, new measurements of the transducer height above the bottom substrate and its position relative to a fixed shore location were updated in an EXCEL worksheet so that beam coverage at the new location could be evaluated.

Before 2001, the right- and left-bank transducers were deployed directly across the river from each other, and complete beam coverage for the entire middle portion of the river was accomplished by extending the counting range for both banks to the thalweg (the line delimiting the lowest points along the length of the river bed). Under these conditions, we could be relatively certain that the entire middle portion of the river was insonified. In 2001, river bottom profiles indicated improved beam coverage (in the vertical plane) could be attained on the left bank by moving the transducer approximately 35 m downstream of its original location (Miller et al. 2003). The left-bank transducer has been deployed at this new location since 2001. Because of the offset deployment of the right- and left- bank transducers (Figure 3), it is difficult to determine if there is complete beam coverage to the thalweg (Miller et al. 2004).

Sonar System Calibration

Prior to sonar sampling, HTI performed reciprocity calibrations with a naval standard transducer to ensure consistent target strength parameters for among-year sonar comparisons. Calibrations were verified at the calibration facility with a 38.1-mm tungsten carbide sphere (Foote and MacLennan 1984) and verified at the sonar site using the same sphere on 16 May. For each standard sphere measurement, we recorded the maximum background noise level and voltage threshold in addition to the data collected automatically by the onboard signal-processing software.

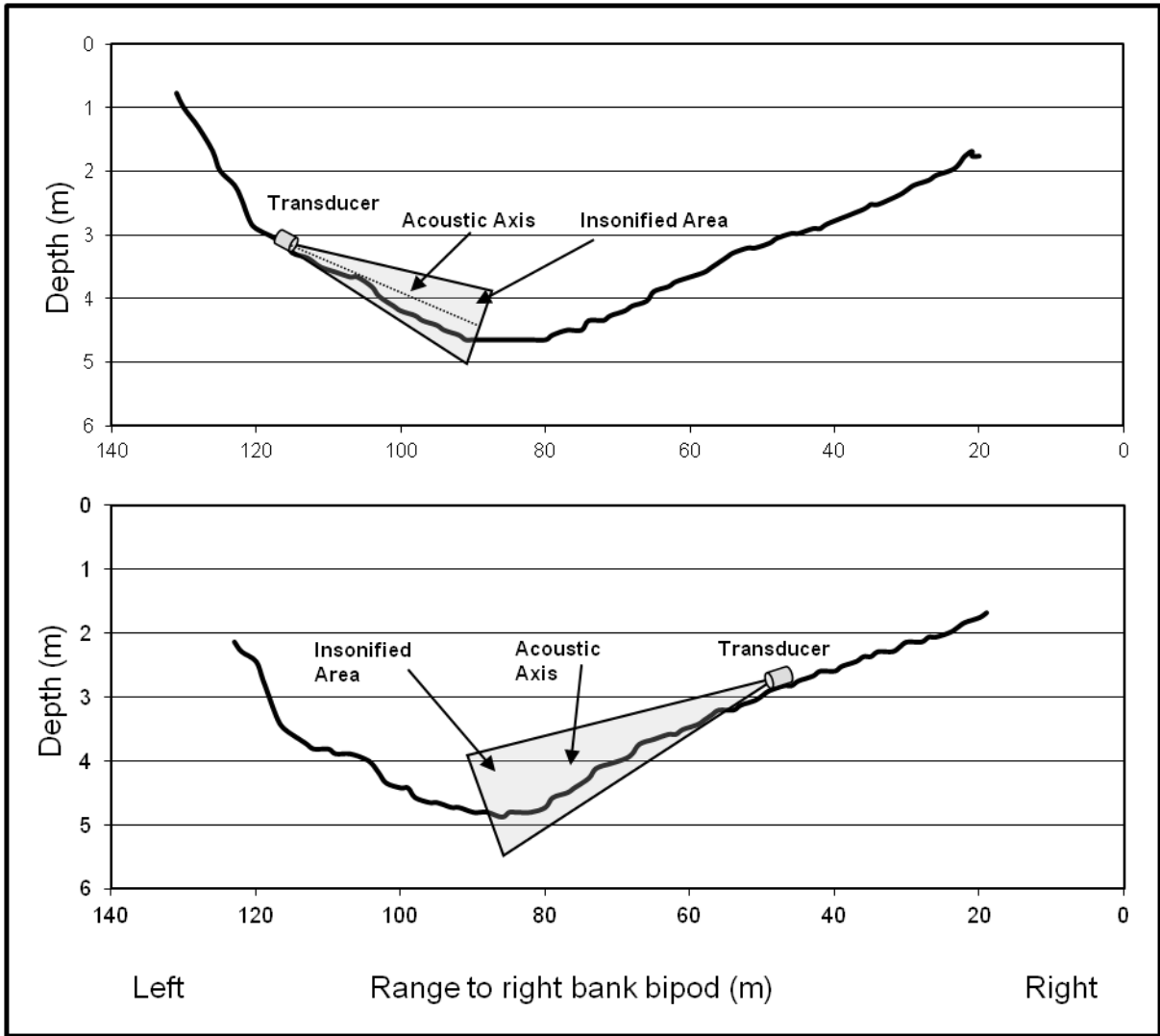


Figure 5.—Bottom profiles by bank for the Kenai River Chinook salmon sonar site with approximate transducer placement and sonar beam coverage for 16 May 2007.

Sampling Procedure

A systematic sample design (Cochran 1977) was used to estimate fish passage from each bank for 20 minutes each hour. Although the sonar system is capable of sampling both banks continuously, data collection was restricted to 20-min samples per hour to limit the data processing time and the number of personnel required to estimate daily fish passage. The equipment was automated to sample the right bank for 20 minutes starting at the top of each hour followed by a 20-min left-bank sample. The system was inactive for the third 20-min period unless ancillary sonar studies were being conducted. This routine was followed 24 hours per day and 7 days per week unless a transducer on one or both banks was inoperable. A test of this sample design in 1999 found no significant difference between estimates of Chinook salmon passage obtained using 1-hour counts and estimates obtained by extrapolating 20-min counts to 1 hour (Miller et al. 2002).

Because fish passage rates are related to tides (Eggers et al. 1995), tide stage was recorded at the top of each hour and at 20 minutes past each hour to coincide with the start of each 20-min

sample. Tide stage was recorded from a staff gauge at the sonar site using water level measured to the nearest 0.25 ft and converted to meters.

Data Collection Parameters

An HTI Model 244 digital echo sounder (DES) was used for data collection. Key data collection parameters (echo sounder settings) are listed in Table 2 with complete summaries by bank in Appendices B1 and B2. Most echo sounder settings were identical for each bank and remained consistent throughout the sample period. High power and low gain settings were used to maximize SNR. The transmitted pulse width was set relatively low to maximize resolution of individual fish and SNR.

Table 2.–Hydroacoustics Technology Inc. model 244 digital echo sounder settings used in 2007.

Echo Sounder Parameters	Value
Transmit Power	25 dB
System Gain (G_r)	-18 dB
Time Varying Gain	$40\log_{10}R$
Transmitted Pulse Width	0.20 msec
Ping Rate Right Bank	11 pings/sec
Ping Rate Left Bank	16 pings/sec

Data Acquisition

DES performed the initial filtering of returned echoes based on user-selected criteria (Table 3, Appendices B1 and B2) that are input via software stored on an external data processing computer (Table 1, Figure 6). DES recorded the start time, date, and number of pings (acoustic pulses) processed for each sample.

Table 3.–Echo acceptance criteria for digital echo processing, 2007.

Bank	Pulse width ^a (ms) at -6 dB	Vertical angle off-axis (°)	Horizontal angle off-axis (°)	Threshold mV (dB)	Minimum range (m)
Right					
0 D _± \$ XI	0.04 to 10.0	-2.5 to 2.0	-5.0 to 5.0	662 (-35 dB)	2.0
Left					
16 May–5 Aug	0.04 to 10.0	-2.5 to 2.0	-5.0 to 5.0	409 (-35 dB)	2.0

^a Pulse width filters have not been used since 1996 (Burwen and Bosch 1998) in order to retain information potentially useful for species classification (Burwen et al. 2003; Fleischman and Burwen 2003).

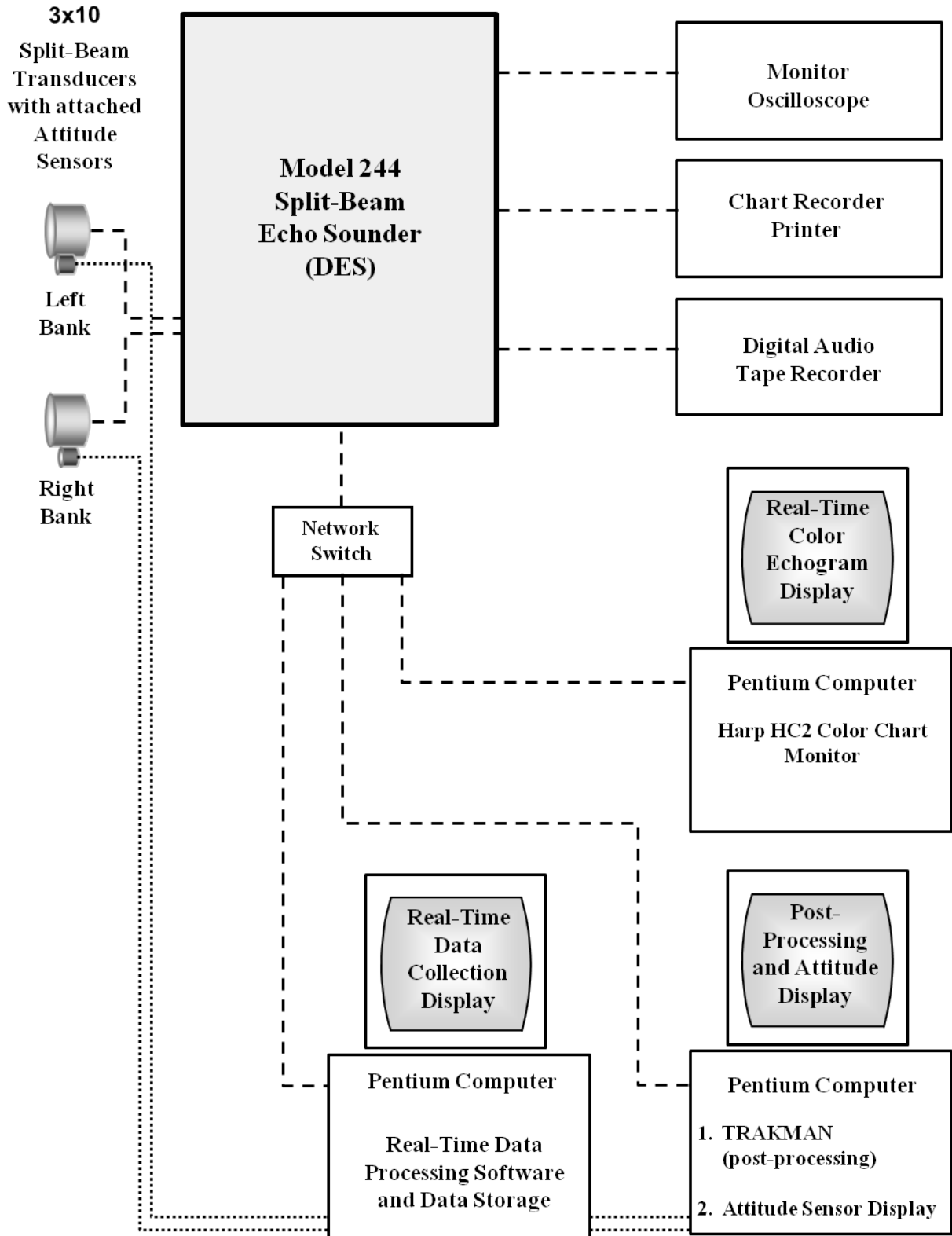


Figure 6.—Diagram of 2007 split-beam sonar system configuration and data flow.

Echoes that originated in the transducer near field (≤ 2.0 m) were excluded because fluctuating sound intensity near the face of the transducer results in unreliable data (Simmonds and MacLennan 2005). Echoes that exceeded maximum vertical and horizontal angles off-axis were also excluded to prevent consideration of unreliable data near the edge of the sonar beam.

Voltage thresholds were used to exclude most background noise from spurious sources such as boat wake, the river bottom, and the water surface. Collection of data from unwanted noise causes data management problems and makes it difficult to distinguish echoes originating from valid fish targets. The level of background noise is determined largely by the dimensions of the sonar beam in relation to the depth of the river. Because the water level at the sonar site is strongly influenced by tidal stage (vertical fluctuations of more than 4 m), the background noise fluctuates periodically, with the lowest noise levels during high tide and the highest levels during falling and low tides. Voltage thresholds corresponding to a -35 dB target on-axis were selected for each bank as the lowest threshold that would exclude background noise at low tide when noise was at a maximum.

For each echo passing initial filtering criteria, DES wrote information in ASCII file format (*.RAW files). This file provided a record of all raw echo data, which could then be used by other post-processing software. A uniquely-named file was produced for each sample hour. The file stored the following statistics for each tracked echo: 1) distance from the transducer, 2) sum channel voltage produced by the echo, 3) pulse widths measured at -6 dB, -12 dB, and -18 dB down from the peak voltage, 4) up-down (vertical) angle, left-right (horizontal) angle, and 5) multiplexer port.

The sum channel voltage from DES was also output to a printer, to a Nicolet 310 digital storage oscilloscope, and to a Harp HC2 color chart monitor. Output to the printer was filtered only by a voltage threshold, which was set equal to the DES threshold. Real-time echograms were produced for each sample. The echograms were used for data backup and transducer aiming, and to aid in manual target tracking. Voltage output to the oscilloscope and color monitor was not filtered. Monitoring the unfiltered color echogram ensured that sub-threshold targets were not being unintentionally filtered. Advanced features on the digital oscilloscope aided in performing field calibrations with a standard target and in monitoring the background noise level relative to the voltage threshold level.

Fish Tracking and Echo Counting

Using HTI proprietary software called TRAKMAN 1400 (version 1.31), echoes (from the *.RAW files) were manually grouped (tracked) into fish traces. TRAKMAN produces an electronic chart recording for all valid echoes collected during a 20-min sample. Selected segments of the chart can be enlarged and echoes viewed on a Cartesian grid. Echoes that displayed a sequential progression through the beam were selected by the user and classified into fish traces (targets). TRAKMAN then produced 3 output files. The first file contained each echo that was tracked from a valid target (*.MEC file) and included the following data for each echo: estimated X (left-right), Y (up-down), and Z (distance from the transducer) coordinates in meters, where the transducer face is the origin of the coordinate system; pulse widths measured at -6 dB, -12 dB, and -18 dB amplitude levels; combined beam pattern factor in dB; and target strength in dB. The second fixed-record ASCII file (*.MFS file) summarized data from all echoes associated with an individual tracked target and output the following fields by target: total number of echoes tracked; starting X, Y, and Z coordinates; distance traveled (m) in the X, Y, and Z

directions; mean velocity (m/sec); and mean target strength (dB). The third file was identical to the *.RAW file described earlier except that it contained only those echoes combined into tracked targets. Direction of travel was estimated by calculating the simple linear regression of X-axis position (distance up- or downriver from the beam axis) on ping number, for echoes with absolute X-axis angle less than 5 degrees. On the right bank, a target was classified as upstream-bound if the slope of the regression was negative or downstream-bound if the slope was positive. On the left bank the criteria were reversed. Only upstream targets contributed to estimates of Chinook salmon passage. A diagram illustrating data flow can be found in Appendix C1.

Downstream moving targets (and occasionally upstream moving targets during a strong flood tide) were further classified as fish or debris primarily by looking at the angle of passage and degree of movement in the Z-axis (distance from transducer) as the target moved through the acoustic beam. For debris, the angle of passage through the beam is constant with little change in the range as it passes through the beam. Consequently, debris resembles a line drawn on the echogram with a straightedge. A fish typically leaves a meandering trace that reflects some level of active movement as it passes through the acoustic beam. Separate summary files were generated for tracked targets classified as debris (i.e., *.DEC and *.DFS files). Except for debris, only targets comprising echoes displaying fish-like behavior were tracked. Echoes from structures, boat wakes, and sport-fishing tackle were ignored.

Data Analysis

Tidal and Temporal Distribution

Falling tide was defined as the period of decreasing staff-gauge readings, low tide as the period of low static readings, and rising tide as the period of both increasing readings and high static readings (i.e., high slack tide). The rising and high slack tides were combined into one category because of the very short duration of high slack tide at the sonar site. Data from both banks were combined to summarize fish passage by tide stage (falling, low, and rising) for both upstream and downstream traveling fish. Data were first filtered using target strength and range criteria.

Spatial Distribution

Knowledge of the spatial distribution of fish is desirable for developing strategies for insonifying a specific area, for determining appropriate transducer beam dimensions, and for evaluating the probability of detecting fish near the edge of the acoustic beam (Mulligan and Kieser 1996).

Fish range (Z-axis) distributions (distance from shore) for each bank were plotted separately for upstream and downstream moving targets. Fish range distributions were calculated using the mean distance from transducer for each target. Before 2000, range distribution comparisons were made using z_m , the distance from the face of the transducer to the target location (Miller et al. 2002). These comparisons provided information on distribution of fish targets from the face of the transducer. However, the comparisons were poor descriptors of actual fish range distributions across the river because tripod/transducer locations change throughout the season. Beginning in 2000, estimates of distance from bank were standardized to the nearest shore transducer deployment for that bank based on distances to a fixed point (cable bipod) on the right bank (Figures 3 and 4):

$$z_a = z_m + |z_t - z_n| \quad (1)$$

where

- z_a = adjusted range (in meters),
- z_t = distance (in meters) from right bank bipod to transducer, and
- z_n = distance (in meters) from right bank bipod to nearest shore (right bank or left bank) deployment location.

Range distribution plots were produced with the adjusted (standardized) range estimates allowing for comparisons of actual fish target locations across the river. The end range in these distribution graphs was the maximum distance covered (generally to the thalweg) by the sonar beam on that particular bank.

Vertical distributions were plotted by direction of travel (upstream and downstream) and tide stage. Vertical distributions were calculated from the midpoint angle off-axis⁸ in the vertical plane as follows:

$$\theta_v = \arcsin \frac{v_s + \left(\frac{d_v}{2}\right)}{z_m} \quad (2)$$

where

- θ_v = vertical angle-off-axis midpoint (degrees),
- v_s = starting vertical coordinate (in meters), and
- d_v = distance traveled in vertical direction (in meters).

Upstream Midriver Fish Passage Estimates

The following procedures are used to estimate the number of salmon of all species that migrate upstream past the sonar site in midriver, where midriver is defined as at least 15 m from the right-bank transducer and at least 10 m from the left-bank transducer. This “unfiltered”⁹ estimate is used as the basis for all other estimates described herein. The remaining estimates pertain only to Chinook salmon, and differ in the manner in which species classification is carried out.

As mentioned above, the sonar operated 20 minutes per hour from each bank of the river, 24 hours per day. The number of salmon-sized fish (hydroacoustic variable y) passing midriver and upstream through the sonar beams during day i was estimated as

$$\hat{y}_i = 24 \hat{\bar{y}}_i \quad (3)$$

where

$$\hat{\bar{y}}_i = \frac{1}{n_i} \sum_{j=1}^{n_i} \hat{y}_{ij}, \quad (4)$$

⁸ Axis or acoustic axis refers to the center of the beam in either the vertical or horizontal plane.

⁹ These are known in-house as “unfiltered” estimates in the sense that TS and time-varying range thresholds have not been applied. Technically, these counts are still filtered by time-invariant minimum range criteria to exclude fish very close to the transducer. These fish are subject to imperfect detection due to the narrowness of the sonar beams at close range, and have been assumed to be composed almost entirely of sockeye salmon.

where n_i is the total number of hours (j) during which fish passage was estimated¹⁰ for day i , and where

$$\hat{y}_{ij} = \sum_{k=1}^2 \hat{y}_{ijk}, \quad (5)$$

where \hat{y}_{ijk} is the estimate of upstream midriver fish passage on bank k during hour j of day i .

When the sonar was functional on bank k during hour j of day i , then hourly upstream midriver fish passage was estimated as follows:

$$\hat{y}_{ijk} = \frac{60}{m_{ijk}} c_{ijk} \quad (6)$$

where

m_{ijk} = number of minutes (usually 20) sampled from bank k during hour j of day i , and

c_{ijk} = number of upstream-bound fish greater than 15 m from the right-bank transducer and greater than 10 m from the left-bank transducer, for bank k , hour j , and day i .

When the sonar system was functional on one bank but not the other, the passage on the non-functional bank k' was estimated from passage on the functional bank k as follows:

$$\hat{y}_{ijk'} = \hat{R}_{ikt} \hat{y}_{ijk}, \quad (7)$$

where the estimated bank-to-bank ratio R_{ikt} , for day i and tide stage t is calculated by pooling counts from all hours at tide stage t (set J_t) during the previous 2 days (to ensure adequate sample size):

$$\hat{R}_{ikt} = \frac{\sum_{j \in J_t} \hat{y}_{(i-2)jk'} + \sum_{j \in J_t} \hat{y}_{(i-1)jk'}}{\sum_{j \in J_t} \hat{y}_{(i-2)jk} + \sum_{j \in J_t} \hat{y}_{(i-1)jk}}. \quad (8)$$

The variance of the estimates of y , due to systematic sampling in time, was approximated (successive difference model, Wolter 1985), with adjustments for missing data, as

$$\hat{V}[\hat{y}_i] \cong 24^2 (1-f) \frac{\sum_{j=2}^{24} \phi_{ij} \phi_{i(j-1)} (\hat{y}_{ij} - \hat{y}_{i(j-1)})^2}{2 \sum_{j=1}^{24} \phi_{ij} \sum_{j=2}^{24} \phi_{ij} \phi_{i(j-1)}} \quad (9)$$

where f is the sampling fraction (proportion of time sampled daily, usually 0.33), and ϕ_{ij} is 1 if \hat{y}_{ij} exists for hour j of day i , or 0 if not.

¹⁰ Hours for which passage was not estimated include hours when equipment on both banks was not functional (<1% of time).

The total estimate of upstream midriver fish passage during the period of sonar operation, and its variance, was the sum of all daily estimates:

$$\hat{Y} = \sum_i \hat{y}_i, \text{ and} \quad (10)$$

$$\hat{V}[\hat{Y}] = \sum_i \hat{V}[\hat{y}_i]. \quad (11)$$

Target Strength (TS)-based Chinook Salmon Passage Estimates

To produce TS-based estimates, upstream fish counts (c_{ijk}) were filtered using 2 criteria: target strength (greater than -28 dB) and distance from the transducer (greater than customized range thresholds, see below). TS-based estimates were the standard metric for comparison with escapement goals. Although target strength and range thresholds do not exclude all sockeye salmon (see Introduction; also Eggers 1994 and Burwen et al. 1995), we continued their use for historical comparability, while we developed other means of discriminating between fish species.

Range thresholds differed by bank and over time. Range thresholds were changed when transducer tripods were moved or when fish distribution and behavior indicated that species discrimination could be improved. The left-bank range threshold was 10 m from 20 May to 10 June, 15 m from 11 June to 4 July, and 12 m from 5 July to 4 August. The right-bank range threshold was 15 m for the entire season (Figure 4).

Target strength was calculated for individual echoes and averaged for each fish trace (Appendix A1). TS-based daily passage estimates for day i , \hat{y}_{TSi} , were calculated using equations 3–10 after substituting c'_{ijk} for c_{ijk} , where

c'_{ijk} = number of upstream-bound fish on bank k meeting range and target-strength criteria during t_{ijk} .

Additionally, for TS-based estimates, some sample hours were excluded when there was evidence (greater than 50% of targets in closely-spaced groups) of increased sockeye salmon abundance. Under these conditions, and at the discretion of the project leader, the entire hourly sample was dropped and the daily estimate was based on the remaining samples. Censored hourly samples are listed in Appendix D1.

Variance estimates consider only sampling error due to temporal expansion, not error due to imperfect detection or tracking of fish, nor error due to imperfect species classification. Therefore, equation 11 represents only a minimal estimate of variance.

Downstream TS-based Chinook salmon passage¹¹ for day i was estimated as:

$$\hat{x}_{TSi} = \hat{y}_{TSi} \frac{\sum_j \sum_k d_{ijk}}{\sum_j \sum_k c'_{ijk}}, \quad (12)$$

¹¹ These quantities are reported for historical comparability only.

where d_{ijk} is the number of downstream-bound fish on bank k meeting range and target-strength criteria during t_{ijk} .

Net-Apportioned Chinook Salmon Passage Estimates

The “net-apportioned” daily estimate of Chinook salmon passage was calculated by multiplying the upstream midriver fish passage estimate by the estimated proportion of Chinook salmon ($\hat{\pi}_{NETi}$) in 5-in and 7.5-in drift net catches near the sonar site (Eskelin 2010):

$$\hat{y}_{NETi} = \hat{y}_i \hat{\pi}_{NETi} \quad (13)$$

The variance estimate followed Goodman (1960):

$$\hat{\text{var}}(\hat{y}_{NETi}) = \hat{y}_i^2 \hat{\text{var}}(\hat{\pi}_{NETi}) + \hat{\pi}_{NETi}^2 \hat{\text{var}}(\hat{y}_i) - \hat{\text{var}}(\hat{\pi}_{NETi}) \hat{\text{var}}(\hat{y}_i) \quad (14)$$

Echo Length Standard Deviation (ELSD)-based Chinook Salmon Passage Estimates

Alternative estimates based on echo length standard deviation were first produced in 2002, based on work initiated in the mid-1990s that showed ELSD to be a better predictor of fish size than target strength (Burwen et al. 2003). ELSD-based estimates are generated by fitting a statistical species/age mixture model to sonar and netting data. Mixture model methodology is described below.

Mixture Models and Thresholds

Mixture models are useful for extracting information from the observed frequency distribution of a carefully-selected measurement. Imagine being able to observe the exact length, but not the species, of every fish passing the sonar. The distribution of such measurements might look something like Figure 7A. If we have knowledge of the sockeye and Chinook salmon length distributions, the shape of the overall distribution can tell us quite a lot about the relative abundance of sockeye and Chinook salmon. For instance, if we know that sockeye salmon do not exceed 70 cm in length, and that small Chinook salmon are very rare, then we can conclude that the left hand mode of the distribution is almost all sockeye salmon and that the species composition is perhaps 50:50 sockeye to Chinook salmon. Mixture model analysis is merely a quantitative version of this assessment, in which the shape of the overall frequency distribution is modeled and “fitted” until it best approximates the data. Uncertainty is assessed by providing a range of plausible species compositions that could have resulted in the observed frequency distribution.

As another example, imagine that there are substantial numbers of small Chinook salmon, and that there is error in the length measurements. The effect of the measurement error is to cause the modes to begin to overlap, reducing the ability to detect detail in the length distribution and reducing the precision of the estimates (e.g., Figure 7B). Here, the human brain could still hazard a guess about the true species composition, but to quantify the uncertainty is more difficult, and is best accomplished by fitting a mixture model.

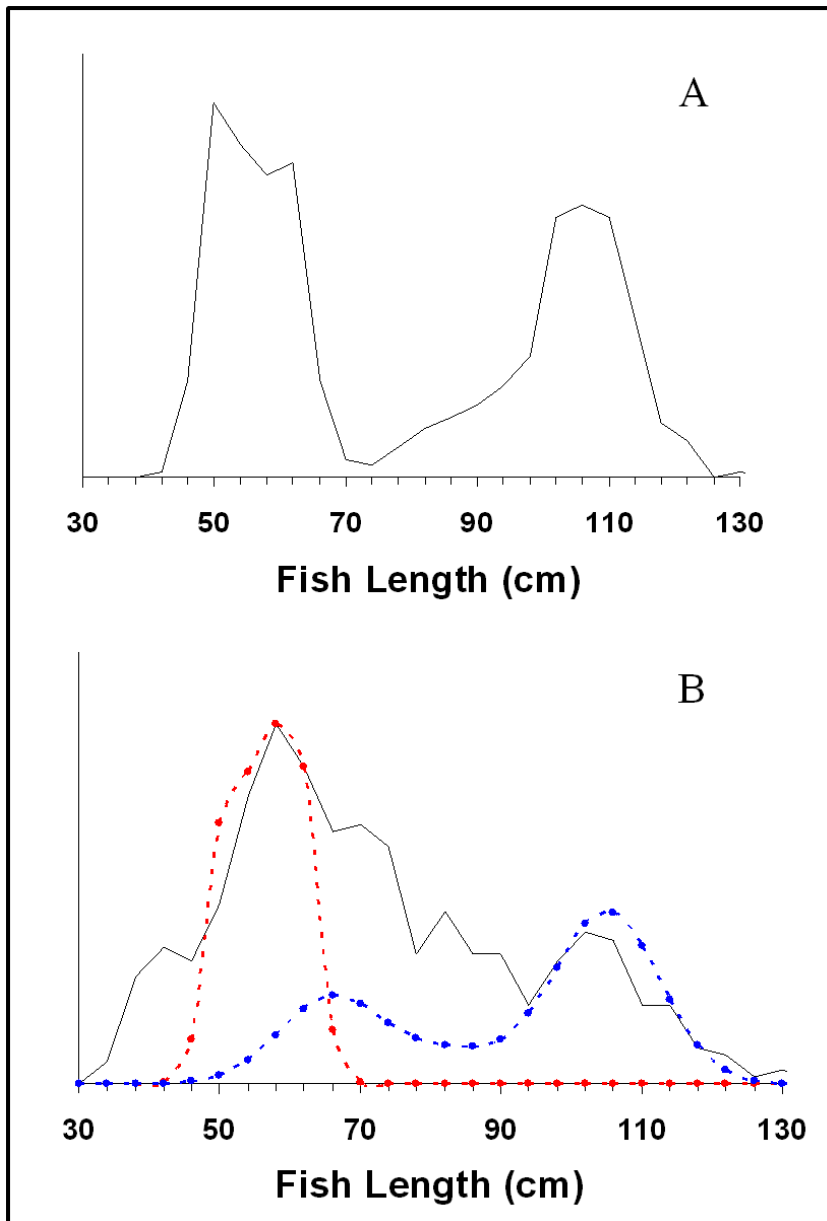


Figure 7.—Hypothetical distributions of fish length measurements (black solid lines) at the Kenai River sonar site. A, Few small Chinook salmon, no measurement error. The true species composition is 50% sockeye salmon, 50% Chinook salmon. B, 40% of Chinook salmon are small; measurement error standard deviation = 10 cm. Distributions of sockeye salmon (red dashed line) and Chinook salmon (blue dashed line) true length are shown. The true species composition is 50% sockeye salmon, 50% Chinook salmon.

Mixture models can also be conducted on measurements of other quantities, like ELSD, that are related to length. Given quantitative knowledge of the relationship between length and ELSD (gleaned from tethered fish experiments, Burwen et al. 2003), it is straightforward to convert from length units to ELSD units by including the slope, intercept, and mean-squared error of the

relationship in the mixture model (Equation 17 below). The more closely related the surrogate measurement is to the one of interest, the more the two distributions will resemble each other and the better the resulting estimate will be. Because ELSD is a reasonably good predictor of fish length (Figure 8)¹², the observed frequency distribution of ELSD supplies valuable information about species composition, even though there is some overlap of ELSD measurements between species. An ELSD distribution with greater mass on the left hand side indicates an abundance of sockeye salmon, whereas more mass on the right hand side indicates more Chinook salmon (Figure 9).

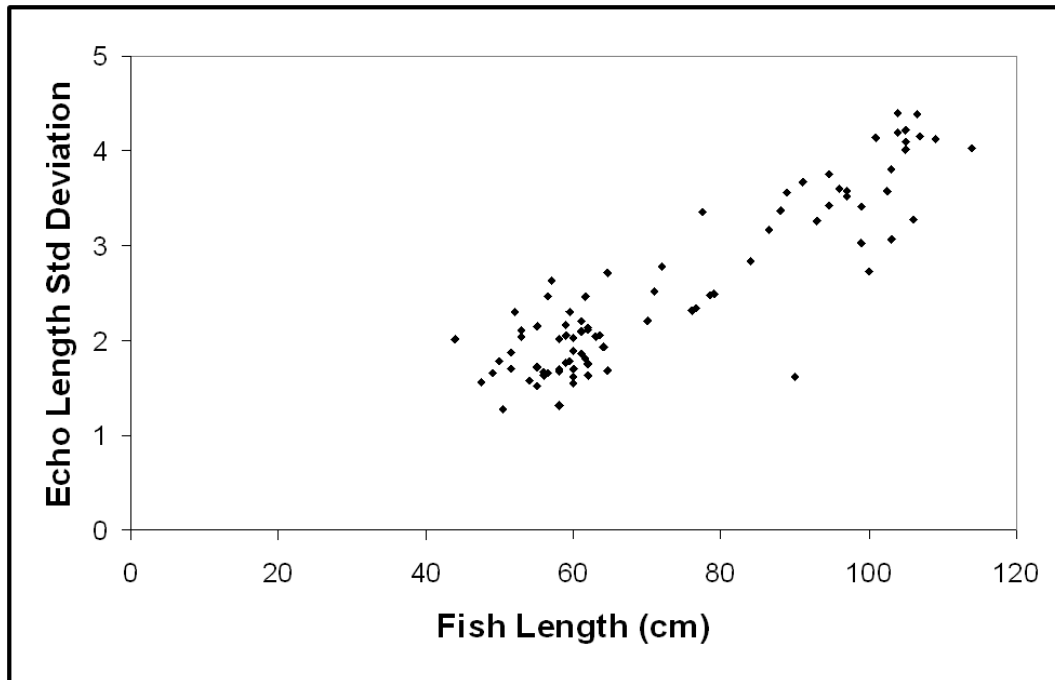


Figure 8.—Echo length standard deviation versus fish length for tethered Pacific salmon in the Kenai River, 1995. Data from Burwen and Fleischman (1998).

The relationship between target strength and fish length is less precise than between ELSD and fish length (Burwen et al. 2003) and it is also less predictable (the relationship changes over time). Furthermore, TS-based species discrimination is implemented in the form of a threshold (TS < -28dB = sockeye salmon, TS > -28dB = Chinook salmon), and the threshold approach has several important drawbacks. When distributions overlap between species, thresholds are unbiased only when compensating errors are equal (e.g., when the number of sockeye salmon exceeding the threshold is equal to the number of Chinook salmon beneath the threshold). But the size of the respective errors depends on the species composition itself (Figure 9): when sockeye salmon are dominant there are more misclassified sockeye salmon than misclassified Chinook salmon (and the resulting estimate of Chinook salmon proportion is too high), and when

¹² ELSD is a good predictor of length, though not as precise as the DIDSON length estimates. DIDSON-measured length will be an excellent candidate for mixture model analysis in the future.

Chinook salmon are dominant there are more misclassified Chinook salmon than misclassified sockeye salmon (and the resulting estimate of Chinook salmon proportion is too low). Thus, threshold-based discrimination is subject to bias that worsens for species proportions near 0 and 1. Furthermore, threshold-based estimates are sensitive to fish size distributions. For instance, in the example illustrated in Figure 9, the number of Chinook salmon misclassified as sockeye salmon (number with $ELSD < 2.7$) depends largely on the relative abundance of small Chinook salmon, which changes over time.¹³

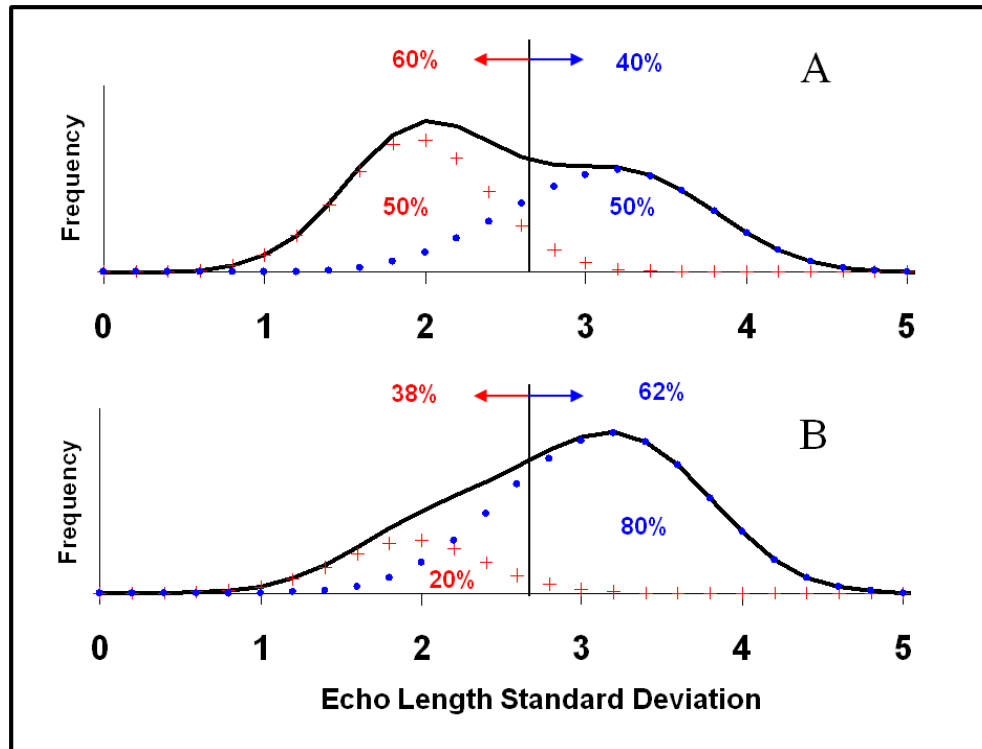


Figure 9.—An example of threshold-based discrimination of Chinook and sockeye salmon. Threshold-based discrimination is subject to bias when discriminating variables are imprecise. Solid lines are simulated frequency distributions of echo length standard deviation arising from component distributions due to sockeye salmon (plus symbols) and Chinook salmon (solid symbols). A, If the true species composition is 50% sockeye salmon to 50% Chinook salmon, and a threshold criterion of 2.7 is used, estimated species composition will be 60:40. B, Using the threshold criterion above, if the true species composition is 20:80, estimated species composition will be 38:62.

The mixture model approach explicitly incorporates the expected variability in hydroacoustic measurements (known from tethered fish experiments), as well as current information about fish

¹³ In fact, use of such a threshold by itself does not discriminate Chinook salmon from sockeye salmon, but rather large Chinook salmon from sockeye salmon and small Chinook salmon.

size distributions (from the onsite netting program). As a result, it is not subject to the same pitfalls as thresholds. There is less bias against extreme proportions, and the estimates are germane to the entire population of Chinook salmon, not just those Chinook salmon larger than sockeye salmon. Finally, as long as length and hydroacoustic measurements are paired in time, mixture model estimates of species proportions are insensitive to temporal changes in fish size distribution.

Mixture Model Details¹⁴

Echo length standard deviation (ELSD) was calculated as

$$ELSD = \sqrt{\frac{\sum_{j=1}^{n_E} (EL_j - \overline{EL})^2}{n_E - 1}} \quad (15)$$

where n_E is the number of echoes and EL_j is the length of the j^{th} echo measured in 48 kHz sample units at -12 dB or higher, depending on peak echo amplitude. If peak amplitude was greater than 12 dB above the voltage threshold, then echo length was measured at 12 dB below peak amplitude. If peak amplitude was 6–12 dB above the threshold, echo length was measured at the threshold. If peak amplitude was less than 6 dB above threshold, EL_j was not defined.

Fish traces with fewer than 8 defined measurements of -12dB pulse width ($n_E < 8$) were excluded from the mixture model; they were assumed to be sockeye salmon because they generally occurred at close ranges, where the beam is very narrow. These fish generally comprised only 1–3% of all fish in the dataset.

The probability density function (PDF) of ELSD (denoted here as y , for convenience) was modeled as a weighted mixture of two component distributions arising from sockeye and Chinook salmon (Figure 10),

$$f(y) = \pi_S f_S(y) + \pi_C f_C(y) \quad (16)$$

where $f_S(y)$ and $f_C(y)$ are the PDFs of the sockeye and Chinook salmon component distributions, and the weights π_S and π_C are the proportions of sockeye and Chinook salmon in the population.

Individual observations of y for fish i were modeled as normal random variates whose mean was a linear function of fish length x :

$$y_i = \beta_0 + \beta_1 x_i + \gamma z_i + \varepsilon_i \quad (17)$$

where β_0 is the intercept; β_1 the slope; γ is the mean difference in y between sockeye and Chinook salmon after controlling for length; z_i equals 1 if fish i was a sockeye salmon, or 0 if Chinook salmon; and the error ε_i is normally distributed with mean 0 and variance σ^2 .

Thus, the component distributions $f_S(y)$ and $f_C(y)$ were functions of the length distributions $f_S(x)$ and $f_C(x)$ and the linear model parameters β_0 , β_1 , γ , and σ^2 (Figure 10). The species proportions π_S and π_C were the parameters of interest.

¹⁴ Statistical notation in this section may overlap with the notation used in the remainder of the report. Specifically, the meaning of variables x , y , and z are unique to this section.

Length measurements were obtained from fish captured by gillnets (e.g., Eskelin 2010) immediately downstream of the sonar site. Length data were paired with hydroacoustic data from the same time periods.

Sockeye salmon and Chinook salmon return from the sea to spawn at several discrete ages. We modeled sockeye and Chinook salmon length distributions as 3-component normal age mixtures:

$$f_S(x) = \theta_{S1}f_{S1}(x) + \theta_{S2}f_{S2}(x) + \theta_{S3}f_{S3}(x) \quad (18)$$

$$f_C(x) = \theta_{C1}f_{C1}(x) + \theta_{C2}f_{C2}(x) + \theta_{C3}f_{C3}(x) \quad (19)$$

where θ_{Ca} and θ_{Sa} are the proportions of Chinook and sockeye salmon belonging to age component a and the distributions

$$f_{Sa}(x) \sim N(\mu_{Sa}, \tau_{Sa}^2), \text{ and} \quad (20)$$

$$f_{Ca}(x) \sim N(\mu_{Ca}, \tau_{Ca}^2) \quad (21)$$

where μ is mean length-at-age and τ is the standard deviation. The overall design was therefore a mixture of (transformed) mixtures. That is, the observed hydroacoustic data were modeled as a 2-component mixture (sockeye salmon and Chinook salmon) of echo length standard deviation (y), each component of which was transformed from a 3-component normal age mixture of fish length (x).

Bayesian statistical methods were employed because they provided realistic estimates of uncertainty and the ability to incorporate auxiliary information. We implemented the Bayesian mixture model in WinBUGS (Bayes Using Gibbs Sampler; Gilks et al. 1994). Bayesian methods require that prior probability distributions be formulated for all unknowns in the model (Gelman et al. 2004). Species proportions π_S and π_C were assigned an uninformative Dirichlet (1,1) prior. Age proportions $\{\theta_{Sa}\}$ and $\{\theta_{Ca}\}$ were assigned informative Dirichlet priors based on a hierarchical analysis of historical data (Appendix E2). Likewise, informative normal priors based on historical data were used for the length-at-age means μ and standard deviations τ (Appendix E2). Informative priors were used for regression parameters β_0 , β_1 , γ , and σ^2 based on linear statistical models of tethered fish data reported by Burwen et al. (2003).

WinBUGS uses Markov chain Monte Carlo methods to sample from the joint posterior distribution of all unknown quantities in the model. We started 3 Markov chains for each run and monitored Gelman-Rubin statistics to assess convergence (Gelman et al. 2004). Burn-in periods of 10,000 or more samples were used. Samples were thinned 10 to 1, and at least 10,000 samples per chain were retained.

The end product of a Bayesian analysis is the joint posterior probability distribution of all unknowns in the model. For point estimates, posterior means were used. Posterior standard deviations were reported as analogues to the standard error of an estimate from a classical (non-Bayesian) statistical analysis.

Sample size limitations occasionally necessitated pooling the data over more than 1 day. The WinBUGS code for the ELSD mixture model is in Appendix E1. Figure 10 is a flow chart with major components of the ELSD mixture model. See also Fleischman and Burwen (2003).

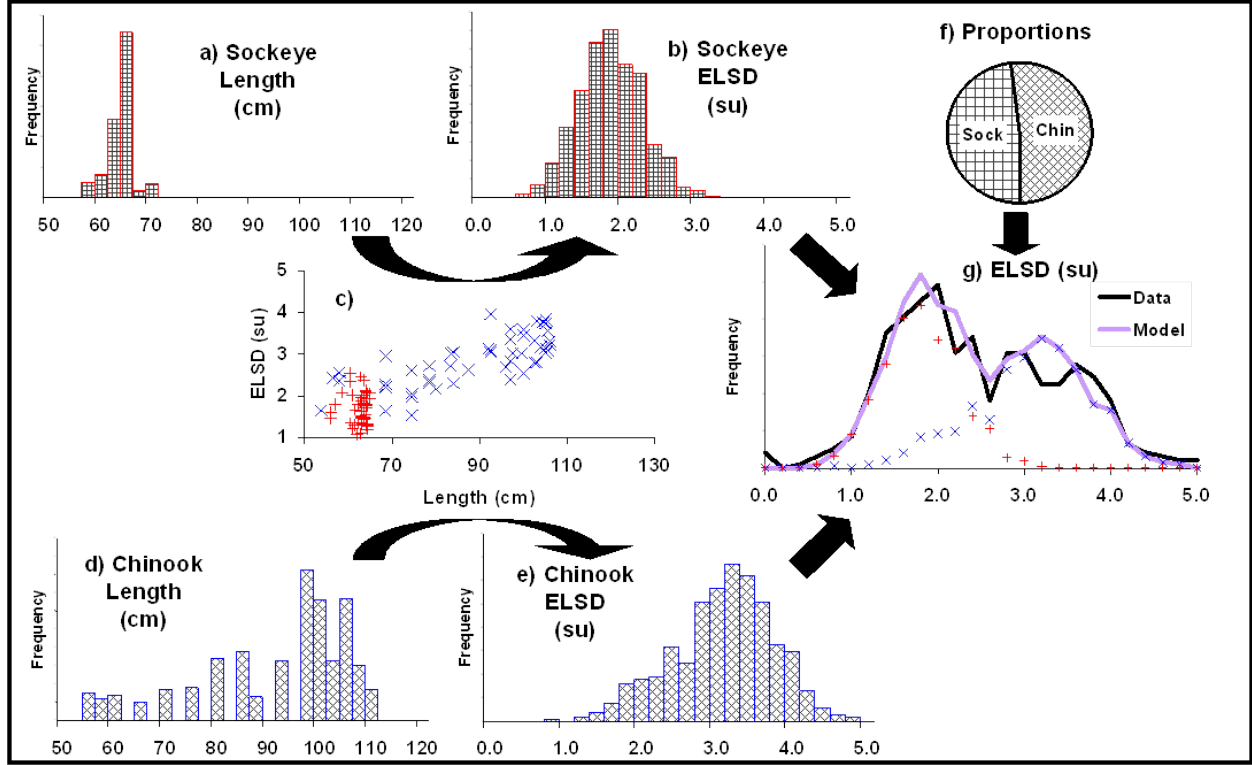


Figure 10.–Flow chart of a mixture model. The frequency distribution of echo length standard deviation (ELSD, panel g) is modeled as a weighted mixture of species-specific ELSD distributions (panels b and e), which in turn are the products of species-specific size distributions (panels a and d) and the relationship between ELSD and fish length (panel c). The weights (species proportions, panel f) are the parameters of interest. Plus symbol = sockeye salmon, x = Chinook salmon. Checkered pattern = sockeye salmon, cross-hatched = Chinook salmon. Units for ELSD are 48 kHz digital sampling units.

Behavior-Censored ELSD Mixture Model Chinook Salmon Passage Estimates

Behavior-censored ELSD mixture model estimates of daily Chinook salmon passage were obtained as follows. First, the proportion p_{Mi} of sonar-sampled fish that satisfied the sample size criterion ($n_E \geq 8$) and the proportion p_{Bi} that satisfied the behavior criterion (fish could not be less than 1 m of range from another fish) for day i were calculated. Then the ELSD frequency distribution from fish meeting both criteria was analyzed with the mixture model methods described above, yielding $\hat{\pi}_{Ci}$, the posterior mean of the Chinook salmon fraction in the reduced data set for day i .

The estimated number of Chinook salmon passing during day i was then

$$\hat{y}_{ELi} = \hat{y}_i \hat{\pi}_{Ci} p_{Mi} p_{Bi} \quad (22)$$

with estimated variance

$$\hat{\text{var}}(\hat{y}_{ELi}) = \left[\hat{y}_i^2 \hat{\text{var}}(\hat{\pi}_{Ci}) + \hat{\pi}_{Ci}^2 \hat{\text{var}}(\hat{y}_i) - \hat{\text{var}}(\hat{\pi}_{Ci}) \hat{\text{var}}(\hat{y}_i) \right] \hat{p}_{Mi}^2 \hat{p}_{Bi}^2 \quad (23)$$

where $\hat{\text{var}}(\hat{\pi}_{Ci})$ was the squared posterior standard deviation from the mixture model. Uncertainty about p_{Mi} and p_{Bi} was ignored because it was negligible compared to $\hat{\text{var}}(\hat{\pi}_{Ci})$.

Expansion for Missing Days

The sonar was not operational until 20 May in 2007, 4 days after the usual starting date of 16 May. Passage estimates were expanded for the missing days as follows. Early-run passage estimates (for 16 May–30 June; \hat{Y}_e) were expanded for these missing days by dividing by the mean proportion of passage (\bar{p}) for the dates 20 May–30 June for the 19 years (1988–2006) the sonar project has operated:

$$\hat{Y}_e = \frac{\hat{Y}}{\bar{p}} \quad (24)$$

where

$$\bar{p} = \frac{\sum_g P_g}{19}, \quad (25)$$

$$P_g = \frac{\sum_{i=20May}^{30June} \hat{y}_i}{\sum_{i=16May}^{30June} \hat{y}_i}, \quad (26)$$

and where g was the year. The variance of \hat{Y}_e was

$$\hat{V}[\hat{Y}_e] = \hat{V}[\hat{Y}]\bar{p}^{-2} + \hat{V}[\bar{p}^{-1}]\hat{Y}^2 - \hat{V}[\hat{Y}]\hat{V}[\bar{p}^{-1}] \quad (27)$$

where

$$\hat{V}[\bar{p}^{-1}] = \frac{\sum_{g=1}^{19} (p^{-1}_g - \bar{p}^{-1})^2}{19(19-1)}. \quad (28)$$

DUAL-FREQUENCY IDENTIFICATION SONAR (DIDSON) TESTING

A long-range DIDSON, coupled with a high-resolution lens was leased from the manufacturer for evaluation from 16 through 23 July. The high-resolution lens was designed to approximately double the resolution of the standard lens previously tested at this site in 2002 and 2004 (Burwen et al. 2007). The high resolution lens was also designed to increase the range at which DIDSON could operate in high frequency mode (i.e. from 15 m to 30 m) yielding higher resolution images at further ranges than was possible with the standard lens. During the 2007 study, a DIDSON software programmer/engineer worked closely with ADF&G personnel to implement requested features related to displaying and measuring fish from DIDSON images. A detailed description of the DIDSON system configuration can be found in Appendix F1.

DIDSON data were collected on both tethered and free-swimming fish. Tethered fish allowed for almost unlimited sampling of high-quality DIDSON images from individual fish of known size centered in the multibeam array. Data collected on free-swimming fish provided a more realistic view of the actual conditions under which DIDSON images from free-swimming fish would

normally be acquired. All experiments were conducted at the split-beam sonar site (river mile 8.5).

Tethered Fish

Tethered fish experiments were conducted on 16, 18, and 23 July. Tethered fish data were collected on the right bank to take advantage of better signal-to-noise conditions. Live Chinook and sockeye salmon were captured with gillnets and held in live pens or totes until they could be deployed. The configuration was similar to that used for counting migrating salmon with split-beam sonar, i.e., the sonar was mounted near the bank and the beam directed across the river perpendicular to the current so that migrating fish swim through the sonar beam at a near side-aspect orientation. The sonar was mounted on a Remote Ocean Systems PT-25 pan and tilt unit to allow precise aiming and deployed in the river on a tripod-style mount. The DIDSON lens was positioned at a height of 39 cm above the substrate and at a depth approximately 1 m below the surface at low tide. The beam was aimed down at a vertical angle of approximately -3.5° to insonify the near-bottom area where the tethered fish were anticipated to settle. After a tethered fish was deployed, minor adjustments to the aim were made to center the fish in each beam. The vertical aiming angle for insonifying individual tethered fish varied from approximately -2° to -5° . More detail on fish-tethering procedures can be found in Burwen and Fleischman (1998) and Burwen et al. (2007).

Free-Swimming Fish

To maximize the probability of high fish passage rates, DIDSON sampling was scheduled to occur during the anticipated peak of late-run Chinook salmon. Data on free-swimming fish were collected on 21–22 July. For free-swimming fish data collection, the DIDSON was moved to the left bank where it was easier to deploy in a side-by-side configuration with the split-beam transducer (Figure 11). The DIDSON system was programmed to sample the range stratum from 13–23 m providing overlapping coverage with approximately the last 10 m of range insonified by the split-beam system. These data provided the opportunity to evaluate the ability of the DIDSON to detect fish at various distances from the transducer, determine direction of travel for fish and debris, and distinguish among individual fish at high passage rates.

DIDSON-Based Fish Length Measurements

Estimates of fork length were made from images using the manual fish-measuring feature included in the Sound Metrics Corporation (SMC) DIDSON Control and Display software Version 5.13. Noise from stationary structures was removed from the images using DIDSON's algorithm for dynamic background removal. We restricted the number of measured frames to 3, in order to approximate what would be reasonable to attain with free swimming fish. The mean of these 3 measurements was used as an estimate of the DIDSON-based length (DL). Additional detail on procedures and software settings used to obtain manual fish length measurements can be found in Burwen et al. (2010).

Data Analysis

Linear statistical models (Neter et al. 1985) were fitted to assess the relationship between DL and measured fork length (FL), and to test for the effect of range (distance from the transducer) on the measurements. We used DL as the dependent variable.

A mixture model, similar to that used for split-beam ELSD measurements (described on page 25), was used to estimate species composition of free-swimming fish passing the DIDSON. The DIDSON mixture model differed from that used for ELSD in that 1) the discriminatory variable was DL rather ELSD, and 2) there was no γ term in Equation 17. Information about the slope and intercept of the relationship between DL and FL was derived from DIDSON tethered fish data.



Figure 11.–Mounting system for a long-range, high resolution DIDSON (left on mount) and split-beam transducer (right on mount).

RESULTS

SPLIT-BEAM SONAR

System Calibration

During system calibration at the Hydroacoustic Technology Inc. (HTI) calibration facility, the target strength of a 38.1-mm tungsten carbide standard sphere was measured at -38.4 dB for the right-bank transducer and -38.5 dB for the left-bank transducer (HTI 2006; Table 4). The theoretical value for the sphere is -39.5 dB (MacLennan and Simmonds 1992). During a subsequent *in situ* calibration check using the same sphere, mean target strength measured -39.5 dB on the right bank and -37.5 dB on the left bank (Table 4). Small fluctuations in mean target strength are expected during *in situ* calibration checks as target strength can vary with signal to noise ratio (SNR), water temperature, depth, conductivity and other factors.

Table 4.—Results of 2007 *in situ* calibration verifications using a 38.1 mm tungsten carbide standard sphere.

Location	Date	Mean target strength (dB)	SD	N	5 \$ 1 * (P	Noise (mV)	Threshold (mV)
<u>Right Bank</u>							
HTI ^a	20 Nov 06	-38.4	0.71	1,017	6.1	N/A ^b	N/A ^b
Kenai River	16 May 07	-39.5	2.84	461	12.7	125	150
<u>Left Bank</u>							
HTI ^a	20 Nov 06	-38.5	0.43	1,109	6.1	N/A ^b	N/A ^b
Kenai River	16 May 07	-37.5	0.97	926	13.7	50	75

^a Measurements taken at Hydroacoustic Technology Inc. facility during system calibration.

^b Not available or not applicable.

Target Tracking

In 2007, 60,320 targets were manually tracked, 10,115 during the early run and 50,205 during the late run. For the purpose of this report, filtered targets refer to those targets that meet range and target strength (TS) criteria.

The percentage of filtered targets that exhibited upstream movement was 98% for the early run and 97% for the late run (Appendices G1 and G2). Daily upstream percentages varied from 67% to 100% during the early run and from 88% to 99% during the late run.

The number of echoes tracked per filtered target varied by run, bank, and direction of travel. Upstream moving targets averaged 61 echoes (SD = 31) per target on the left bank during the early run and 64 echoes (SD = 36) on the right bank. Downstream moving targets averaged 49 echoes (SD = 30) on the left bank and 54 echoes (SD = 35) on the right bank. During the late run, upstream moving targets averaged 78 echoes (SD = 43) on the left bank and 66 echoes (SD = 38) on the right bank. Downstream moving targets averaged 57 echoes (SD = 40) on the left bank and 51 echoes (SD = 35) per target on the right bank.

Tidal Distribution

Upstream-moving filtered targets were observed mostly during the falling tide for both the early (62.4%) and late (62.9%) runs (Tables 5 and 6, Figure 12). Downstream-moving targets were more evenly distributed between the falling and rising tide stages for both runs.

Table 5.—Percentage of filtered targets by tide stage and direction of travel for the 2007 early run (20 May–30 June).

2007 Early run	Total	Rising	Falling	Low
Upstream				
Row %	100.0%	15.5%	62.4%	22.1%
Column %	97.5%	94.0%	98.2%	98.2%
Downstream				
Row %	100.0%	38.5%	45.2%	16.3%
Column %	2.5%	6.0%	1.8%	1.8%

Note: Test for independence: chi-square = 155.27, df = 2, $P < 0.0001$.

Table 6.—Percentage of filtered targets by tide stage and direction of travel for the 2007 late run (1 July–4 August).

2007 Late run	Total number of fish	Rising	Falling	Low
Upstream				
Row %	100.0%	21.6%	62.9%	15.5%
Column %	96.8%	94.3%	97.7%	96.5%
Downstream				
Row %	100.0%	39.2%	43.9%	16.9%
Column %	3.2%	5.7%	2.3%	3.5%

Note: Test for independence: chi-square = 273.51, df = 2, $P < 0.0001$.

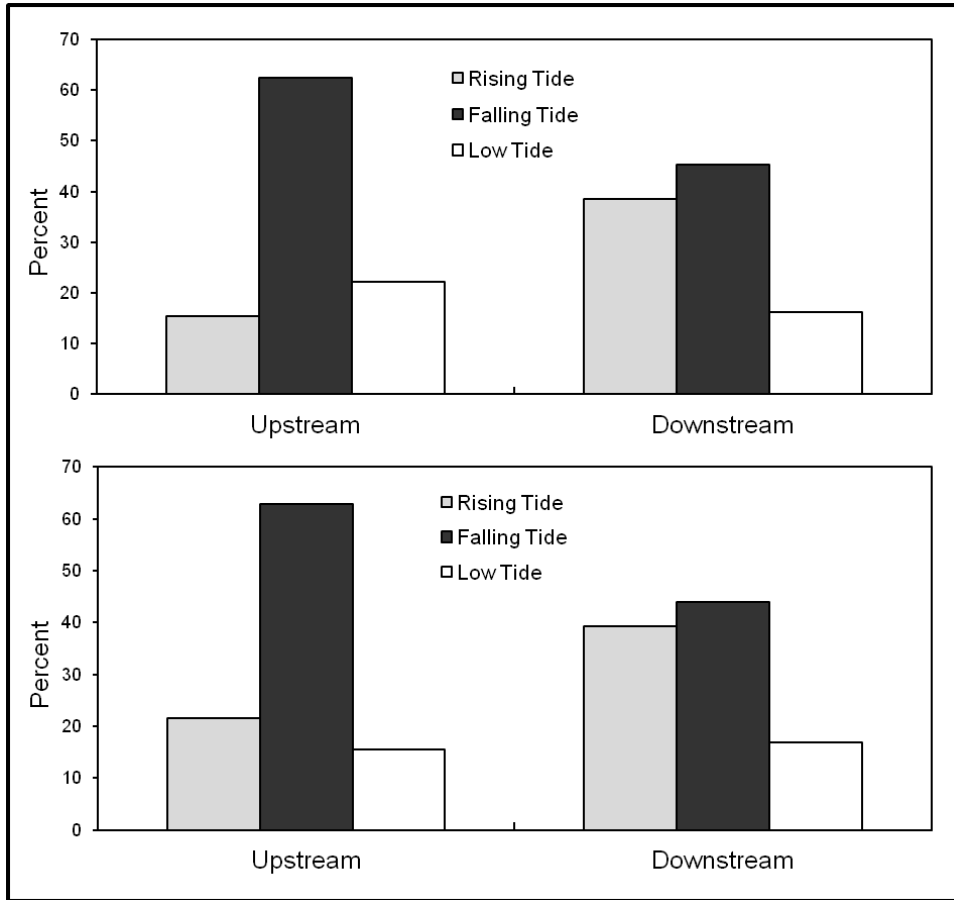


Figure 12.-Percentage of upstream and downstream moving filtered targets by tide stage for the early (top) and late (bottom) runs, Kenai River, 2007.

Note: Data have been filtered by range (distance from transducer) and target strength criteria.

Spatial Distribution

Distribution by Bank

During the early run, more upstream-moving filtered targets were observed on the left bank than on the right bank (Table 7). During the late run, more upstream moving targets were observed on the right bank than on the left bank (Table 8).

Table 7.-Percentage of filtered targets by riverbank and direction of travel for the 2007 early run (20 May–30 June).

Bank	Upstream	Downstream	Upstream and Downstream
Right	38%	70%	38%
Left	62%	30%	62%
Total	100%	100%	100%

Table 8.—Percentage of filtered targets by riverbank and direction of travel for the 2007 late run (1 July–4 August).

Bank	Upstream	Downstream	Upstream and Downstream
Right	53%	51%	28%
Left	47%	49%	72%
Total	100%	100%	100%

Distribution by Range¹⁵

During the early run, upstream-moving filtered targets on the left bank were distributed throughout the insonified range, whereas downstream-moving targets were concentrated further away from the riverbank near the end of the insonified range (Figure 13). Upstream- and downstream-moving filtered targets on the right bank were distributed throughout the range, but upstream-moving filtered targets exhibited peaks in passage near the end of the insonified range (Figure 13).

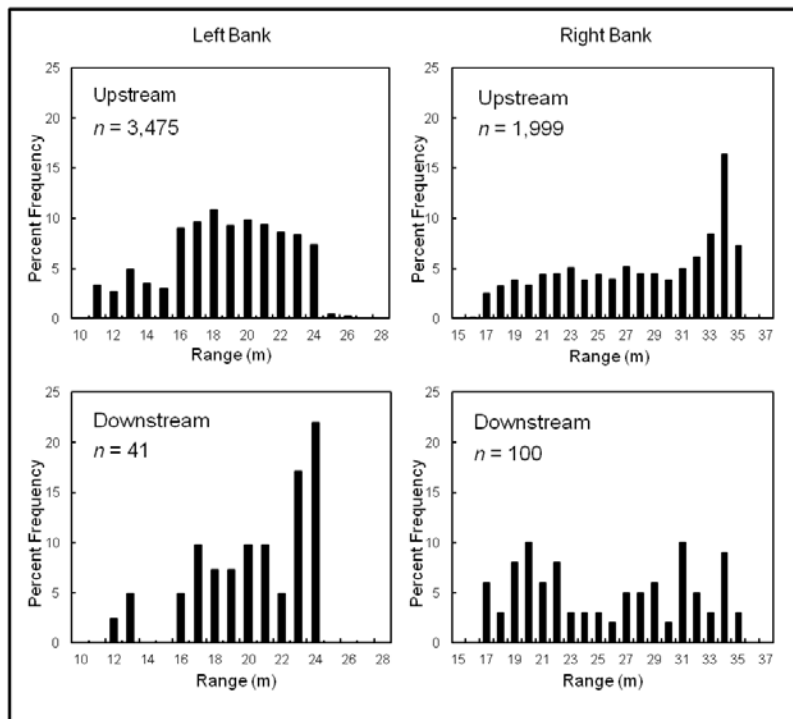


Figure 13.—Standardized distance from transducer (range) of early-run upstream and downstream moving filtered targets by bank, Kenai River, 2007.

Note: Data have been filtered by range and target strength criteria.

¹⁵ Because transducers were moved throughout the season in response to changing water levels (Figure 4), range measurements were standardized (Figures 12–15) to reflect distance from a fixed geographic reference point (see Methods). Hence, the left side of the distributions (in Figures 12–15) reflects the combined effects of range thresholds and the geographic standardization.

During the late run, upstream-moving filtered targets on both banks were relatively evenly distributed throughout the insonified range (Figure 14). Downstream-moving filtered targets on both banks exhibited peaks near the end of the insonified range (Figure 14).

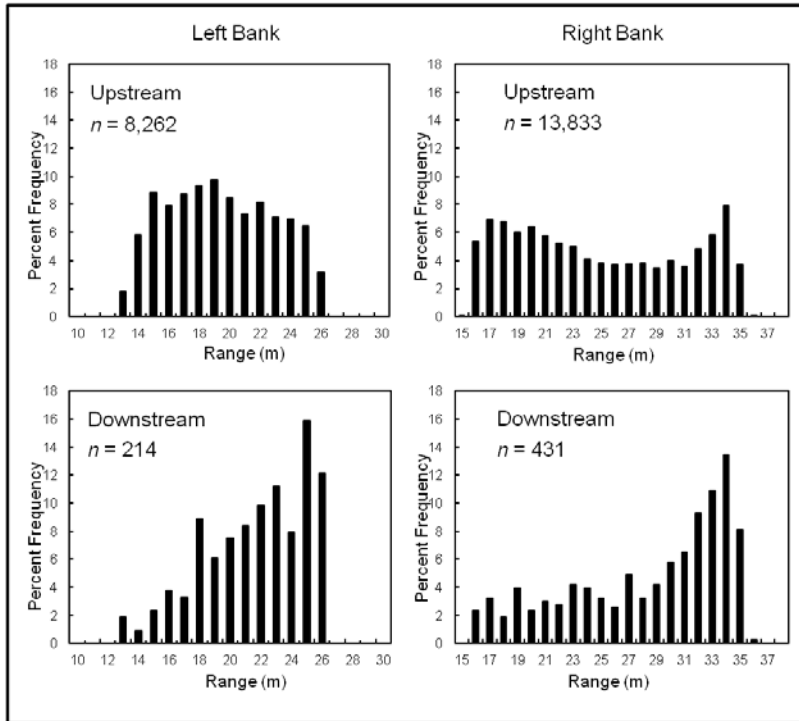


Figure 14.–Standardized distance from transducer (range) of late-run upstream and downstream moving filtered targets by bank, Kenai River, 2007.

Note: Data have been filtered by range and target strength criteria.

The effect of tide stage on the range distribution (distance from shore) of filtered targets on the left bank was small during both the early and late runs (Figures 15 and 16). Range distribution was mostly uniform for all tide stages. Tide stage appeared to have more effect on the right bank. The falling and low tide stages exhibited large peaks in distribution whereas the rising tide stage exhibited a more uniform distribution during both runs (Figures 15 and 16).

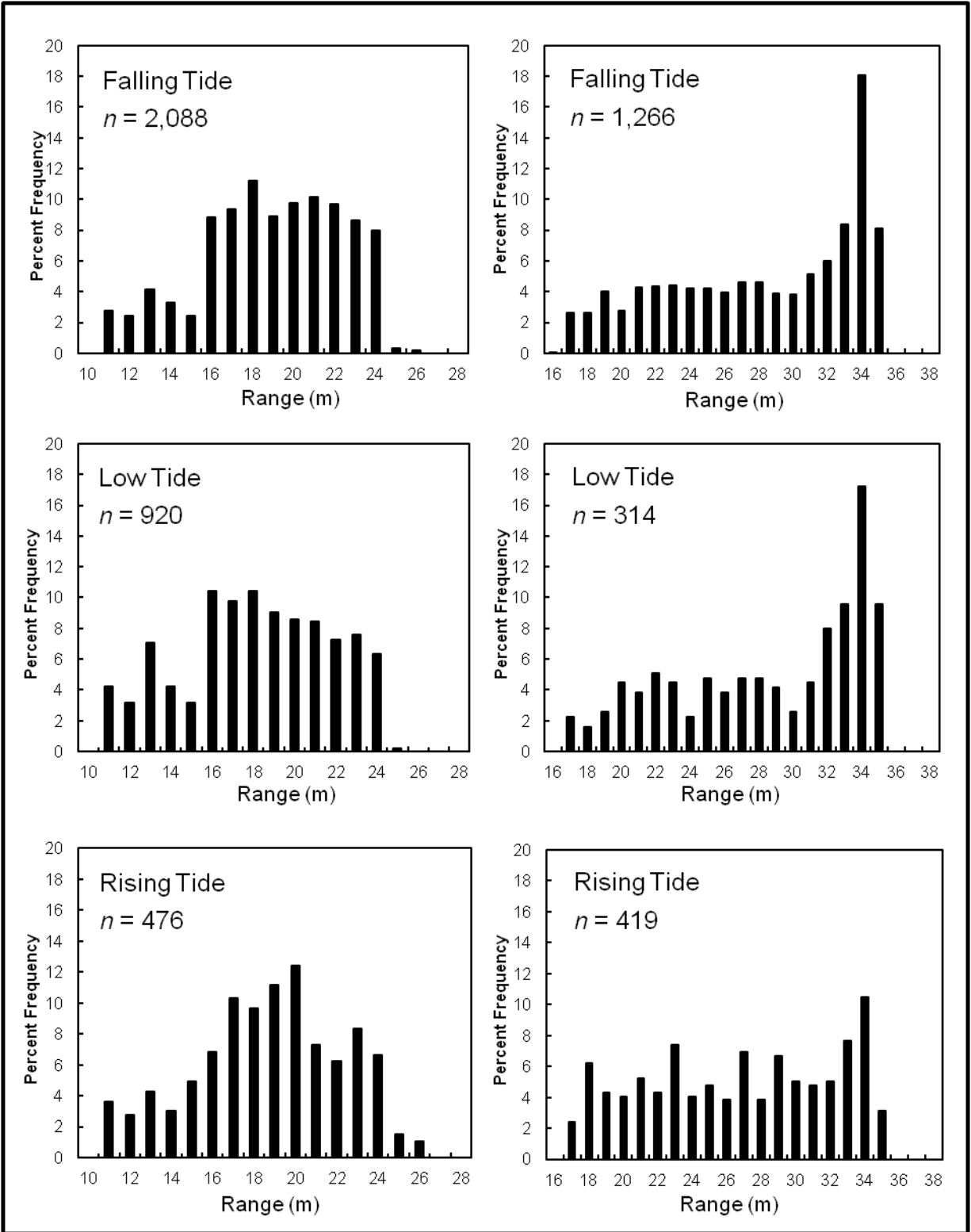


Figure 15.—Standardized distance from transducer (range) of early-run upstream moving filtered targets by tide stage and bank, Kenai River, 2007.

Note: Data have been filtered by range and target strength criteria.

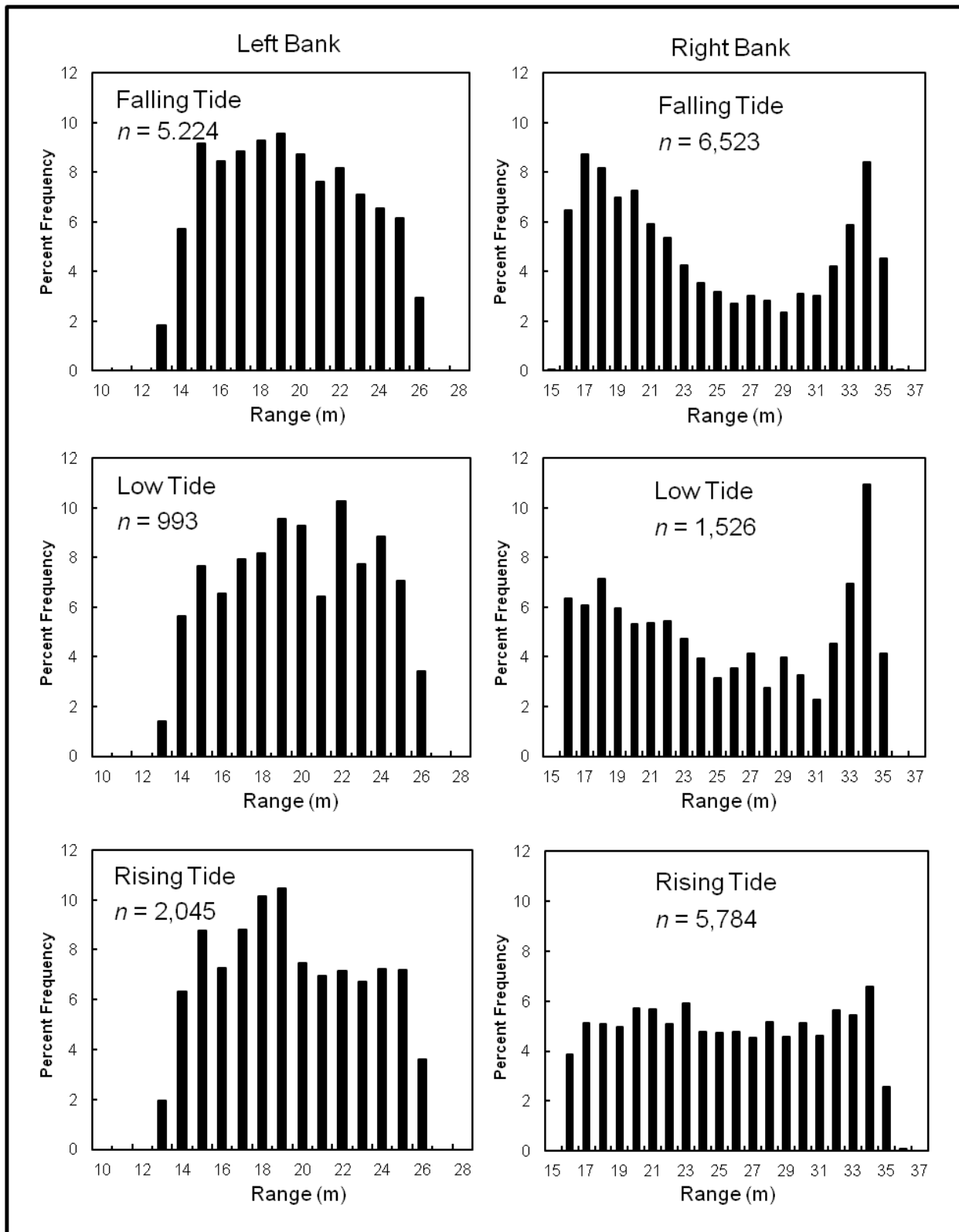


Figure 16.—Standardized distance from transducer (range) of late-run upstream moving filtered targets by tide stage and bank, Kenai River, 2007.

Note: Data have been filtered by range and target strength criteria.

Distribution by Vertical Position

Although filtered targets were generally bottom-oriented during both the early and late runs, vertical distribution did vary by direction of travel, tide stage, and run (Appendices H1 and H2). During the early run, 93% of the upstream-moving filtered targets on the left bank and 74% on the right bank were on or below the acoustic axis (Figure 17). Seventy-eight percent of downstream-moving filtered targets on the left bank and 64% on the right bank were on or below the acoustic axis (Figure 17). Upstream moving targets on the left bank (mean = -0.53° , SD = 0.38, $N = 3,475$) traveled lower ($t = 1.68$, $P = 0.03$) in the water column than downstream targets (mean = -0.38° , SD = 0.51, $N = 41$). There was no significant difference ($t = 1.17$, $P = 0.12$) between the vertical position of upstream-moving filtered targets (mean = -0.08° , SD = 0.32, $N = 1,999$) and downstream-moving filtered targets (mean = -0.04° , SD = 0.33, $N = 100$) on the right bank. On both banks, upstream-moving filtered targets were distributed slightly higher in the water column during rising tides (Figure 18).

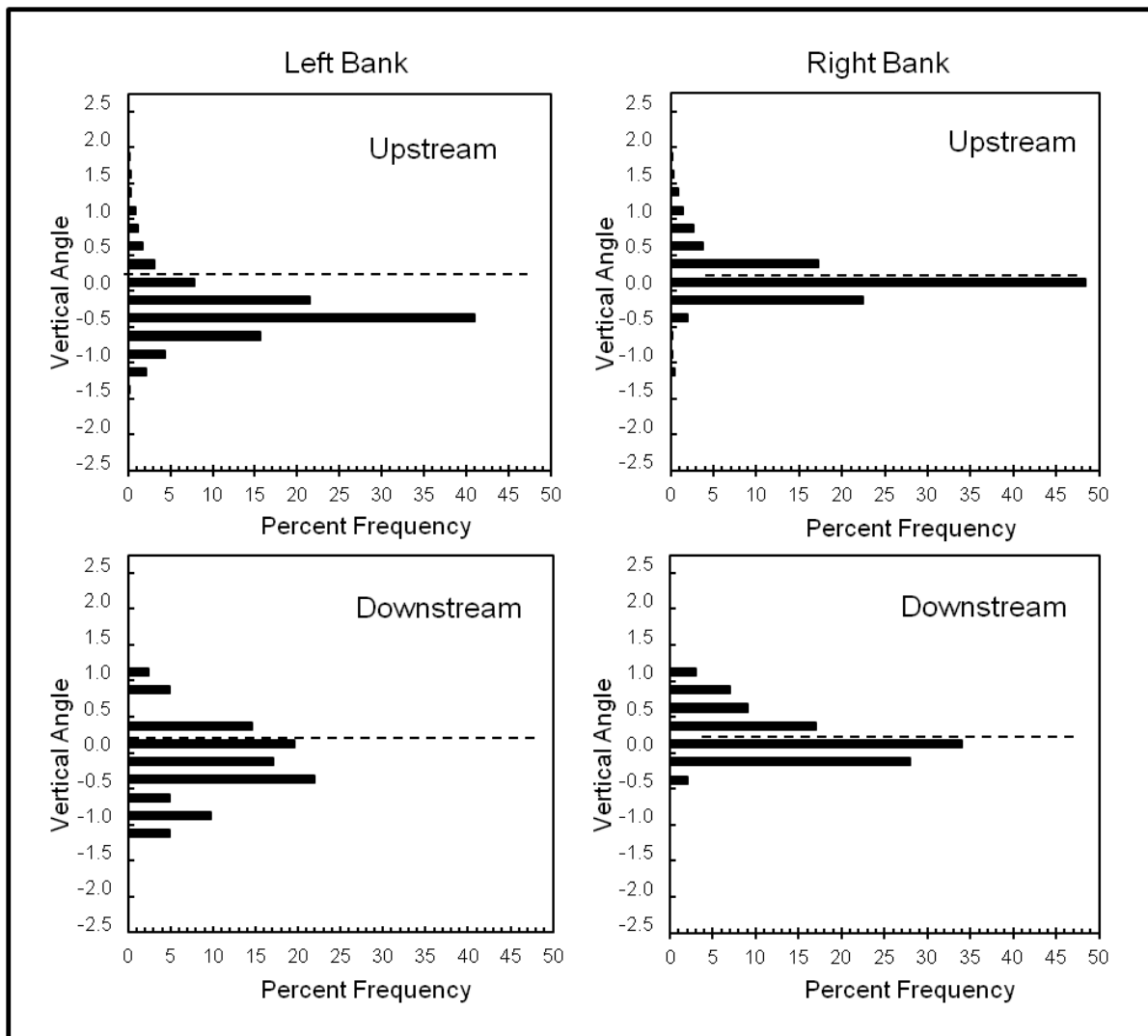


Figure 17.–Vertical distributions above and below the acoustic axis of early-run upstream and downstream moving filtered targets by bank, Kenai River, 2007.

Note: Data have been filtered by range (distance from transducer) and target strength criteria. Acoustic axis = 0.0.

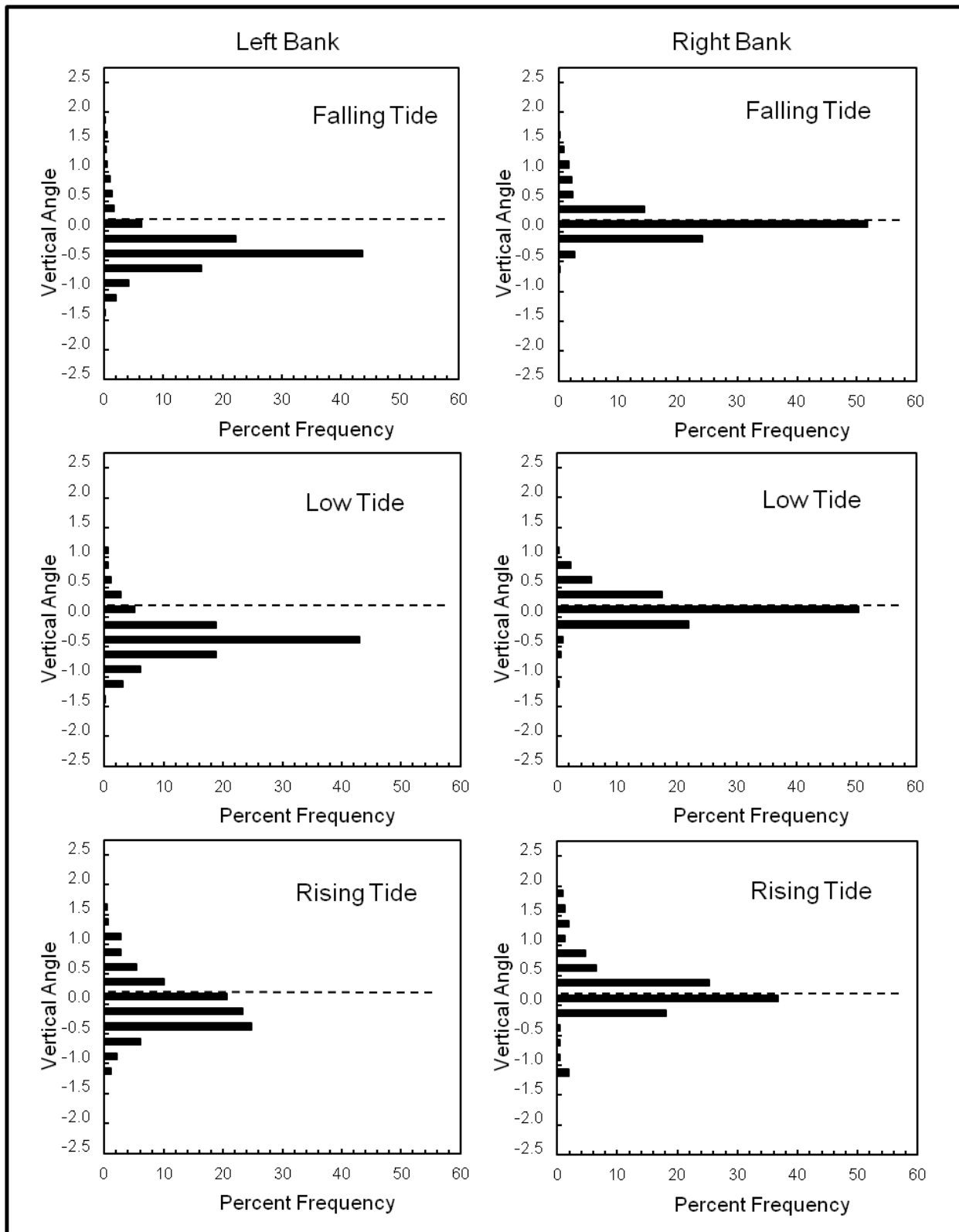


Figure 18.—Vertical distributions above and below the acoustic axis of early-run upstream moving filtered targets by tide stage and bank, Kenai River, 2007.

Note: Data have been filtered by range (distance from transducer) and target strength criteria. Acoustic axis = 0.0.

During the late run, 87% of upstream-moving filtered targets on the left bank and 64% on the right bank were on or below the acoustic axis (Figure 19). Seventy-five percent of downstream-moving filtered targets on the left bank and 52% on the right bank were on or below the acoustic axis (Figure 19). Upstream-moving filtered targets on the left bank (mean = -0.38° , SD = 0.37, $N = 8,262$) were lower ($t = 4.68$, $P < 0.001$) in the water column than downstream-moving filtered targets (mean = -0.24° , SD = 0.46, $N = 214$). Similarly, upstream-moving filtered targets on the right bank (mean = -0.12° , SD = 0.32, $N = 13,833$) traveled lower ($t = 6.33$, $P < 0.001$) in the water column than downstream-moving filtered targets (mean = -0.00° , SD = 0.36, $N = 431$). Vertical distribution of upstream-moving targets was slightly higher during the rising tide on both banks (Figure 20).

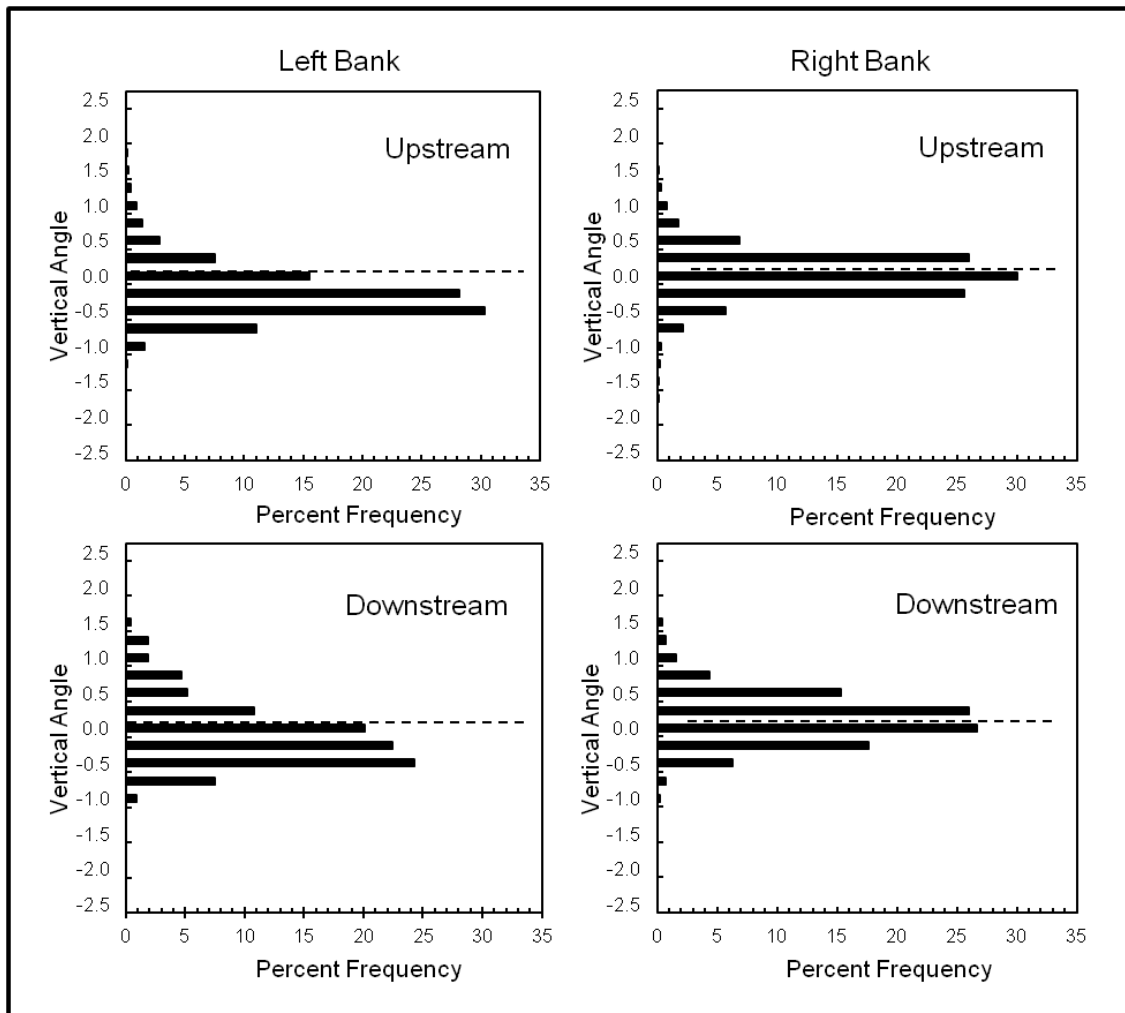


Figure 19.—Vertical distributions above and below the acoustic axis of late-run upstream and downstream moving filtered targets by bank, Kenai River, 2007.

Note: Data have been filtered by range (distance from transducer) and target strength criteria. Acoustic axis = 0.0.

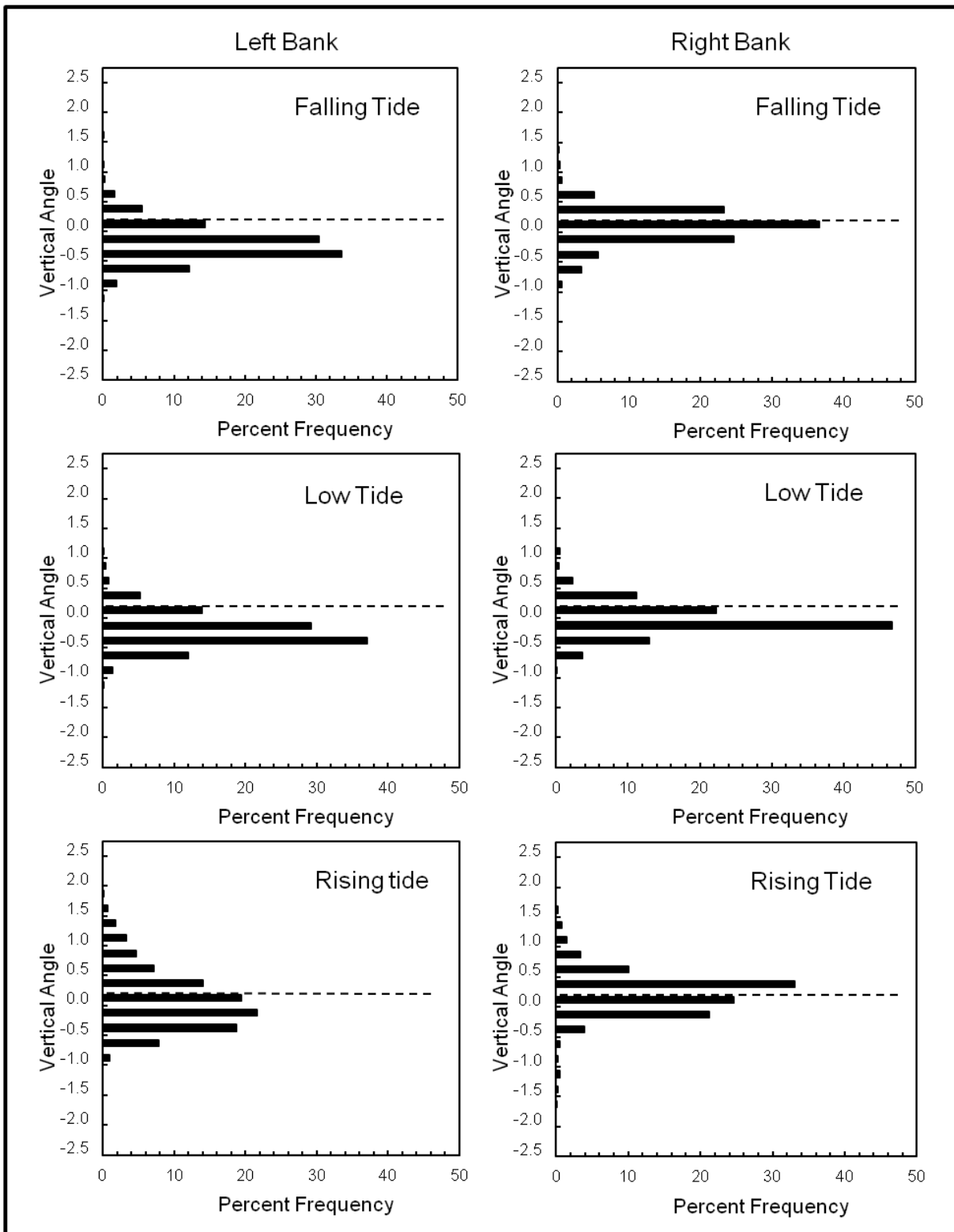


Figure 20.—Vertical distributions above and below the acoustic axis of late-run upstream moving filtered targets by tide stage and bank, Kenai River, 2007.

Note: Data have been filtered by range (distance from transducer) and target strength criteria. Acoustic axis = 0.0.

Target Strength

Target strength distributions varied by bank, direction of travel, and run. Mean target strength estimates for all upstream moving targets (unfiltered) during both runs were similar between the left and right banks (Figures 21 and 22). Mean target strength of all upstream and downstream targets varied more on the right bank than on the left bank.

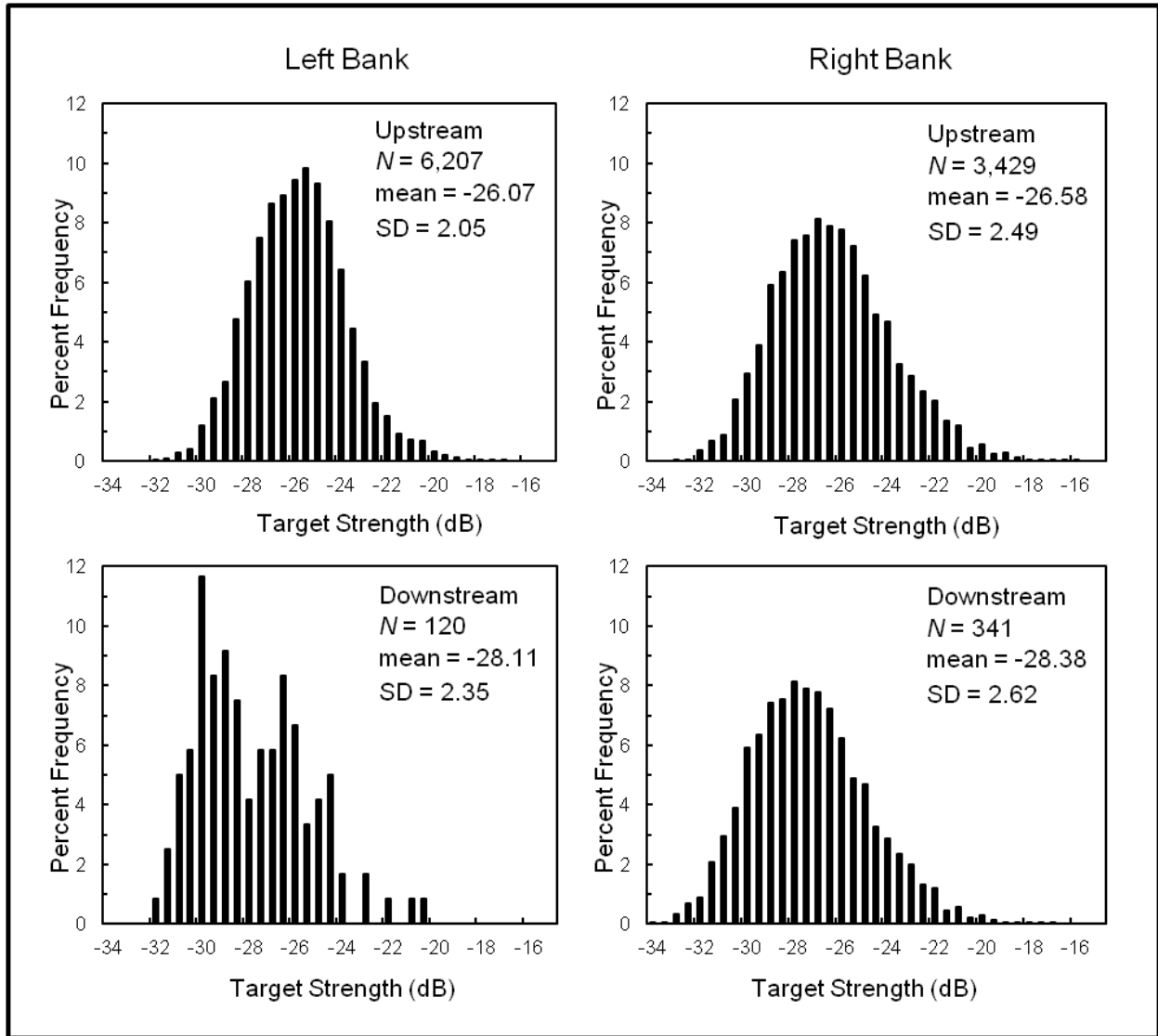


Figure 21.—Early-run target strength (acoustic size) for all upstream and downstream moving targets by bank, Kenai River, 2007.

Note: Data have not been filtered by range (distance from transducer) and target strength criteria.

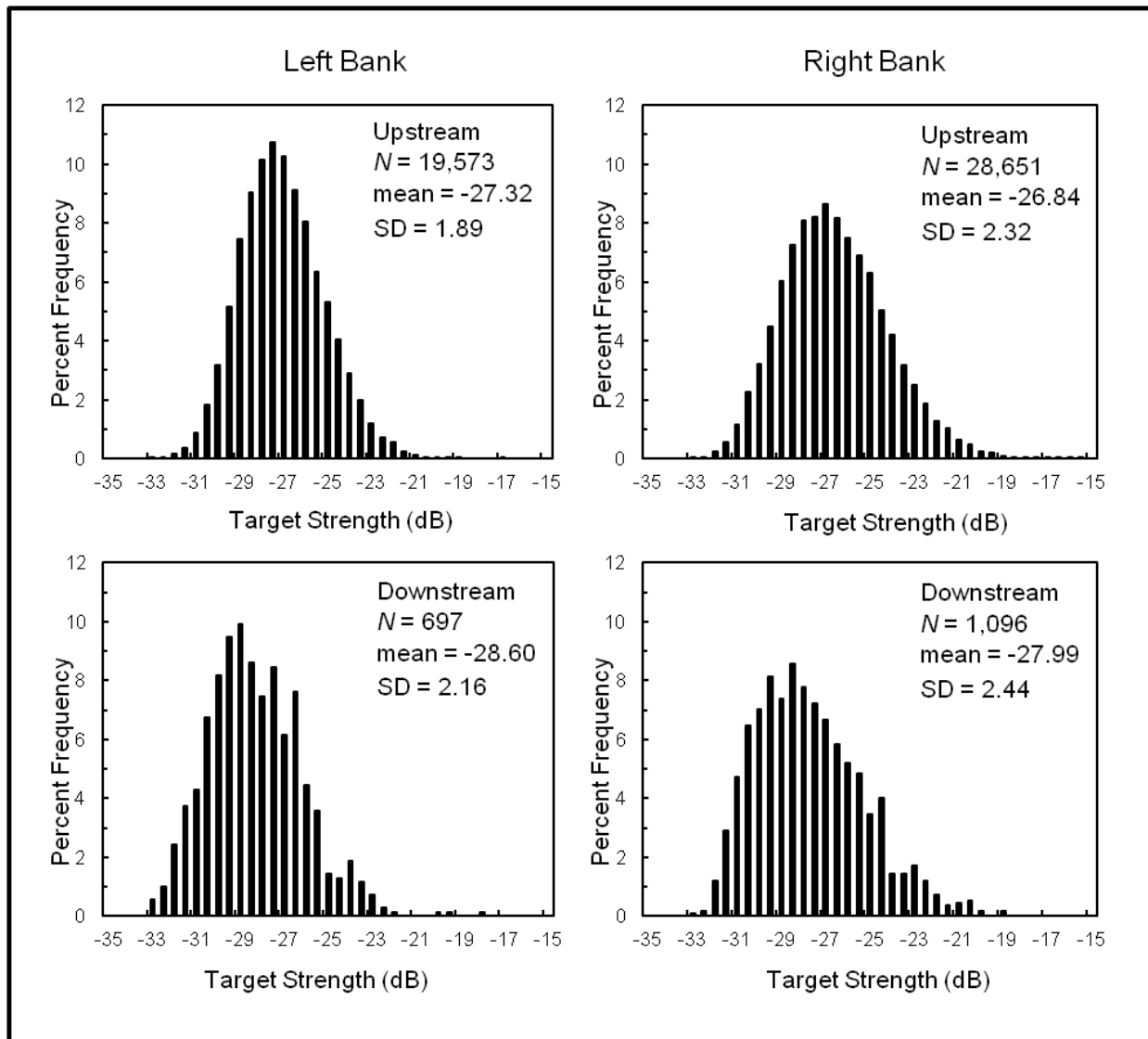


Figure 22.—Late-run target strength (acoustic size) for all upstream and downstream moving targets by bank, Kenai River, 2007.

Note: Data have not been filtered by range (distance from transducer) and target strength criteria.

During the early run on the left bank, mean target strength of filtered targets was similar ($t = -0.83$, $P = 0.21$) among upstream and downstream targets (Table 9). Mean target strength variability was lower for upstream-moving filtered targets ($F = 1.45$, $P = 0.03$). On the right bank, mean target strength was slightly higher ($t = -2.03$, $P = 0.02$) among upstream-moving filtered targets than among downstream-moving filtered targets. Mean target strength variability was similar ($F = 1.13$, $P = 0.19$) among upstream and downstream filtered targets (Table 9).

During the late run on the left bank, mean target strength of filtered targets was similar ($t = -1.62$, $P = 0.05$) among upstream and downstream targets (Table 9). Mean target strength variability was lower for upstream-moving filtered targets ($F = 1.22$, $P > 0.02$). On the right bank during the late run, mean target strength of filtered targets was higher ($t = -3.13$, $P = 0.001$) among

upstream-moving targets, and mean target strength variability was similar ($F = 0.95$, $P = 0.26$; Table 9).

Table 9.—Mean target strength (dB) for upstream and downstream moving filtered targets by riverbank during the early (20 May–30 June) and late (1 July–4 August) runs, 2007.

Location	Upstream mean target strength			Downstream mean target strength		
	(dB)	SD	<i>N</i>	(dB)	SD	<i>N</i>
<u>Early Run</u>						
Left Bank	-25.64	1.46	3,475	-25.87	1.76	41
Right Bank	-25.36	2.00	1,999	-25.77	2.10	100
<u>Late Run</u>						
Left Bank	-26.22	1.33	8,262	-26.38	1.46	214
Right Bank	-25.49	1.83	13,833	-26.77	1.78	431

TS-Based Estimates of Chinook Salmon Passage

Daily TS-based estimates of Chinook salmon passage were generated for 20 May through 4 August. A total of 550 hours of acoustic data were processed from the right bank and 607 hours from the left bank during the 77-day season. This represented 30% of the total available sample time (on average in a 24-hour period) for the right bank and 33% for the left bank.

Estimated upstream¹⁶ Chinook salmon passage from 20 May to 4 August was 58,883 (SE = 741), including 15,904 (SE = 285) early-run fish and 42,979 (SE = 684) late-run fish (Tables 7, 8, 10, and 11). Estimated early-run passage for 16 May to 30 June was 16,217 (SE = 403) fish. Peak daily passage during the early run occurred on 8 June; 50% of the run passed by 12 June (Figure 23). Early run escapement timing was similar to historic mean escapement timing (Figure 23 and Appendix I1). Peak daily passage during the late run occurred on 25 July; 50% of the late run passed by 22 July (Figure 24). Timing of the late run was late compared to historic mean escapement timing (Figure 24 and Appendix I2).

¹⁶ Due to our inability to accurately differentiate between debris and downstream moving fish, only upstream moving targets were used to produce the upstream passage estimate (i.e. no adjustments were made for downstream passage).

Table 10–Daily upstream Chinook salmon passage estimates, early run, 2007.

Date	Left Bank	Right Bank	Daily Total	Cumulative Total
16-May	-	-	62 ^a	62
17-May	-	-	75 ^a	137
18-May	-	-	84 ^a	221
19-May	-	-	92 ^a	313
20-May	18	0	18	331
21-May	39	21	60	391
22-May	42	24	66	457
23-May	30	21	51	508
24-May	52	39	91	599
25-May	42	46	88	687
26-May	66	6	72	759
27-May	39	42	81	840
28-May	78	39	117	957
29-May	111	33	144	1,101
30-May	134	30	164	1,265
31-May	168	84	252	1,517
1-Jun	194	31	225	1,742
2-Jun	150	36	186	1,928
3-Jun	213	64	277	2,205
4-Jun	242	61	303	2,508
5-Jun	416	103	519	3,027
6-Jun	401	204	605	3,632
7-Jun	598	398	996	4,628
8-Jun	777	369	1,146	5,774
9-Jun	509	222	731	6,505
10-Jun	494	153	647	7,152
11-Jun	293	195	488	7,640
12-Jun	511	213	724	8,364
13-Jun	479	237	716	9,080
14-Jun	363	303	666	9,746
15-Jun	410	288	698	10,444
16-Jun	284	210	494	10,938
17-Jun	287	183	470	11,408
18-Jun	144	126	270	11,678
19-Jun	263	223	486	12,164
20-Jun	188	94	282	12,446
21-Jun	152	131	283	12,729
22-Jun	188	132	320	13,049
23-Jun	242	243	485	13,534
24-Jun	137	139	276	13,810
25-Jun	108	87	195	14,005
26-Jun	114	136	250	14,255
27-Jun	186	134	320	14,575
28-Jun	362	279	641	15,216
29-Jun	176	258	434	15,650
30-Jun	215	352	567	16,217
16 May–30 June Total	-	-	16,217	
20 May–30 June Total	9,915	5,989	15,904	

^a Extreme tides and debris prevented sampling 16–19 May. Daily passage for 16–19 May was estimated using total passage from 20 May to 30 June and the mean proportion of passage from 16 to 19 May for years 1988–2006.

Table 11.—Daily upstream Chinook salmon passage estimates, Kenai River sonar, late run, 2007.

Date	Left Bank	Right Bank	Daily Total	Cumulative Total
1-Jul	293	316	609	609
2-Jul	138	263	401	1,010
3-Jul	146	304	450	1,460
4-Jul	227	274	501	1,961
5-Jul	253	253	506	2,467
6-Jul	228	282	510	2,977
7-Jul	253	325	578	3,555
8-Jul	506	545	1,051	4,606
9-Jul	254	347	601	5,207
10-Jul	236	264	500	5,707
11-Jul	398	529	927	6,634
12-Jul	236	474	710	7,344
13-Jul	197	330	527	7,871
14-Jul	431	606	1,037	8,908
15-Jul	524	758	1,282	10,190
16-Jul	297	370	667	10,857
17-Jul	359	417	776	11,633
18-Jul	858	871	1,729	13,362
19-Jul	838	916	1,754	15,116
20-Jul	1,159	994	2,153	17,269
21-Jul	950	727	1,677	18,946
22-Jul	1,397	1,354	2,751	21,697
23-Jul	890	1,011	1,901	23,598
24-Jul	1,585	1,423	3,008	26,606
25-Jul	1,525	1,965	3,490	30,096
26-Jul	1,202	1,457	2,659	32,755
27-Jul	1,304	2,053	3,357	36,112
28-Jul	905	874	1,779	37,891
29-Jul	527	332	859	38,750
30-Jul	524	398	922	39,672
31-Jul	764	576	1,340	41,012
1-Aug	386	480	866	41,878
2-Aug	161	169	330	42,208
3-Aug	123	274	397	42,605
4-Aug ^a	149	225	374	42,979
Total	20,223	22,756	42,979	

^a Sampling was terminated on 4 August following three consecutive days of passage less than 1% of the cumulative passage.

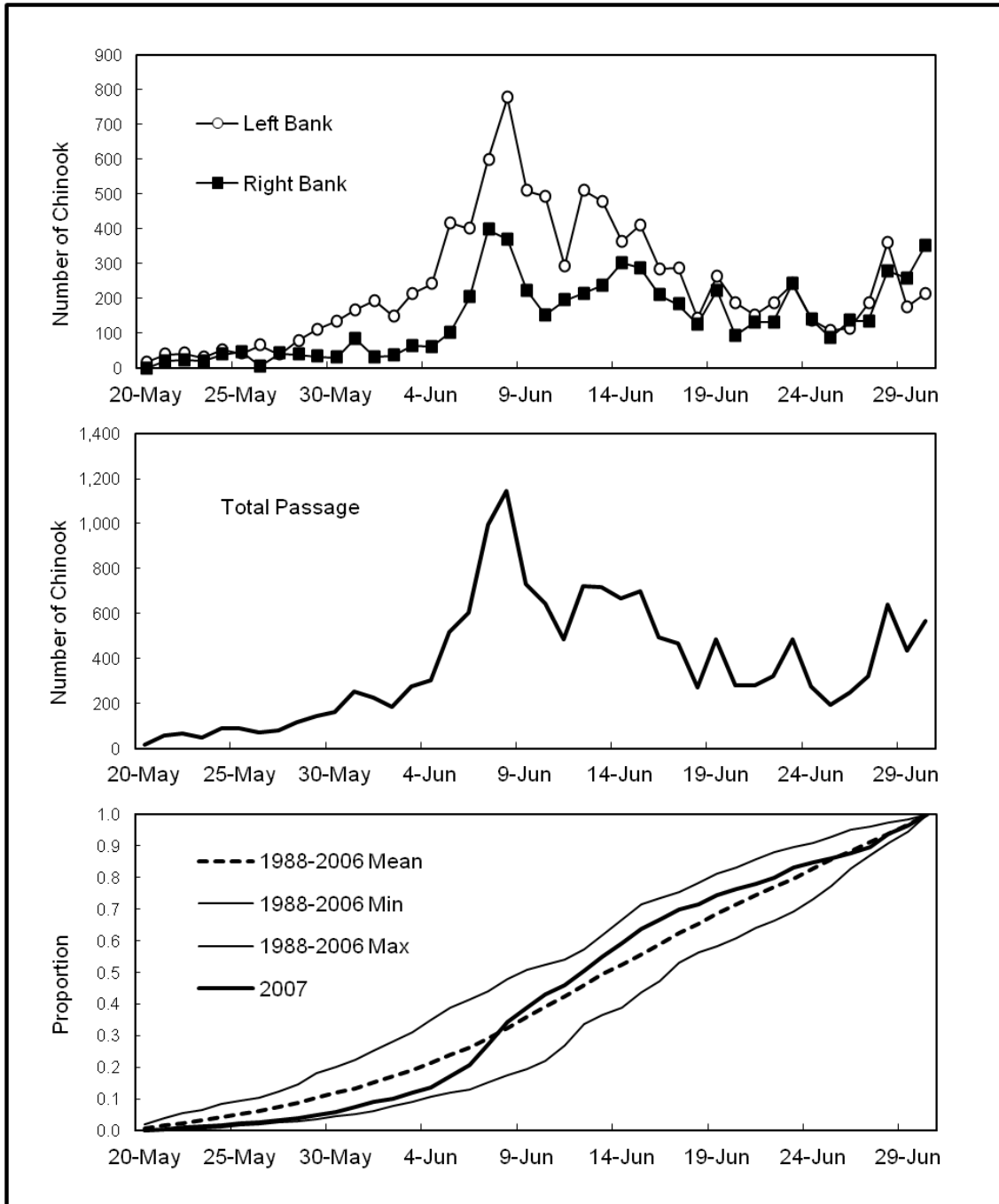


Figure 23.—Daily sonar passage estimates by bank (top), total passage (center), and historical cumulative proportions (bottom) for the Chinook salmon early run returning to the Kenai River, 2007.

Note: mean in bottom panel is based on estimates of total passage for 1988–1997 and upstream passage for 1998–2006

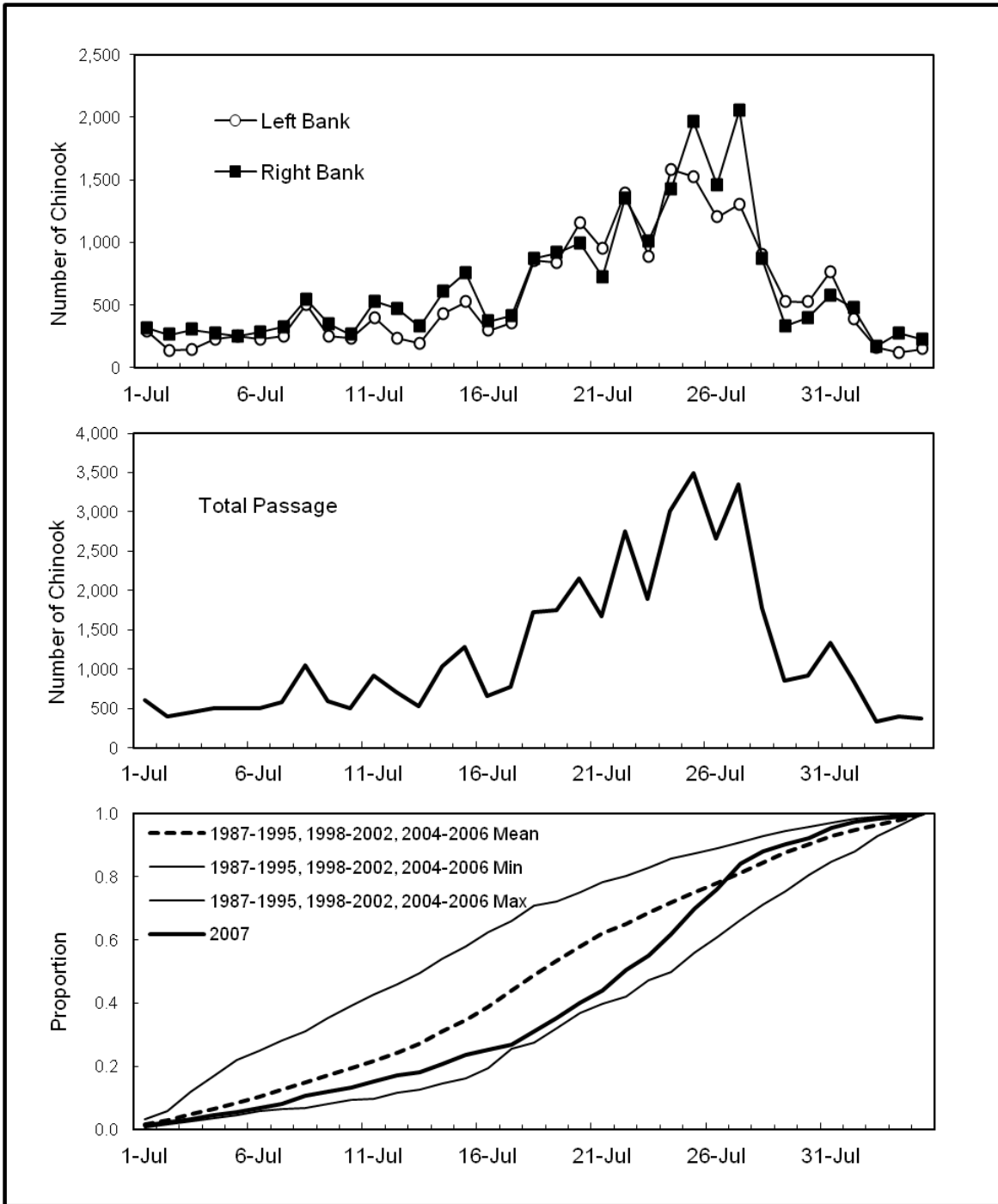


Figure 24.—Daily sonar passage estimates by bank (top), total passage (center), and historical cumulative proportions (bottom) for the Chinook salmon late run returning to the Kenai River, 2007.

Note: Mean in bottom panel is based on passage through 4 August and on estimates of total passage for 1987–1997 and upstream passage for 1998–2006.

Alternative Estimates of Chinook Salmon Passage

Net-apportioned estimates of upstream Chinook salmon passage in 2007 were 4,516 (SE = 299) fish for the early run and 29,455 (SE = 1516) fish for the late run (Appendices J1–J2). Peak daily passage based on net-apportioned estimates occurred on 9 June for the early run and 20 July for the late run.

Behavior-censored ELSD-based estimates of upstream Chinook salmon passage were 8,716 (SE = 350) fish for the early run and 28,915 (SE = 1168) fish for the late run (Appendices J1–J2). Peak daily passage based on behavior-censored ELSD-based estimates occurred on 8 June for the early run and 21 July for the late run.

DIDSON TESTING

Tethered Fish

The DIDSON supplied for this study was operable in “high-resolution mode” to only 23 m, rather than to 30 m as originally planned. However, we were able to collect data on 18 Chinook and sockeye salmon of varied lengths out to 21 m. The 23 m range limitation has since been resolved and a similarly configured DIDSON system should produce similarly high-resolution images over the maximum range allowed by high-frequency operation (~30 m).

Lengths of tethered fish measured manually from DIDSON images (DL) were highly correlated with the actual fish lengths (FL) (Figure 25; $R^2 = 0.90$, RMSE = 5.8 cm). FL alone explained 90% of the total variation in DL. There was no apparent effect of range on DIDSON estimates of fish length, given true length (Figure 26; $P > 0.20$). The intercept of the regression between DL and FL was positive, and the slope was slightly less than one (Figure 25). Thus there was a slight negative bias in the DIDSON length estimates for all fish over 17 cm. For example, the expected length measurement, based on DIDSON images, from a 40-cm sockeye salmon would be 38 cm; and the expected measurement from a 90-cm Chinook salmon would be 84 cm. More details on 2007 DIDSON tethered fish results can be found in Burwen et al. (2010).

Free-Swimming fish

Frequency distributions of DIDSON length measurements were consistent with direct measurements of fish sampled by an inriver netting program. We were able to successfully model DIDSON length data as a species/age mixture, using methods developed for split-beam ELSD data (Figure 27). By fitting such a model, it becomes possible to estimate the abundance of Chinook salmon of all sizes, including small Chinook salmon that cannot be individually distinguished from sockeye salmon. On 21 and 22 July, application of the DIDSON length mixture model resulted in estimates of 8.5% and 34% Chinook salmon, respectively, for fish passing 13–23 m from the left-bank tripod. The corresponding estimates derived from application of the ELSD mixture model to matching split-beam data were 13% and 32% Chinook salmon.

Efforts to detect, track, and measure fish using DIDSON software during periods of high fish passage were successful. To reveal any hardware or software problems related to high-density passage rates, DIDSON sampling was scheduled to occur from 16–23 July, 2007 during the anticipated peak of late-run Chinook salmon passage. Project personnel were able to track and measure free-swimming fish during some of the highest days of fish passage (e.g. 22 July was the 4th highest day of fish passage during the 2007 season with 2,751 fish).

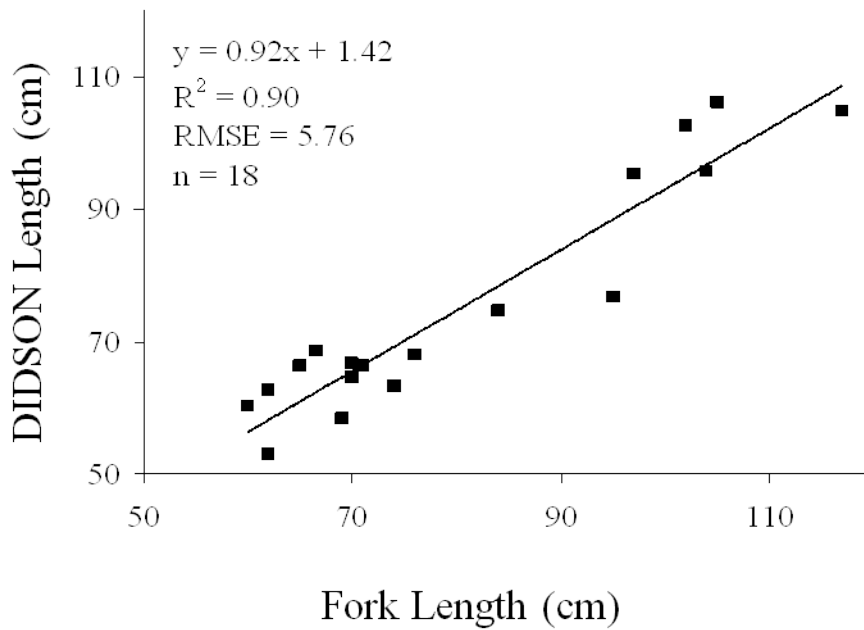


Figure 25.—DIDSON-based length (DL) measures with fork length (FL) for tethered fish insonified by the long-range DIDSON fitted with a high-resolution lens.

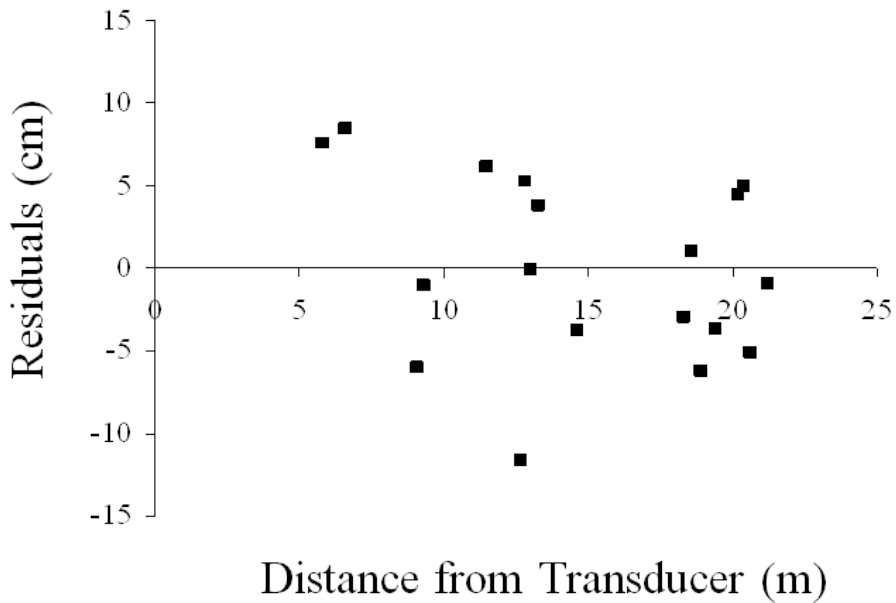


Figure 26.—Plot of residuals (observed-expected) with range of DIDSON-based length (DL) measures versus fork length (FL).

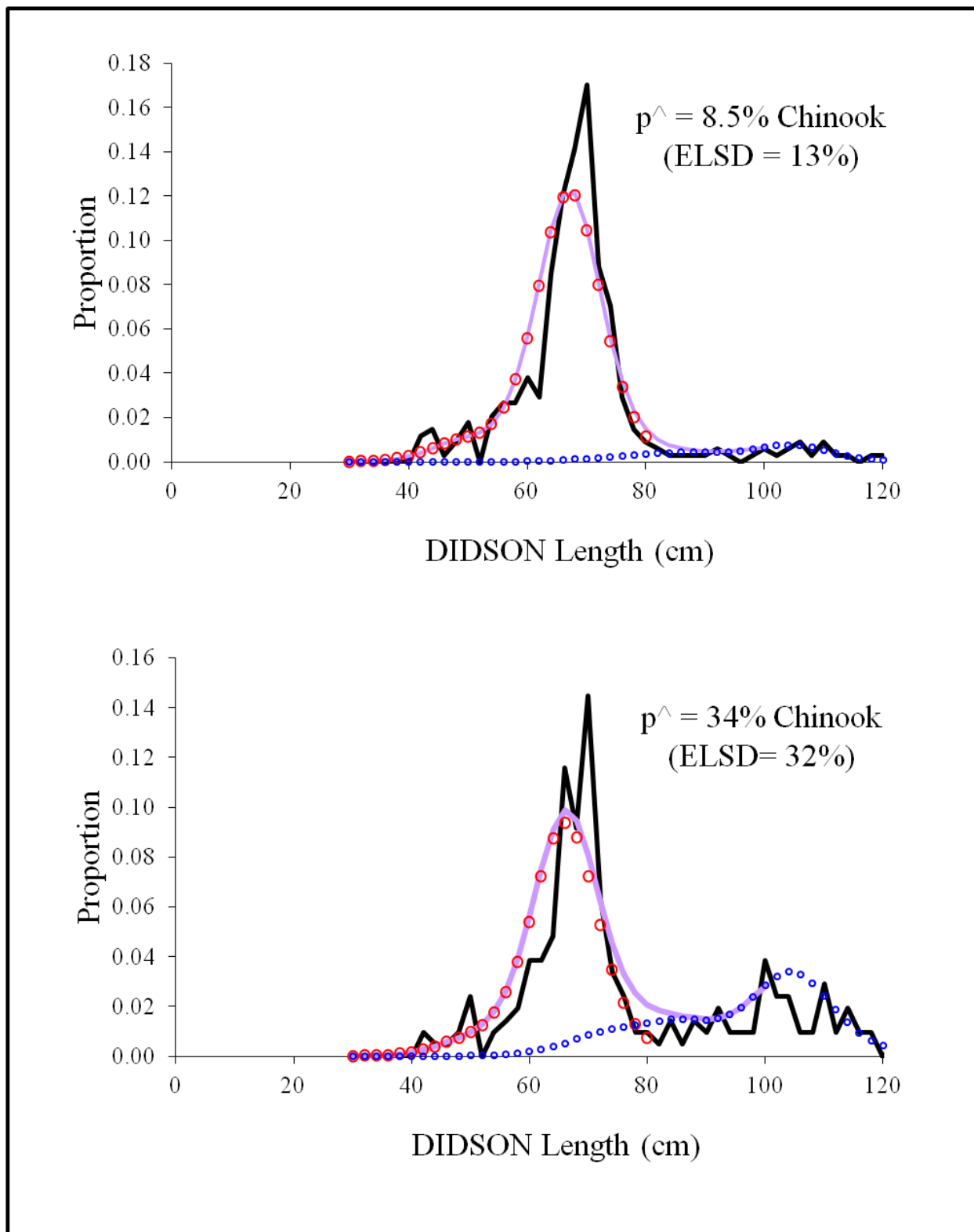


Figure 27.—Species / age mixture model fitted to observed DIDSON length frequency data (solid line), 21 July (top) and 22 July (bottom) 2007. Fitted sockeye and Chinook salmon length distributions (large and small circles) and fitted overall length distributions (shaded line) are also shown. Posterior medians of Chinook salmon proportion are given, with corresponding ELSD-based quantities in parentheses.

DISCUSSION

ACCURACY OF PASSAGE ESTIMATES

Sonar estimates of Chinook salmon passage are subject to potential biases from several sources, including 1) imperfect target detection (fish swimming above, below, or behind the effective beam; or not meeting the voltage threshold), 2) errors in target tracking (including direction of travel), and 3) inaccurate species discrimination. Bias from imperfect target detection and tracking are generally small, consistent, or negative (resulting in conservative estimates). For more details about target detection see Miller et al. (2007a). At present, we are more concerned about species discrimination errors, which could hypothetically occur in either direction, and which have the potential to be large in magnitude.

Through a series of research projects in the mid- and late-1990s, we learned that our current species discrimination algorithm, based on target strength and range thresholds, is less than satisfactory. Target strength is an imprecise predictor of fish size and species; many sockeye salmon exceed the -28 dB target strength threshold and many Chinook salmon do not (Burwen and Fleischman 1998). Although only a small fraction of sockeye salmon swim beyond our range thresholds, they can comprise more than 50% of mid-channel fish (Burwen et al. 1998). Under these circumstances range thresholds are ineffective and Chinook salmon passage can be overestimated.

Beginning in 2002, in response to these shortcomings, we began censoring hourly samples of TS-based estimates of Chinook salmon passage, and developed alternative net-apportioned (see page 21) and ELSD-based estimates (see page 21) of Chinook salmon passage.

Historically, we have also compared sonar estimates of Chinook salmon passage with several other indices of Chinook and sockeye salmon abundance to aid in evaluating accuracy of the sonar estimates. These indices include Chinook salmon catch per unit effort (CPUE) from the inriver netting program (see Introduction), Chinook salmon CPUE estimated by an onsite creel survey of the lower river sport fishery (Eskelin 2010), and daily estimates of sockeye salmon at the river mile-19 sonar site.

The river mile-19 sockeye salmon sonar site, located upriver of the Chinook salmon sonar site, provides an index of inriver sockeye salmon abundance. This sonar project is conducted from 1 July to mid August by ADF&G Division of Commercial Fisheries and targets sockeye salmon near shore (Westerman and Willette 2010). Although travel time between the river mile-8.5 Chinook salmon sonar site and the river mile-19 sockeye salmon sonar site varies, we believe it averages 1 to 2 days. This project identifies periods when sockeye salmon are abundant and when the potential for misclassifying sockeye as Chinook salmon may be high.

2007 Early Run

The 2007 early-run TS-based sonar passage estimate of 15,904 Chinook salmon¹⁷ (20 May–30 June; Table 10) was close to the 1988–2006 average of 16,480 (Appendix I1).

¹⁷ Fourteen of 2,016 hourly samples were censored to produce this estimate (Appendix D1). Inclusion of all available hourly samples, regardless of the presence of grouping behavior, would have generated an early-run estimate (20 May–30 June) of 16,295 (SE = 300).

Both alternative estimators (net-apportioned and ELSD-based) were lower than the TS-based estimate. The early-run total net-apportioned estimate was 4,516 (SE = 299), which is 72% less than the TS-based estimate of 15,904 (Appendix J1). The early-run total ELSD-based estimate of 8,716 (SE = 350) Chinook salmon was 45% lower than the TS-based estimate (Appendix J1). Daily Chinook salmon net-apportioned estimates were substantially lower than the TS-based estimates throughout most of the early run (Figure 28). ELSD-based estimates were also lower than TS-based estimates throughout much of the early run, particularly during the first half of June (Figure 28). Both alternative estimates have been lower than the TS-based estimate for the early run since 2005.

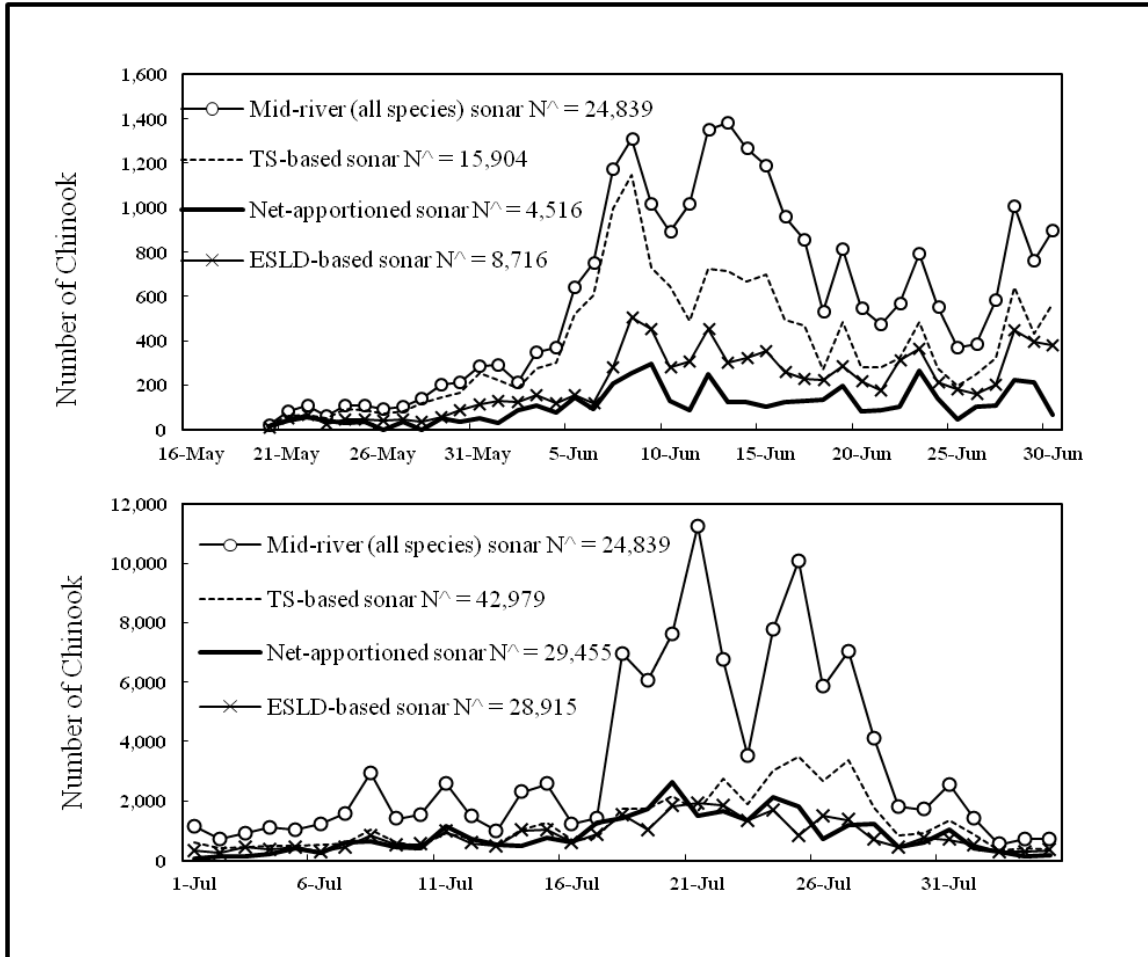


Figure 28.—Estimated upstream fish passage in mid-river (all species), TS-based (Chinook salmon only), net-apportioned (alternative estimate Chinook salmon only) and behavior-censored ELSD-based sonar (alternative estimate, Chinook salmon only), early- (20 May–30 June; top) and late-run (1 July–4 August; bottom), Kenai River, 2007.

Sonar passage estimates and gillnet CPUE tracked each other over the short term, but the relationship appeared to change over time (Figure 29). General trends in increasing and decreasing passage were observed from both methods, but the relative magnitude of the increases and decreases varied through time, especially during peak daily sonar passage that occurred from 7 June through 9 June. River discharge and water clarity did not completely explain these variations (Figure 29).

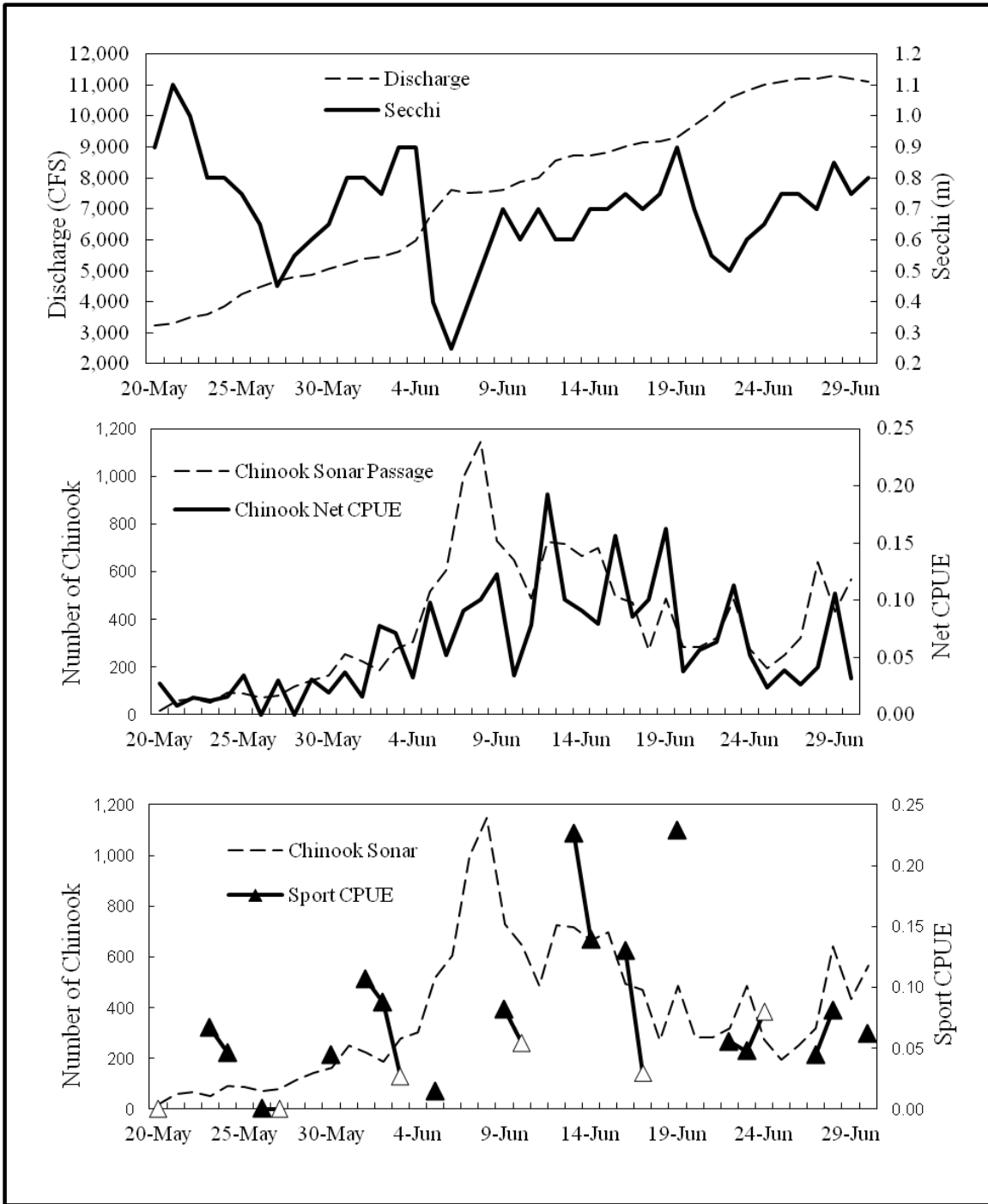


Figure 29.—Daily discharge rates collected at the Soldotna Bridge, Secchi disk readings taken at the sonar site, Chinook salmon TS-based sonar passage estimates, inriver gillnet CPUE, and Chinook salmon sport fish CPUE, early run (20 May–30 June), Kenai River, 2007.

Based on gillnet CPUE estimates, sockeye salmon were present at the sonar site throughout June, with the highest sockeye salmon CPUE estimates observed 11–16 June (Figure 30). Although peak sockeye salmon net CPUE did not coincide with peak Chinook salmon sonar passage, gillnet CPUE estimates illustrate increased sockeye salmon presence during early to mid June with the possibility of species misclassification during this time.

The above comparisons suggest that the TS-based estimator may have misclassified sockeye salmon as Chinook salmon during the first two weeks of June, probably resulting in an overestimate of Chinook salmon passage for the early run.

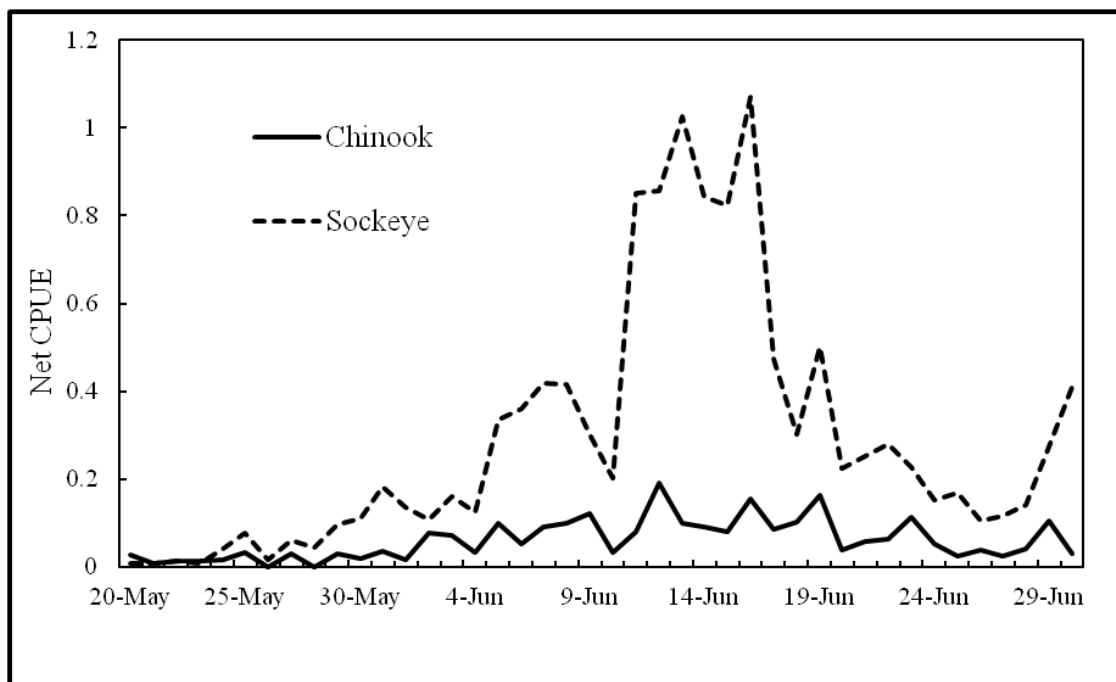


Figure 30.—Daily Chinook and sockeye salmon inriver gillnetting CPUE, early run (20 May–30 June), Kenai River, 2007.

2007 Late Run

The 2007 late-run TS-based passage estimate of 42,979 Chinook salmon¹⁸ through 4 August was close to the 1988–2006 average of 42,929 (Appendix I2).

Both alternative estimators (net-apportioned and ELSD-based) were lower than the TS-based estimate. The late-run net-apportioned sonar estimate of 29,455 (SE = 1,516) Chinook salmon was 31% lower than the TS-based sonar estimate (Appendix J2). Likewise, the cumulative censored ELSD estimate of 28,915 (SE = 1,168) Chinook salmon was 32% lower than the TS-based sonar estimate (Appendix J2). This is the first time that both alternative estimates have been lower than the TS-based estimate for the late run.

Daily Chinook salmon gillnet CPUE (Figure 31), net-apportioned sonar estimates (Figure 28), and censored ELSD estimates all indicated daily TS-based Chinook salmon sonar passage estimates may have been too high during the third week in July. Although the TS-based estimate peaked between 24 and 27 July, Chinook salmon gillnet CPUE decreased during this time (Figure 31). Similarly, the daily net-apportioned and ELSD-based estimates, both of which tracked the TS-based estimate closely during much of the late run, were significantly less than the TS-based estimate during the third week in July (Figure 28; Appendix J2).

¹⁸ Of 1,680 samples, 182 were censored to produce this estimate (Appendix D1). Inclusion of all available hourly samples, regardless of the presence of grouping behavior, would have generated a late-run estimate through 4 August of 68,266 (SE = 1,425).

Sockeye salmon gillnet CPUE and river mile-19 sockeye salmon sonar estimates (Figure 31) both indicate the presence of sockeye salmon at the Chinook salmon sonar site throughout the late run, with highest peaks in passage occurring during the last two weeks of July. Peak sockeye salmon gillnet CPUE did not always align with days of peak Chinook salmon sonar passage, but did confirm an increased presence of sockeye salmon throughout the second half of July.

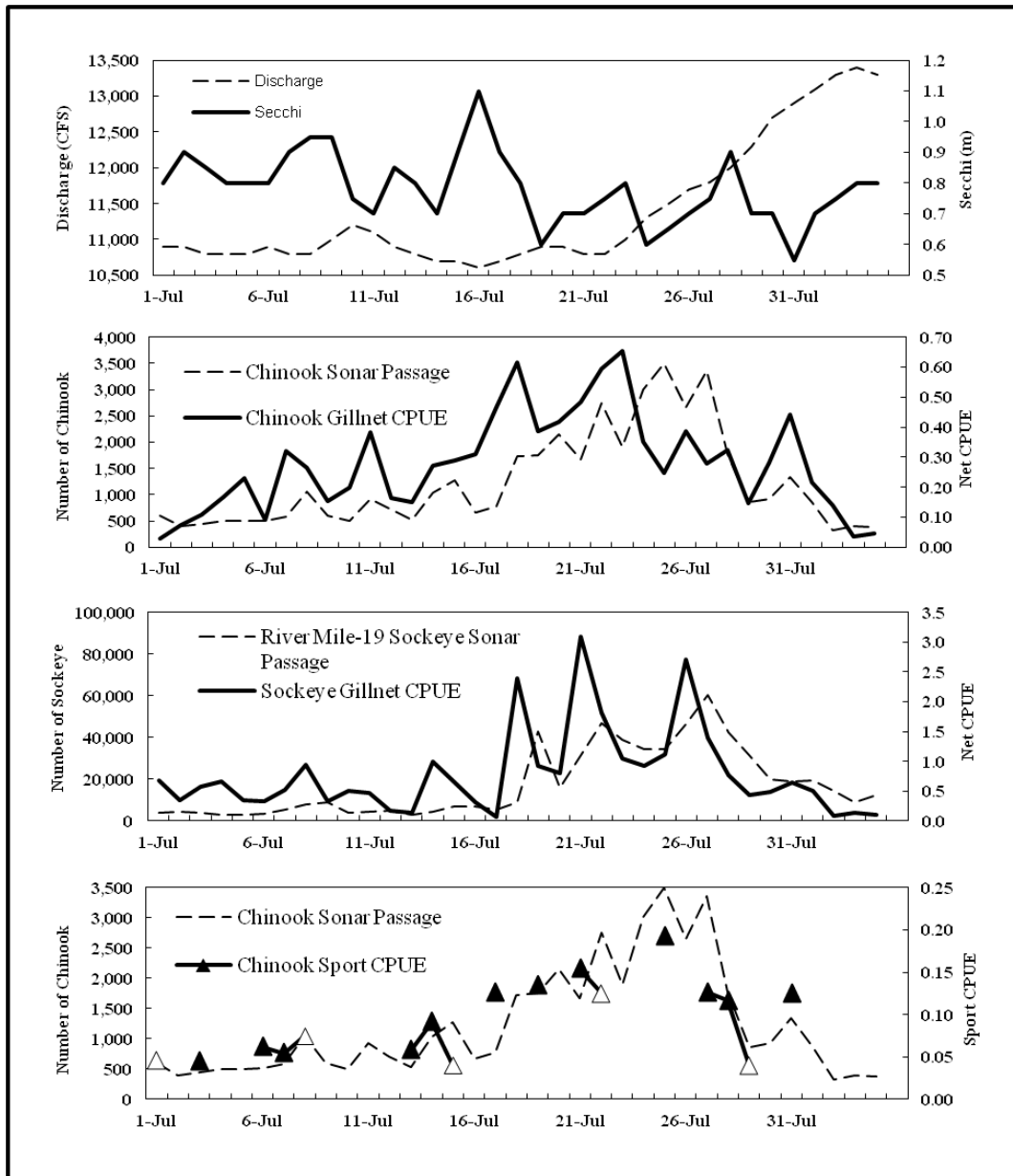


Figure 31.—Daily discharge rates collected at the Soldotna Bridge, Secchi disk readings taken at the sonar site, Chinook salmon sonar passage estimates, inriver Chinook salmon gillnet CPUE, river mile-19 sockeye salmon sonar passage estimates and gillnet CPUE, and Chinook salmon sport fish CPUE, late run (1 July–4 August), Kenai River, 2007.

Note: River discharge taken from USGS (2007). River mile-19 sockeye sonar estimates taken from Westerman and Willette (2010). Net CPUE and sport fish CPUE taken from Eskelin (2010). The Chinook salmon sport fishery was closed by regulation on 31 July, so sport fish CPUE data were not available after this date. Open triangles are days when only unguided anglers were allowed to fish.

SUMMARY AND OUTLOOK

Species discrimination continues to be the weak link in our ability to accurately estimate Chinook salmon passage in the Kenai River. Both alternative estimates, based on netting and echo length data, were lower than filtered TS-based sonar estimates for early and late runs in 2007. Note that early-run ELSD mixture model estimates presented herein differ¹⁹ from previously published estimates, having been filtered to remove fish swimming in close proximity to one another. Late-run ELSD mixture model estimates have not previously been published.

The results of DIDSON testing in 2007 were very promising. A prototype high-resolution lens attachment was successfully deployed with a long-range DIDSON, and accurate length measurements proved feasible to ranges of at least 21 m; estimates of species composition derived from DIDSON length data matched up well with ELSD-based estimates; and high passage rates did not present any special difficulty. DIDSON-derived fish measurements of fish behavior may also contain additional information on species identity (Mueller et al. 2010). With these advances, DIDSON technology now appears to be the best long-term solution to obtaining accurate estimates of Chinook salmon passage in the Kenai River. Acquisition of a DIDSON system and continued testing are planned for 2008.

ACKNOWLEDGMENTS

We would like to thank Mark Jensen for his assistance in overseeing the day-to-day operation of the project, for providing computer programming and networking support, and for his assistance in reducing and analyzing the data. We would also like to thank Linda Lowder, Mike Hopp, Andrew Pfeiffer, and Jordan Chilson for meticulously collecting the sonar data and for their high level of motivation throughout a long field season. We would like to express our gratitude to Melissa Brown with Hi-Lo Charters for allowing us to use her dock for project deployment and breakdown. Finally, thanks to Sport Fish Division staff in Soldotna who provided logistical support throughout the season.

REFERENCES CITED

- Alexandersdottir, M., and L. Marsh. 1990. Abundance estimates of the escapement of Chinook salmon into the Kenai River, Alaska, by analysis of tagging data, 1989. Alaska Department of Fish and Game, Fishery Data Series No. 90-55, Anchorage. <http://www.sf.adfg.state.ak.us/FedAidPDFs/fds90-55.pdf>
- Bernard, D. R., and P. A. Hansen. 1992. Mark-recapture experiments to estimate the abundance of fish: a short course given by the Division of Sport Fish, Alaska Department of Fish and Game in 1991. Alaska Department of Fish and Game, Special Publication No. 92-4, Anchorage. <http://www.sf.adfg.state.ak.us/FedAidPDFs/sp92-04.pdf>
- Bosch, D., and D. Burwen. 1999. Estimates of Chinook salmon abundance in the Kenai River using split-beam sonar, 1997. Alaska Department of Fish and Game, Fishery Data Series No. 99-3, Anchorage. <http://www.sf.adfg.state.ak.us/FedAidPDFs/fds99-03.pdf>
- Bosch, D., and D. Burwen. 2000. Estimates of Chinook salmon abundance in the Kenai River using split-beam sonar, 1998. Alaska Department of Fish and Game, Fishery Data Series No. 00-12, Anchorage. <http://www.sf.adfg.state.ak.us/FedAidPDFs/fds00-12.pdf>

¹⁹ Because of the filtering, the new estimates are smaller than the previous estimates.

REFERENCES CITED (Continued)

- Burger, C. V., R. L. Wilmot, and D. B. Wangaard. 1985. Comparison of spawning areas and times for two runs of Chinook salmon (*Oncorhynchus tshawytscha*) in the Kenai River, Alaska. *Canadian Journal of Fisheries and Aquatic Sciences* 42(4):693-700.
- Burwen, D., and D. Bosch. 1998. Estimates of Chinook salmon abundance in the Kenai River using split-beam sonar, 1996. Alaska Department of Fish and Game, Fishery Data Series No. 98-2, Anchorage. <http://www.sf.adfg.state.ak.us/FedAidPDFs/fds98-02.pdf>
- Burwen, D., J. Hasbrouck, and D. Bosch. 2000. Investigations of alternate sites for Chinook salmon sonar on the Kenai River. Alaska Department of Fish and Game, Fishery Data Series No. 00-43, Anchorage. <http://www.sf.adfg.state.ak.us/FedAidPDFs/fds00-43.pdf>
- Burwen, D. L., and D. E. Bosch. 1995a. Estimates of Chinook salmon abundance in the Kenai River using dual-beam sonar, 1993. Alaska Department of Fish and Game, Fishery Data Series No. 95-31, Anchorage. <http://www.sf.adfg.state.ak.us/FedAidPDFs/fds95-31.pdf>
- Burwen, D. L., and D. E. Bosch. 1995b. Estimates of Chinook salmon abundance in the Kenai River using dual-beam sonar, 1994. Alaska Department of Fish and Game, Fishery Data Series No. 95-38, Anchorage. <http://www.sf.adfg.state.ak.us/FedAidPDFs/fds95-38.pdf>
- Burwen, D. L., and D. E. Bosch. 1996. Estimates of Chinook salmon abundance in the Kenai River using split-beam sonar, 1995. Alaska Department of Fish and Game, Fishery Data Series No. 96-9, Anchorage. <http://www.sf.adfg.state.ak.us/FedAidPDFs/fds96-09.pdf>
- Burwen, D. L., D. E. Bosch, and S. J. Fleischman. 1995. Evaluation of hydroacoustic assessment techniques for Chinook salmon on the Kenai River using split-beam sonar. Alaska Department of Fish and Game, Fishery Data Series No. 95-45, Anchorage. <http://www.sf.adfg.state.ak.us/FedAidPDFs/fds95-45.pdf>
- Burwen, D. L., D. E. Bosch, and S. J. Fleischman. 1998. Evaluation of hydroacoustic assessment techniques for Chinook salmon on the Kenai River, 1995. Alaska Department of Fish and Game, Fishery Data Series No. 98-3, Anchorage. <http://www.sf.adfg.state.ak.us/FedAidPDFs/fds98-03.pdf>
- Burwen, D. L., and S. J. Fleischman. 1998. Evaluation of side-aspect target strength and pulse width as hydroacoustic discriminators of fish species in rivers. *Canadian Journal of Fisheries and Aquatic Sciences* 55(11):2492-2502.
- Burwen, D. L., S. J. Fleischman, and J. D. Miller. 2007. Evaluation of a dual-frequency imaging sonar for estimating fish size in the Kenai River. Alaska Department of Fish and Game, Fishery Data Series No. 07-44, Anchorage. <http://www.sf.adfg.state.ak.us/FedAidPDFs/fds07-44.pdf>
- Burwen, D. L., S. J. Fleischman, and J. D. Miller. 2010. Accuracy and precision of manual fish length measurements from DIDSON sonar images. *Transactions of the American Fisheries Society*, 139:1306-1314.
- Burwen, D. L., S. J. Fleischman, J. D. Miller, and M. E. Jensen. 2003. Time-based signal characteristics as predictors of fish size and species for a side-looking hydroacoustic application in a river. *ICES Journal of Marine Science* 60:662-668.
- Carlson, J. A., and M. Alexandersdottir. 1989. Abundance estimates of the escapement of Chinook salmon into the Kenai River, Alaska, by analysis of tagging data, 1988. Alaska Department of Fish and Game, Fishery Data Series No. 107, Juneau. <http://www.sf.adfg.state.ak.us/FedAidPDFs/fds-107.pdf>
- Cochran, W. G. 1977. *Sampling techniques*, 3rd edition. John Wiley and Sons, New York.
- Conrad, R. H. 1988. Abundance estimates of the escapement of Chinook salmon into the Kenai River, Alaska, by analysis of tagging data, 1987. Alaska Department of Fish and Game, Fishery Data Series No. 67, Juneau. <http://www.sf.adfg.state.ak.us/FedAidPDFs/fds-067.pdf>

REFERENCES CITED (Continued)

- Conrad, R. H., and L. L. Larson. 1987. Abundance estimates for Chinook salmon (*Oncorhynchus tshawytscha*) in the escapement into the Kenai River, Alaska, by analysis of tagging data, 1986. Alaska Department of Fish and Game, Fishery Data Series No. 34, Juneau. <http://www.sf.adfg.state.ak.us/FedAidPDFs/fds-034.pdf>
- Eggers, D. M. 1994. On the discrimination of sockeye and Chinook salmon in the Kenai River based on target strength determined with 420 kHz dual-beam sonar. Alaska Fishery Research Bulletin 1(2):125-139. Alaska Department of Fish and Game, Juneau.
- Eggers, D. M., P. A. Skvorc, and D. L. Burwen. 1995. Abundance estimate for Chinook salmon in the Kenai River using dual-beam sonar. Alaska Department of Fish and Game. Alaska Fishery Research Bulletin 2(1):1-22.
- Ehrenberg, J. E. 1983. A review of *in situ* target strength estimation techniques. FAO (Food and Agriculture Organization of the United Nations) Fisheries Report 300:85-90.
- Eskelin, A. 2007. Chinook salmon creel survey and inriver gillnetting study, lower Kenai River, Alaska, 2005. Alaska Department of Fish and Game, Fishery Data Series No. 07-87, Anchorage. <http://www.sf.adfg.state.ak.us/FedAidPDFs/fds07-87.pdf>
- Eskelin, A. 2010. Chinook salmon creel survey and inriver gillnetting study, lower Kenai River, Alaska, 2007. Alaska Department of Fish and Game, Fishery Data Series No. 10-63, Anchorage. <http://www.sf.adfg.state.ak.us/FedAidpdfs/FDS10-63.pdf>
- Fleischman, S. J., and D. L. Burwen. 2003. Mixture models for the species apportionment of hydroacoustic data, with echo-envelope length as the discriminatory variable. ICES Journal of Marine Science 60:592-598.
- Foote, K. G., and D. N. MacLennan. 1984. Comparison of copper and tungsten carbide calibration spheres. Journal of the Acoustical Society of America 75:612-616.
- Gamblin, M., L. E. Marsh, P. Berkahn, and S. Sonnichsen. 2004. Area management report for the recreational fisheries of the Northern Kenai Peninsula, 2000 and 2001. Alaska Department of Fish and Game, Fishery Management Report No. 04-04, Anchorage. <http://www.sf.adfg.state.ak.us/FedAidPDFs/fmr04-04.pdf>
- Gelman, A., J. B. Carlin, H. S. Stern, and D. B. Rubin. 2004. Bayesian Data Analysis, 3rd edition. Chapman and Hall, Boca Raton, Florida.
- Gilks, W. R., A. Thomas, and D. J. Spiegelhalter. 1994. A language and program for complex Bayesian modeling. The Statistician 43:169-178. <http://www.mrc-bsu.cam.ac.uk/bugs> Accessed 01/2010.
- Goodman, L. A. 1960. On the exact variance of products. Journal of the American Statistical Association 55:708-713.
- Hammarstrom, S. L., and J. J. Hasbrouck. 1998. Estimation of the abundance of late-run Chinook salmon in the Kenai River based on exploitation rate and harvest, 1996. Alaska Department of Fish and Game, Fishery Data Series No. 98-6, Anchorage. <http://www.sf.adfg.state.ak.us/FedAidPDFs/fds98-06.pdf>
- Hammarstrom, S. L., and J. J. Hasbrouck. 1999. Estimation of the abundance of late-run Chinook salmon in the Kenai River based on exploitation rate and harvest, 1997. Alaska Department of Fish and Game, Fishery Data Series No. 99-8, Anchorage. <http://www.sf.adfg.state.ak.us/FedAidPDFs/fds99-08.pdf>
- Hammarstrom, S. L., L. Larson, M. Wenger, and J. Carlon. 1985. Kenai Peninsula Chinook and coho salmon studies. Alaska Department of Fish and Game. Federal Aid in Fish Restoration. Annual Performance Report, 1984-1985, Project F-9-17(26)G-II-L, Juneau. [http://www.sf.adfg.state.ak.us/FedAidPDFs/FREDf-9-17\(26\)G-II-L.pdf](http://www.sf.adfg.state.ak.us/FedAidPDFs/FREDf-9-17(26)G-II-L.pdf)
- Hammarstrom, S. L., and L. L. Larson. 1986. Kenai River salmon escapement. Alaska Department of Fish and Game. Federal Aid in Fish Restoration, Annual Performance Report, 1985-1986, Project F-10-1, 27 (S-32-2), Juneau. [http://www.sf.adfg.state.ak.us/FedAidPDFs/FREDf-10-1\(27\)S-32-1,2,4,5.pdf](http://www.sf.adfg.state.ak.us/FedAidPDFs/FREDf-10-1(27)S-32-1,2,4,5.pdf)

REFERENCES CITED (Continued)

- Howe, A. L., G. Fidler, A. E. Bingham, and M. J. Mills. 1996. Harvest, catch, and participation in Alaska sport fisheries during 1995. Alaska Department of Fish and Game, Fishery Data Series No. 96-32, Anchorage. <http://www.sf.adfg.state.ak.us/FedAidPDFs/fds96-32.pdf>
- Howe, A. L., G. Fidler, and M. J. Mills. 1995. Harvest, catch, and participation in Alaska sport fisheries during 1994. Alaska Department of Fish and Game, Fishery Data Series No. 95-24, Anchorage. <http://www.sf.adfg.state.ak.us/FedAidPDFs/fds95-24.pdf>
- Howe, A. L., R. J. Walker, C. Olnes, K. Sundet, and A. E. Bingham. 2001a. Revised Edition. Harvest, catch, and participation in Alaska sport fisheries during 1996. Alaska Department of Fish and Game, Fishery Data Series No. 97-29 (revised), Anchorage. [http://www.sf.adfg.state.ak.us/FedAidPDFs/fds97-29\(revised\).pdf](http://www.sf.adfg.state.ak.us/FedAidPDFs/fds97-29(revised).pdf)
- Howe, A. L., R. J. Walker, C. Olnes, K. Sundet, and A. E. Bingham. 2001b. Revised Edition. Harvest, catch, and participation in Alaska sport fisheries during 1997. Alaska Department of Fish and Game, Fishery Data Series No. 98-25 (revised), Anchorage. [http://www.sf.adfg.state.ak.us/FedAidPDFs/fds98-25\(revised\).pdf](http://www.sf.adfg.state.ak.us/FedAidPDFs/fds98-25(revised).pdf)
- Howe, A. L., R. J. Walker, C. Olnes, K. Sundet, and A. E. Bingham. 2001c. Revised Edition. Participation, catch, and harvest in Alaska sport fisheries during 1998. Alaska Department of Fish and Game, Fishery Data Series No. 99-41 (revised), Anchorage. [http://www.sf.adfg.state.ak.us/FedAidPDFs/fds99-41\(revised\).pdf](http://www.sf.adfg.state.ak.us/FedAidPDFs/fds99-41(revised).pdf)
- Howe, A. L., R. J. Walker, C. Olnes, K. Sundet, and A. E. Bingham. 2001d. Participation, catch, and harvest in Alaska sport fisheries during 1999. Alaska Department of Fish and Game, Fishery Data Series No. 01-08, Anchorage. <http://www.sf.adfg.state.ak.us/FedAidPDFs/fds01-08.pdf>
- HTI (Hydroacoustic Technology Inc.). 1996. Model 340 digital echo processor (split-beam) operator's manual, version 1.6 Hydroacoustic Technology Inc., Seattle, WA.
- HTI (Hydroacoustic Technology Inc.). 1997. Model 241/243/244 split-beam digital echo sounder system operator's manual, version 1.6. Hydroacoustic Technology Inc., Seattle, WA.
- HTI (Hydroacoustic Technology Inc.). 2006. Transducer calibration for HTI Model 244 split-beam system, November 20, 2006. Report of Hydroacoustic Technology, Inc. to Alaska Department of Fish and Game, Division of Sport Fish, Anchorage.
- Jennings, G. B., K. Sundet, and A. E. Bingham. 2007. Participation, catch, and harvest in Alaska sport fisheries during 2004. Alaska Department of Fish and Game, Fishery Data Series No. 07-40, Anchorage. <http://www.sf.adfg.state.ak.us/FedAidPDFs/fds07-40.pdf>
- Jennings, G. B., K. Sundet, and A. E. Bingham. 2009a. Estimates of participation, catch, and harvest in Alaska sport fisheries during 2005. Alaska Department of Fish and Game, Fishery Data Series No. 09-47, Anchorage. <http://www.sf.adfg.state.ak.us/FedAidPDFs/FDS09-47.pdf>
- Jennings, G. B., K. Sundet, and A. E. Bingham. 2009b. Estimates of participation, catch, and harvest in Alaska sport fisheries during 2006. Alaska Department of Fish and Game, Fishery Data Series No. 09-54, Anchorage. <http://www.sf.adfg.state.ak.us/FedAidPDFs/FDS09-54.pdf>
- Jennings, G. B., K. Sundet, and A. E. Bingham. 2010. Estimates of participation, catch, and harvest in Alaska sport fisheries during 2007. Alaska Department of Fish and Game, Fishery Data Series No. 10-02, Anchorage. <http://www.sf.adfg.state.ak.us/FedAidpdfs/Fds10-02.pdf>
- Jennings, G. B., K. Sundet, A. E. Bingham, and D. Sigurdsson. 2004. Participation, catch, and harvest in Alaska sport fisheries during 2001. Alaska Department of Fish and Game, Fishery Data Series No. 04-11, Anchorage. <http://www.sf.adfg.state.ak.us/FedAidPDFs/fds04-11.pdf>
- Jennings, G. B., K. Sundet, A. E. Bingham, and D. Sigurdsson. 2006a. Participation, catch, and harvest in Alaska sport fisheries during 2002. Alaska Department of Fish and Game, Fishery Data Series No. 06-34, Anchorage. <http://www.sf.adfg.state.ak.us/FedAidpdfs/fds06-34.pdf>

REFERENCES CITED (Continued)

- Jennings, G. B., K. Sundet, A. E. Bingham, and D. Sigurdsson. 2006b. Participation, catch, and harvest in Alaska sport fisheries during 2003. Alaska Department of Fish and Game, Fishery Data Series No. 06-44, Anchorage. <http://www.sf.adfg.state.ak.us/FedAidpdfs/fds06-44.pdf>
- MacLennan, D. N., and E. J. Simmonds. 1992. Fisheries acoustics. Chapman & Hall, London, UK.
- Marsh, L. E. 2000. Angler effort and harvest of Chinook salmon by the recreational fisheries in the lower Kenai River, 1998. Alaska Department of Fish and Game, Fishery Data Series No. 00-21, Anchorage. <http://www.sf.adfg.state.ak.us/FedAidPDFs/fds00-21.pdf>
- McBride, D. N., M. Alexandersdottir, S. Hammarstrom, and D. Vincent-Lang. 1989. Development and implementation of an escapement goal policy for the return of Chinook salmon to the Kenai River. Alaska Department of Fish and Game, Fishery Manuscript No. 8, Juneau. <http://www.sf.adfg.state.ak.us/FedAidPDFs/fms-008.pdf>
- Miller, J. D., D. Bosch, and D. Burwen. 2002. Estimates of Chinook salmon abundance in the Kenai River using split-beam sonar, 1999. Alaska Department of Fish and Game, Fishery Data Series No. 02-24, Anchorage. <http://www.sf.adfg.state.ak.us/FedAidPDFs/fds02-24.pdf>
- Miller, J. D., and D. Burwen. 2002. Estimates of Chinook salmon abundance in the Kenai River using split-beam sonar, 2000. Alaska Department of Fish and Game, Fishery Data Series No. 02-09, Anchorage. <http://www.sf.adfg.state.ak.us/FedAidPDFs/fds02-09.pdf>
- Miller, J. D., D. L. Burwen, and S. J. Fleischman. 2003. Estimates of Chinook salmon abundance in the Kenai River using split-beam sonar, 2001. Alaska Department of Fish and Game, Fishery Data Series No. 03-03, Anchorage. <http://www.sf.adfg.state.ak.us/FedAidPDFs/fds03-03.pdf>
- Miller, J. D., D. L. Burwen, and S. J. Fleischman. 2004. Estimates of Chinook salmon abundance in the Kenai River using split-beam sonar, 2002. Alaska Department of Fish and Game, Fishery Data Series No. 04-29, Anchorage. <http://www.sf.adfg.state.ak.us/FedAidPDFs/fds04-29.pdf>
- Miller, J. D., D. L. Burwen, and S. J. Fleischman. 2005. Estimates of Chinook salmon abundance in the Kenai River using split-beam sonar, 2003. Alaska Department of Fish and Game, Fishery Data Series No. 05-59, Anchorage. <http://www.sf.adfg.state.ak.us/FedAidPDFs/fds05-59.pdf>
- Miller, J. D., D. L. Burwen, and S. J. Fleischman. 2007a. Estimates of Chinook salmon abundance in the Kenai River using split-beam sonar, 2004. Alaska Department of Fish and Game, Fishery Data Series No. 07-57, Anchorage. <http://www.sf.adfg.state.ak.us/FedAidPDFs/fds07-57.pdf>
- Miller, J. D., D. L. Burwen, and S. J. Fleischman. 2007b. Estimates of Chinook salmon abundance in the Kenai River using split-beam sonar, 2005. Alaska Department of Fish and Game, Fishery Data Series No. 07-92, Anchorage. <http://www.sf.adfg.state.ak.us/FedAidpdfs/Fds07-92.pdf>
- Miller, J. D., D. L. Burwen, and S. J. Fleischman. 2010. Estimates of Chinook salmon passage in the Kenai River using split-beam sonar, 2006. Alaska Department of Fish and Game, Fishery Data Series No. 10-40, Anchorage. <http://www.sf.adfg.state.ak.us/FedAidpdfs/FDS10-40.pdf>
- Mills, M. J. 1979. Alaska statewide sport fish harvest studies. Alaska Department of Fish and Game, Federal Aid in Fish Restoration, Annual Performance Report 1978-1979, Project F-9-11(20)SW-I-A, Juneau. [http://www.sf.adfg.state.ak.us/FedAidPDFs/FREDF-9-11\(20\)SW-I-A.pdf](http://www.sf.adfg.state.ak.us/FedAidPDFs/FREDF-9-11(20)SW-I-A.pdf)
- Mills, M. J. 1980. Alaska statewide sport fish harvest studies. Alaska Department of Fish and Game. Federal Aid in Fish Restoration, Annual Performance Report, 1979-1980, Project F-9-12(21) SW-I-A, Juneau. [http://www.sf.adfg.state.ak.us/FedAidPDFs/FREDF-9-12\(21\)SW-I-A.pdf](http://www.sf.adfg.state.ak.us/FedAidPDFs/FREDF-9-12(21)SW-I-A.pdf)
- Mills, M. J. 1981a. Alaska statewide sport fish harvest studies. 1979 data. Alaska Department of Fish and Game, Federal Aid in Fish Restoration, Annual Performance Report 1980-1981, Project F-9-13(22a)SW-I-A, Juneau. [http://www.sf.adfg.state.ak.us/FedAidPDFs/FREDF-9-13\(22a\)SW-I-A.pdf](http://www.sf.adfg.state.ak.us/FedAidPDFs/FREDF-9-13(22a)SW-I-A.pdf)

REFERENCES CITED (Continued)

- Mills, M. J. 1981b. Alaska statewide sport fish harvest studies. 1980 data. Alaska Department of Fish and Game, Federal Aid in Fish Restoration, Annual Performance Report 1980-1981, Project F-9-13(22b)SW-I-A, Juneau. [http://www.sf.adfg.state.ak.us/FedAidPDFs/FREDF-9-13\(22b\)SW-I-A.pdf](http://www.sf.adfg.state.ak.us/FedAidPDFs/FREDF-9-13(22b)SW-I-A.pdf)
- Mills, M. J. 1982. Alaska statewide sport fish harvest studies. Alaska Department of Fish and Game, Federal Aid in Fish Restoration, Annual Performance Report 1981-1982, Project F-9-14(23)SW-I-A, Juneau. [http://www.sf.adfg.state.ak.us/FedAidPDFs/FREDF-9-14\(23\)SW-I-A.pdf](http://www.sf.adfg.state.ak.us/FedAidPDFs/FREDF-9-14(23)SW-I-A.pdf)
- Mills, M. J. 1983. Alaska statewide sport fish harvest studies. Alaska Department of Fish and Game, Federal Aid in Fish Restoration, Annual Performance Report 1982-1983, Project F-9-15(24)SW-I-A, Juneau. [http://www.sf.adfg.state.ak.us/FedAidPDFs/FREDF-9-15\(24\)SW-I-A.pdf](http://www.sf.adfg.state.ak.us/FedAidPDFs/FREDF-9-15(24)SW-I-A.pdf)
- Mills, M. J. 1984. Alaska statewide sport fish harvest studies. Alaska Department of Fish and Game, Federal Aid in Fish Restoration, Annual Performance Report 1983-1984, Project F-9-16(25)SW-I-A, Juneau. [http://www.sf.adfg.state.ak.us/FedAidPDFs/FREDF-9-16\(25\)SW-I-A.pdf](http://www.sf.adfg.state.ak.us/FedAidPDFs/FREDF-9-16(25)SW-I-A.pdf)
- Mills, M. J. 1985. Alaska statewide sport fish harvest studies. Alaska Department of Fish and Game, Federal Aid in Fish Restoration, Annual Performance Report 1984-1985, Project F-9-17(26)SW-I-A, Juneau. [http://www.sf.adfg.state.ak.us/FedAidPDFs/FREDF-9-17\(26\)SW-I-A.pdf](http://www.sf.adfg.state.ak.us/FedAidPDFs/FREDF-9-17(26)SW-I-A.pdf)
- Mills, M. J. 1986. Alaska statewide sport fish harvest studies. Alaska Department of Fish and Game, Federal Aid in Fish Restoration, Annual Performance Report 1985-1986, Project F-10-1(27)RT-2, Juneau. [http://www.sf.adfg.state.ak.us/FedAidPDFs/FREDF-10-1\(27\)RT-2.pdf](http://www.sf.adfg.state.ak.us/FedAidPDFs/FREDF-10-1(27)RT-2.pdf)
- Mills, M. J. 1987. Alaska statewide sport fisheries harvest report, 1986. Alaska Department of Fish and Game, Fishery Data Series No. 2, Juneau. <http://www.sf.adfg.state.ak.us/FedAidPDFs/fds-002.pdf>
- Mills, M. J. 1988. Alaska statewide sport fisheries harvest report, 1987. Alaska Department of Fish and Game, Fishery Data Series No. 52, Juneau. <http://www.sf.adfg.state.ak.us/FedAidPDFs/fds-052.pdf>
- Mills, M. J. 1989. Alaska statewide sport fisheries harvest report, 1988. Alaska Department of Fish and Game, Fishery Data Series No. 122, Juneau. <http://www.sf.adfg.state.ak.us/FedAidPDFs/fds-122.pdf>
- Mills, M. J. 1990. Harvest and participation in Alaska sport fisheries during 1989. Alaska Department of Fish and Game, Fishery Data Series No. 90-44, Anchorage. <http://www.sf.adfg.state.ak.us/FedAidPDFs/fds90-44.pdf>
- Mills, M. J. 1991. Harvest, catch, and participation in Alaska sport fisheries during 1990. Alaska Department of Fish and Game, Fishery Data Series No. 91-58, Anchorage. <http://www.sf.adfg.state.ak.us/FedAidPDFs/fds91-58.pdf>
- Mills, M. J. 1992. Harvest, catch, and participation in Alaska sport fisheries during 1991. Alaska Department of Fish and Game, Fishery Data Series No. 92-40, Anchorage. <http://www.sf.adfg.state.ak.us/FedAidPDFs/fds92-40.pdf>
- Mills, M. J. 1993. Harvest, catch, and participation in Alaska sport fisheries during 1992. Alaska Department of Fish and Game, Fishery Data Series No. 93-42, Anchorage. <http://www.sf.adfg.state.ak.us/FedAidPDFs/fds93-42.pdf>
- Mills, M. J. 1994. Harvest, catch, and participation in Alaska sport fisheries during 1993. Alaska Department of Fish and Game, Fishery Data Series No. 94-28, Anchorage. <http://www.sf.adfg.state.ak.us/FedAidPDFs/fds94-28.pdf>
- Mueller, A. M., D. L. Burwen, K. Boswell, and T. K. Mulligan. 2010. Tail beat patterns in DIDSON echograms and their potential use for species identification and bioenergetics studies. . Transactions of the American Fisheries Society, 139:900-910.
- Mulligan, T. J., and R. Kieser. 1996. A split-beam echo-counting model for riverine use. International Council for the Exploration of the Sea Journal of Marine Science 53:403-406.

REFERENCES CITED (Continued)

- Neter, J., W. Wasserman, and M. H. Kutner. 1985. Applied linear statistical models. 2nd edition. Richard D. Irwin, Inc., Homewood, Illinois.
- Reimer, A. 2004. Chinook salmon creel survey and inriver gillnetting study, lower Kenai River, Alaska, 2002. Alaska Department of Fish and Game, Fishery Data Series No. 04-28, Anchorage. <http://www.sf.adfg.state.ak.us/FedAidPDFs/fds04-28.pdf>
- Reimer, A. M., W. W. Jones, and L. E. Marsh. 2002. Chinook salmon creel survey and inriver gillnetting study, lower Kenai River, Alaska, 1999 and 2000. Alaska Department of Fish and Game, Fishery Data Series No. 02-25, Anchorage. <http://www.sf.adfg.state.ak.us/FedAidPDFs/fds02-25.pdf>
- Simmonds, J., and D. MacLennan. 2005. 2nd edition. Fisheries acoustics: theory and practice. Blackwell Science, Ames, Iowa.
- USDA (United States Department of Agriculture). 1992. Kenai River landowner's guide. Prepared by the U. S. Department of Agriculture, Soil conservation Service (SCS) for the Kenai Soil and Water Conservation District, Kenai, Alaska.
- USGS (United States Geological Survey). 2007. USGS Surface-Water Daily Statistics for Alaska. USGS site #15266300, Kenai River at Soldotna Alaska, water year 2007, accessed October 17, 2007. <http://waterdata.usgs.gov/ak/nwis/>
- Walker, R. J., C. Olnes, K. Sundet, A. L. Howe, and A. E. Bingham. 2003. Participation, catch, and harvest in Alaska sport fisheries during 2000. Alaska Department of Fish and Game, Fishery Data Series No. 03-05, Anchorage. <http://www.sf.adfg.state.ak.us/FedAidPDFs/fds03-05.pdf>
- Westerman, D. L., and T. M. Willette. 2010. Upper Cook Inlet salmon escapement studies, 2007. Alaska Department of Fish and Game, Fishery Data Series No. 10-14, Anchorage. <http://www.sf.adfg.state.ak.us/FedAidpdfs/FDS10-14.pdf>
- Wolter, K. M. 1985. Introduction to variance estimation. Springer-Verlag, New York.
- WRCC (Western Region Climate Center). 2008. Kenai FAA Airport, Alaska. Website Western U.S. Climate Historical Summaries, Climatological Data Summaries, Alaska, accessed February 4, 2008. <http://www.wrcc.dri.edu/cgi-bin/cliMAIN.pl?4546>

APPENDIX A: TARGET STRENGTH ESTIMATION

Appendix A1.–The sonar equation used to estimate target strength in decibels with dual- and split-beam applications.

Target strength (TS), in decibels (dB), of an acoustic target located at range R (in meters), θ degrees from the maximum response axis (MRA) in one plane and ϕ degrees from the MRA in the other plane is estimated as:

$$TS = 20 \log_{10}(V_o) - SL - G_r + 40 \log_{10}(R) + 2\alpha R - G_{TVG} - 2B(\theta, \phi),$$

where:

- V_o = voltage of the returned echo, output by the echo sounder;
- SL = source level of transmitted signal in dB;
- G_r = receiver gain in dB;
- $40\log_{10}(R)$ = two-way spherical spreading loss in dB;
- $2\alpha R$ = two-way absorption loss in dB where α is the absorption coefficient;
- G_{TVG} = time-varied gain correction of the echo sounder; and
- $2B(\theta, \phi)$ = two-way loss due to position of the target off of the MRA.

The source level and gain are measured during calibration and confirmed using *in situ* standard sphere measurements. The time-varied gain correction compensates for spherical spreading loss. Absorption loss ($2\alpha R$) was ignored in this study.

In practice, the location of the target in the beam (θ and ϕ) is not known, so $B(\theta, \phi)$ must be estimated in order to estimate target strength. Dual-beam and split-beam sonar differ in how they estimate $B(\theta, \phi)$, also called the beam pattern factor.

Dual-beam sonar (Ehrenberg 1983) uses one wide and one narrow beam. The system transmits on the narrow beam only and receives on both. The ratio between the voltages of the received signals is used to estimate beam pattern factor

$$B(\theta, \phi) = 20 \log(V_N/V_W) \bullet WBDO,$$

where V_N is the voltage of the returned echo on the narrow beam, V_W is the voltage of the echo on the wide beam, and WBDO is the wide beam drop-off correction, specific to each transducer, and estimated at calibration.

Split-beam sonar (MacLennan and Simmonds 1992) estimates target location (angles θ and ϕ of the target from the MRA) directly, not just the beam pattern factor ($B[\theta, \phi]$). Split-beam transducers are divided into four quadrants, and θ and ϕ are estimated by comparing the phases of signals received by opposing pairs of adjacent quadrants. The beam pattern factor is a function of θ and ϕ , determined during laboratory calibration.

APPENDIX B: SYSTEM PARAMETERS

Appendix B1.–Example of system parameters used for data collection on the right bank (transducer 733).

Parameter Number	Subfield Number ^a	Parameter Value	Parameter Description
100	-1	1	MUX argument #1 - multiplexer port to activate
101	-1	0	percent - sync pulse switch, ping rate determiner NUS ^b
102	-1	13201	maxp - maximum number of pings in a block NUS
103	-1	32767	maxbott - maximum bottom range in samples NUS
104	-1	13	N_th_layer - number of threshold layers
105	-1	5	max_tbp - maximum time between pings (in pings)
106	-1	5	min_pings - minimum number of pings per fish
507	-1	FED5	timval - 0xFED5 corresponds to about 20 kHz NUS
108	-1	1	mux_on - means multiplexing enabled on board NUS
109	-1	200	mux_delay - samples delay between sync and switching NUS
110	-1	0	decimate_mask - decimate input samples flag NUS
112	-1	1	echogram_on - flag for digital echo processor (DEP) echogram enable 0=off, 1=on
113	-1	1	Hourly Sampling flag 1=On 0=Off
118	-1	5	maxmiss - maximum number of missed pings in auto bottom
119	-1	0	bottom-0=fix,1=man,2=scope,3=acq_chan1,4=acq_chan2,5=auto_1,6=auto_chan2
120	-1	0	sb_int_code - sb only=0, sb-int: 40log a bot=1, 20log=2
121	-1	0	sb_int_code2 - sb only=0, sb-int 40log eg=0, 20log=2
122	-1	13	N_int_layers-number of integration strata
123	-1	13	N_int_th_layers - number of integration threshold strata
124	-1	0	int_print - print integrator interval results to printer
125	-1	0	circular element transducer flag for bpf calculation
126	-1	80	grid spacing for Model 404 DCR (in samples, 16 s/m)
127	-1	1	TRIG argument #1 - trigger source
128	-1	0	TRIG argument #2 - digital data routing
130	-1	0	TVG Blank (0=Both Start/End,1=Stop Only,2=Start Only,3=None)
200	-1	20	sigma flag 0.0 = no sigma, else sigma is output
201	-1	221.96	sl - transducer source level
202	-1	-172.54	gn - transducer through system gain at one meter
203	-1	-18	rg - receiver gain used to collect data
204	-1	2.8	narr_ax_bw - vertical nominal beam width
205	-1	10	wide_ax_bw - horizontal axis nominal beam width
206	-1	0	narr_ax_corr - vertical axis phase correction
207	-1	0	wide_ax_corr - horizontal axis phase correction
208	-1	11.0011	ping_rate - pulses per second
209	-1	0	echogram start range in meters
210	-1	35.2	echogram stop range in meters
211	-1	662	echogram threshold in millivolts
212	-1	13.2	print width in inches
213	-1	0	Chirp Bandwidth (0.0 = CHIRP OFF)
214	-1	20	Sampling within Hour Ending Time (in Decimal Minutes)
215	-1	1500	Speed of Sound (m/s)
216	-1	200	Transducer Frequency (kHz)
217	-1	-2.5	min_angoff_v - minimum angle off axis vertical
218	-1	2	max_angoff_v - maximum angle off axis vertical
219	-1	-5	min_angoff_h - minimum angle off axis horiz.

-continued-

Appendix B1.–Page 2 of 3.

Parameter Number	Subfield Number ^a	Parameter Value	Parameter Description
220	-1	5	max_angoff_h - maximum angle off axis horiz.
221	-1	-24	max_dB_off - maximum angle off in dB
222	-1	-16.0459	ux - horizontal electrical to mechanical angle ratio
223	-1	-32.173	uy - vertical electrical to mechanical angle ratio
224	-1	0	ud_coef_a - a coeff. for up-down beam pattern eq.
225	-1	0.0002	ud_coef_b - b coeff. for up-down beam pattern eq.
226	-1	-2.5626	ud_coef_c - c coeff. for up-down beam pattern eq.
227	-1	0.0095	ud_coef_d - d coeff. for up-down beam pattern eq.
228	-1	-0.1036	ud_coef_e - e coeff. for up-down beam pattern eq.
229	-1	0	lr_coef_a - a coeff. for left-rt beam pattern eq.
230	-1	0	lr_coef_b - b coeff. for left-rt beam pattern eq.
231	-1	-0.2093	lr_coef_c - c coeff. for left-rt beam pattern eq.
232	-1	0.0007	lr_coef_d - d coeff. for left-rt beam pattern eq.
233	-1	-0.0002	lr_coef_e - ecoeff. for left-rt beam pattern eq.
234	-1	4	maximum fish velocity in meters per second
235	-1	1	Echo Scope Bottom Location
236	-1	0.4	maxpw - pulse width search window size
238	-1	34.7	bottom - bottom depth in meters
239	-1	0	init_slope - initial slope for tracking in m/ping
240	-1	0.2	exp_cont - exponent for expanding tracking window
241	-1	0.2	max_ch_rng - maximum change in range in m/ping
242	-1	0.04	pw_criteria->min_pw_6-min -6 dB pulse width
243	-1	10	pw_criteria->max_pw_6-max -6 dB pulse width
244	-1	0.04	pw_criteria->min_pw_12 - min -12 dB pulse width
245	-1	10	pw_criteria->max_pw_12 - max -12 dB pulse width
246	-1	0.04	pw_criteria->min_pw_18 - min -18 dB pulse width
247	-1	10	pw_criteria->max_pw_18 - max -18 dB pulse width
249	-1	10	maximum voltage to allow in .RAW file
250	-1	0.2	TX argument #1 - pulse width in milliseconds
251	-1	25	TX argument #2 - transmit power in dB-watts
252	-1	-12	RX argument #1 - receiver gain
253	-1	90.9	REP argument #1 - ping rate in ms per ping
254	-1	10	REP argument #2 - pulsed cal tone separation
255	-1	1	TVG argument #1 - Time Varying Gain (TVG) start range in meters
256	-1	100	TVG argument #2 - TVG end range in meters
257	-1	40	TVG argument #3 - TVG function (XX Log Range)
258	-1	-6	TVG argument #4 - TVG gain
259	-1	0	TVG argument #5 - alpha (spreading loss) in dB/Km
260	-1	0.2	minimum absolute distance fish must travel in x plane
261	-1	0.2	minimum absolute distance fish must travel in y plane
262	-1	0.2	minimum absolute distance fish must travel in z plane
263	-1	2	bottom_window - auto tracking bottom window (m)
264	-1	3	bottom_threshold - auto tracking bottom threshold (V)
265	-1	11.2	TVG argument #7 - 20/40 log crossover (meters)
266	-1	0	rotator - which rotator to aim
267	-1	0	aim_pan - transducer aiming angle in pan (x, lf/rt)
268	-1	0	aim_tilt - transducer aiming angle in tilt (y, u/d)

-continued-

Appendix B1.–Page 3 of 3.

Parameter Number	Subfield Number ^a	Parameter Value	Parameter Description
401	0	1	th_layer[0] – bottom of first threshold layer (m)
401	1	5	th_layer[1] – bottom of second threshold layer (m)
401	2	10	th_layer[2] – bottom of third threshold layer (m)
401	3	15	th_layer[3] – bottom of fourth threshold layer (m)
401	4	20	th_layer[4] – bottom of fifth threshold layer (m)
401	5	25	th_layer[5] – bottom of sixth threshold layer (m)
401	6	30	th_layer[6] – bottom of seventh threshold layer (m)
401	7	35	th_layer[7] – bottom of eighth threshold layer (m)
401	8	40	th_layer[8] – bottom of ninth threshold layer (m)
401	9	45	th_layer[9] – bottom of tenth threshold layer (m)
401	10	50	th_layer[10] – bottom of eleventh threshold layer (m)
401	11	55	th_layer[11] – bottom of twelfth threshold layer (m)
401	12	60	th_layer[12] – bottom of thirteenth threshold layer (m)
402	0	662	th_val[0], threshold for 1 st layer in millivolts
402	1	662	th_val[1], threshold for 2 nd layer in millivolts
402	2	662	th_val[2], threshold for 3 rd layer in millivolts
402	3	662	th_val[3], threshold for 4 th layer in millivolts
402	4	662	th_val[4], threshold for 5 th layer in millivolts
402	5	662	th_val[5], threshold for 6 th layer in millivolts
402	6	662	th_val[6], threshold for 7 th layer in millivolts
402	7	662	th_val[7], threshold for 8 th layer in millivolts
402	8	662	th_val[8], threshold for 9 th layer in millivolts
402	9	662	th_val[9], threshold for 10 th layer in millivolts
402	10	662	th_val[10], threshold for 11 th layer in millivolts
402	11	662	th_val[11], threshold for 12 th layer in millivolts
402	12	9999	th_val[12], threshold for 13 th layer in millivolts
405	0	100	Integration threshold value for layer 1 (mV)
405	1	100	Integration threshold value for layer 2 (mV)
405	2	100	Integration threshold value for layer 3 (mV)
405	3	100	Integration threshold value for layer 4 (mV)
405	4	100	Integration threshold value for layer 5 (mV)
405	5	100	Integration threshold value for layer 6 (mV)
405	6	100	Integration threshold value for layer 7 (mV)
405	7	100	Integration threshold value for layer 8 (mV)
405	8	100	Integration threshold value for layer 9 (mV)
405	9	100	Integration threshold value for layer 10 (mV)
405	10	100	Integration threshold value for layer 11 (mV)
405	11	100	Integration threshold value for layer 12 (mV)
405	12	9999	Integration threshold value for layer 13 (mV)
602	-1	1017536	Echo sounder serial number
604	-1	306733	Transducer serial number
605	-1	Spd-4	Echogram paper speed
606	-1	9_pin	Echogram resolution
607	-1	Board_External	Trigger option
608	-1	LeftToRight	River flow direction

Note: Start Processing at Port 1 -FILE_PARAMETERS- Sunday 1 July 12:00:08 2007.

Note: Data processing parameters used in collecting this file for Port 1.

^a -1 = unique record/field; other values represent the threshold layer number.

^b NUS = not user selectable.

Appendix B2.–Example of system parameters used for data collection on the left bank (transducer 738).

Parameter Number	Subfield Number ^a	Parameter Value	Parameter Description
100	-1	2	MUX argument #1 - multiplexer port to activate
101	-1	0	percent - sync pulse switch, ping rate determiner NUS ^b
102	-1	19200	maxp - maximum number of pings in a block NUS
103	-1	32767	maxbott - maximum bottom range in samples NUS
104	-1	293	N_th_layer - number of threshold layers
105	-1	5	max_tbp - maximum time between pings (in pings)
106	-1	5	min_pings - minimum number of pings per fish
507	-1	FED5	timval - 0xFED5 corresponds to about 20 kHz NUS
108	-1	1	mux_on - means multiplexing enabled on board NUS
109	-1	200	mux_delay - samples delay between sync and switching NUS
110	-1	0	decimate_mask - decimate input samples flag NUS
112	-1	1	echogram_on - flag for digital echo processor (DEP) echogram enable 0=off, 1=on
113	-1	1	Hourly Sampling flag 1=On 0=Off
118	-1	5	maxmiss - maximum number of missed pings in auto bottom
119	-1	0	bottom-0=fix,1=man,2=scope,3=acq_chan1,4=acq_chan2,5=auto_1,6=auto_chan2
120	-1	0	sb_int_code - sb only=0, sb-int: 40log a bot=1, 20log=2
121	-1	0	sb_int_code2 - sb only=0, sb-int 40log eg=0, 20log=2
122	-1	293	N_int_layers-number of integration strata
123	-1	293	N_int_th_layers - number of integration threshold strata
124	-1	0	int_print - print integrator interval results to printer
125	-1	0	circular element transducer flag for bpf calculation
126	-1	80	grid spacing for Model 404 DCR (in samples, 16 s/m)
127	-1	1	TRIG argument #1 - trigger source
128	-1	0	TRIG argument #2 - digital data routing
130	-1	0	TVG Blank (0=Both Start/End,1=Stop Only,2=Start Only,3=None)
200	-1	20	sigma flag 0.0 = no sigma, else sigma is output
201	-1	219.14	sl - transducer source level
202	-1	-173.91	gn - transducer through system gain at one meter
203	-1	-18	rg - receiver gain used to collect data
204	-1	2.8	narr_ax_bw - vertical nominal beam width
205	-1	10	wide_ax_bw - horizontal axis nominal beam width
206	-1	0	narr_ax_corr - vertical axis phase correction
207	-1	0	wide_ax_corr - horizontal axis phase correction
208	-1	16	ping_rate - pulses per second
209	-1	0	echogram start range in meters
210	-1	25	echogram stop range in meters
211	-1	409	echogram threshold in millivolts
212	-1	13.2	print width in inches
213	-1	0	Chirp Bandwidth (0.0 = CHIRP OFF)
214	-1	40	Sampling within Hour Ending Time (in Decimal Minutes)
215	-1	1500	Speed of Sound (m/s)
216	-1	200	Transducer Frequency (kHz)
217	-1	-2.5	min_angoff_v - minimum angle off axis vertical
218	-1	2	max_angoff_v - maximum angle off axis vertical
219	-1	-5	min_angoff_h - minimum angle off axis horiz.

-continued-

Appendix B2.–Page 2 of 3.

Parameter Number	Subfield Number ^a	Parameter Value	Parameter Description
220	-1	5	max_angoff_h - maximum angle off axis horiz.
221	-1	-24	max_dB_off - maximum angle off in dB
222	-1	-16.1638	ux - horizontal electrical to mechanical angle ratio
223	-1	-54.0298	uy - vertical electrical to mechanical angle ratio
224	-1	0	ud_coef_a - a coeff. for up-down beam pattern eq.
225	-1	0.0007	ud_coef_b - b coeff. for up-down beam pattern eq.
226	-1	-2.5031	ud_coef_c - c coeff. for up-down beam pattern eq.
227	-1	-0.0778	ud_coef_d - d coeff. for up-down beam pattern eq.
228	-1	-0.169	ud_coef_e - e coeff. for up-down beam pattern eq.
229	-1	0	lr_coef_a - a coeff. for left-rt beam pattern eq.
230	-1	0	lr_coef_b - b coeff. for left-rt beam pattern eq.
231	-1	-0.2222	lr_coef_c - c coeff. for left-rt beam pattern eq.
232	-1	0.0001	lr_coef_d - d coeff. for left-rt beam pattern eq.
233	-1	-0.0002	lr_coef_e - ecoeff. for left-rt beam pattern eq.
234	-1	4	maximum fish velocity in meters per second
235	-1	1	Echo Scope Bottom Location
236	-1	0.4	maxpw - pulse width search window size
238	-1	23.9	bottom - bottom depth in meters
239	-1	0	init_slope - initial slope for tracking in m/ping
240	-1	1	exp_cont - exponent for expanding tracking window
241	-1	0	max_ch_rng - maximum change in range in m/ping
242	-1	0.04	pw_criteria->min_pw_6-min -6 dB pulse width
243	-1	10	pw_criteria->max_pw_6-max -6 dB pulse width
244	-1	0.04	pw_criteria->min_pw_12 - min -12 dB pulse width
245	-1	10	pw_criteria->max_pw_12 - max -12 dB pulse width
246	-1	0.04	pw_criteria->min_pw_18 - min -18 dB pulse width
247	-1	10	pw_criteria->max_pw_18 - max -18 dB pulse width
249	-1	10	maximum voltage to allow in .RAW file
250	-1	0.2	TX argument #1 - pulse width in milliseconds
251	-1	25	TX argument #2 - transmit power in dB-watts
252	-1	-12	RX argument #1 - receiver gain
253	-1	62.5	REP argument #1 - ping rate in ms per ping
254	-1	10	REP argument #2 - pulsed cal tone separation
255	-1	2	TVG argument #1 - TVG start range in meters
256	-1	100	TVG argument #2 - TVG end range in meters
257	-1	40	TVG argument #3 - TVG function (XX Log Range)
258	-1	-6	TVG argument #4 - TVG gain
259	-1	0	TVG argument #5 - alpha (spreading loss) in dB/Km
260	-1	0.2	minimum absolute distance fish must travel in x plane
261	-1	0.2	minimum absolute distance fish must travel in y plane
262	-1	0.2	minimum absolute distance fish must travel in z plane
263	-1	2	bottom_window - auto tracking bottom window (m)
264	-1	3	bottom_threshold - auto tracking bottom threshold (V)
265	-1	11.2	TVG argument #7 - 20/40 log crossover (meters)
266	-1	0	rotator - which rotator to aim
267	-1	0	aim_pan - transducer aiming angle in pan (x, lf/rt)
268	-1	0	aim_tilt - transducer aiming angle in tilt (y, u/d)

-continued-

Appendix B2.–Page 3 of 3.

Parameter Number	Subfield Number ^a	Parameter Value	Parameter Description
401	0-292	1-30.2	th_layer[0-292], bottom of 1 st threshold layer – bottom of 293 rd threshold layer (i.e. 293 threshold layers in 0.1 m increments and numbered 0 through 292)
402	0-291	409	th_val[0-291], threshold for 1 st through 292 nd layer in millivolts
402	292	9999	th_val[292], threshold for 293 rd layer in millivolts
405	0-291	100	Integration threshold value for layer 1-292 (mV)
405	292	9999	Integration threshold value for layer 293 (mV)
602	-1	1017536	Echo sounder serial number
604	-1	306738	Transducer serial number
605	-1	Spd-4	Echogram paper speed
606	-1	9_pin	Echogram resolution
607	-1	Board_External	Trigger option
608	-1	LeftToRight	River flow direction

Note: Start Processing at Port 2 -FILE_PARAMETERS- Sunday 1 July 12:20:08 2007.

Note: Data processing parameters used in collecting this file for Port 2.

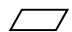
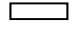


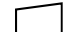


^a -1 = unique record/field; other values represent the threshold layer number.

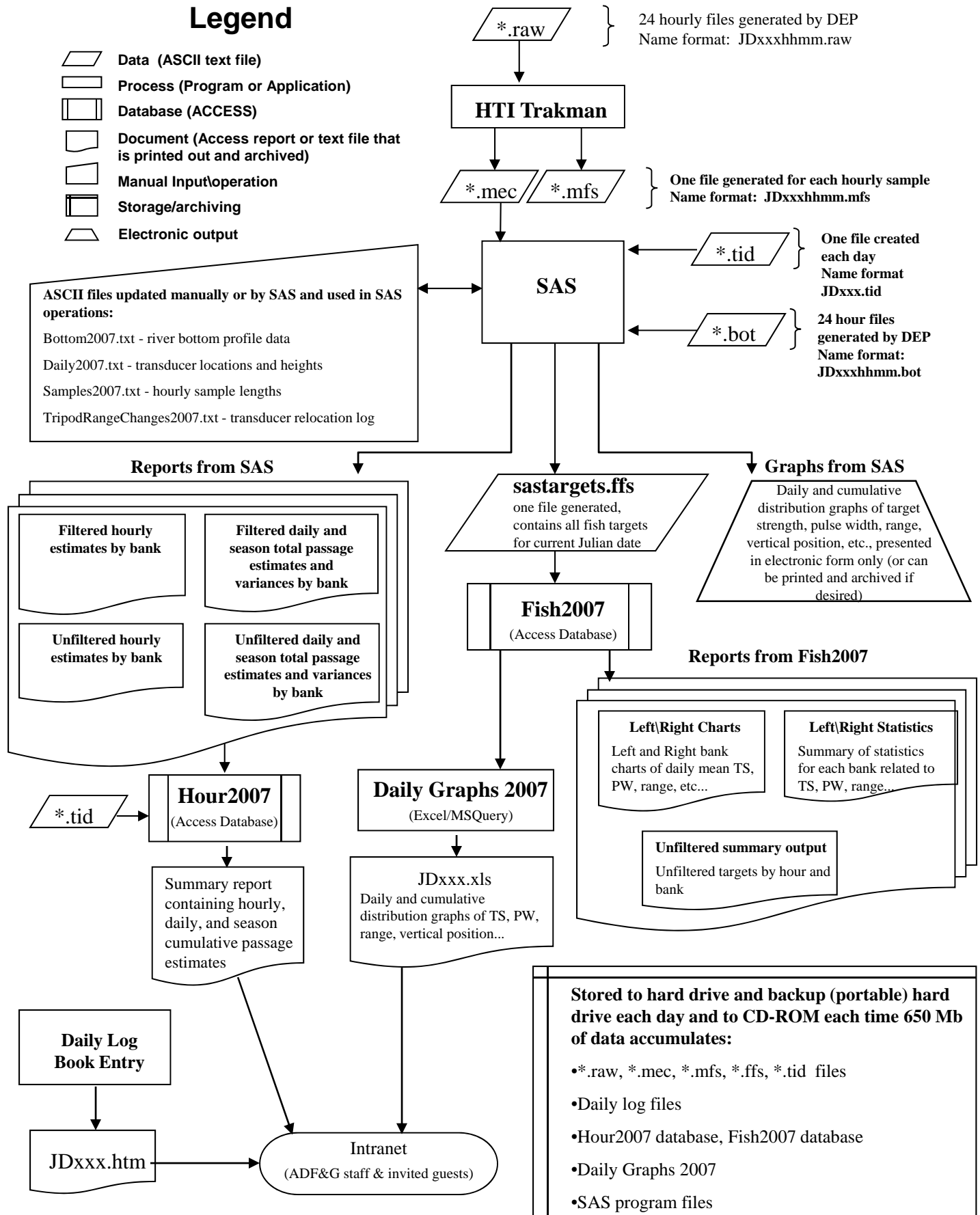
^b NUS = not user selectable.

APPENDIX C: DATA FLOW

Appendix C1.–Data flow diagram for the Kenai River Chinook salmon sonar project, 2007.

Legend

-  Data (ASCII text file)
-  Process (Program or Application)
-  Database (ACCESS)
-  Document (Access report or text file that is printed out and archived)
-  Manual Input/operation
-  Storage/archiving
-  Electronic output



APPENDIX D: EXCLUDED HOURLY SAMPLES

Appendix D1.—Hourly samples excluded by bank from calculation of early- and late-run Chinook salmon daily passage estimates, Kenai River, 2007.

Date	Excluded Sample Hours	
	Left Bank	Right Bank
EARLY RUN		
9-June	0920, 2120	-
10-June	1120	1100
11-June	1620	1600, 1700
14-June	1020, 1220	-
16-June	1320, 1620	1200
20-June	0920	0900
23-June	1720	-
LATE RUN		
1-July	-	0600, 1600, 2100
3-July	-	0700
5-July	2220	2200
6-July	2220	2200
7-July	2020	0900-1100, 2000
8-July	-	1000-1000, 1500, 2100-2200
10-July	-	1200-1300, 2300
11-July	-	0000, 1300-1400
14-July	-	0600
15-July	-	1900
16-July	-	0700, 0900
18-July	1220-1320	0800-1300
19-July	0620, 0820-0920, 1820	0000, 0600-1300
20-July	0720, 1920, 2120	0700-1300, 1900-2200
21-July	0820-1020, 1220-1320, 1520-1620, 1920-2220	0800-1100, 1600, 2000-2200
22-July	1120-1420, 2220	1000-1200, 1500-1700, 2000-2300
23-July	1120	1100-1400, 2100-2300
24-July	1220-1420, 1820, 2320	0000, 0200, 1300-1400, 1600, 1800-2300
25-July	0020-0120, 0620	0000-0800, 1400-2300
26-July	-	0000-0100, 0300-1400, 1600, 1800-1900
27-July	0820	1600-2100
28-July	1620	0200, 1500-1800
29-July	-	1800
30-July	1820	1800
31-July	-	1000-1100
1-August	-	1000
3-August	-	1800
4-August	-	0700, 1900

**APPENDIX E: WINBUGS CODE FOR ECHO-LENGTH
STANDARD DEVIATION (ELSD) MIXTURE MODEL
ESTIMATES OF SPECIES COMPOSITION**

Appendix E1.–WinBUGS code for ELSD mixture model fit to 2007 early- and late-run Kenai River Chinook salmon sonar, gillnetting, and tethered fish data.

```

model{
  beta0 ~ dnorm(0,1.0E-4)
  beta1 ~ dnorm(0,1.0E-4)
  gamma ~ dnorm(0,1.0E-4)
  sigma.elsd ~ dunif(0,2)
  sigma.beta0 ~ dunif(0,2)
  tau.elsd <- 1 / sigma.elsd / sigma.elsd
  tau.beta0 <- 1 / sigma.beta0 / sigma.beta0
  ps[1:2] ~ ddirch(D.species[])
  pa[1,1] ~ dbeta(B1,B2)
  theta1 ~ dbeta(B3,B4)
  pa[1,2] <- theta1 * (1 - pa[1,1])
  pa[1,3] <- 1 - pa[1,1] - pa[1,2]
  pa[2,1] ~ dbeta(0.5,0.5)
  theta2 ~ dbeta(0.5,0.5)
  pa[2,2] <- theta2 * (1 - pa[2,1])
  pa[2,3] <- 1 - pa[2,1] - pa[2,2]
  p.chin <- ps[1] * p_n * p_i
  Lsig[1] <- 75
  Lsig[2] <- 25
  Ltau[1] <- 1 / Lsig[1] / Lsig[1]
  Ltau[2] <- 1 / Lsig[2] / Lsig[2]
  mu[1,1] ~ dnorm(636,0.0006)
  mu[1,2] ~ dnorm(816,0.0070)
  mu[1,3] ~ dnorm(1032,0.0006)
  mu[2,1] ~ dnorm(380,0.003)
  mu[2,2] ~ dnorm(500,0.006)
  mu[2,3] ~ dnorm(580,0.006)
  D.age.sockeye[1] <- 0.01
  D.age.sockeye[2] <- 0.5
  D.age.sockeye[3] <- 3.5
  for (a in 1:3) {
    pa.effective[1,a] <- pa[1,a] * q1.a[a] / inprod(pa[1,],q1.a[])
    pa.effective[2,a] <- pa[2,a]
  }
  for (y in 1:3) {
    beta0.y[y] ~ dnorm(beta0,tau.beta0)
  }
  beta0.predict ~ dnorm(beta0,tau.beta0)
  for (k in 1:141){
    elsd1[k] ~ dnorm(mu.elsd1[k],tau.elsd)
    mu.elsd1[k] <- beta0.y[year[k]] + beta1 * cm75[k] + gamma * sock.indic[k]
  }
  for (i in 1:nfish){
    age[i] ~ dcat(pa.effective[species[i],1:3])
    mefl[i] ~ dnorm(mu[species[i],age[i]],Ltau[species[i]])
  }
  for (j in 1:ntgts){
    species2[j] ~ dcat(ps[])
    age2[j] ~ dcat(pa[species2[j],1:3])
    mefl2[j] ~ dnorm(mu[species2[j],age2[j]],Ltau[species2[j]])
    elsd2[j] ~ dt(mu.elsd2[j],tau.elsd,8)
    cm75t[j] <- (mefl2[j] / 10) - 75;
    sock.indic2[j] <- species2[j] - 1;
    mu.elsd2[j] <- beta0.predict + gamma*sock.indic2[j] + beta1 * cm75t[j]
  }
}

```


Appendix E2.–WinBUGS code for hierarchical age-composition model for development of prior distributions for ELSD mixture model. Prior distributions in green font, likelihoods in blue.

```
#Age Mixture.odc version 6a:
```

```
model {
  #Overall means and std deviations
  for (a in 1:A) {
    sigma[a] ~ dnorm(0,1.0E-4)I(0,)
    tau[a] <- 1 / sigma[a] / sigma[a]
    mu[a] ~ dnorm(0,1.0E-12)I(0,)
  }
  #Dirichlet distributed age proportions across years within weeks
  D.scale ~ dunif(0,1)
  D.sum <- 1 / (D.scale * D.scale)
  for (w in 1:W) {
    pi[w,1] ~ dbeta(0.2,0.4)
    pi.2p[w] ~ dbeta(0.2,0.2)
    pi[w,2] <- pi.2p[w] * (1 - pi[w,1])
    pi[w,3] <- 1 - pi[w,1] - pi[w,2]
    for (y in 1:Y) {
      for (a in 1:A) {
        D[w,y,a] <- D.sum * pi[w,a]
        g[w,y,a] ~ dgamma(D[w,y,a],1)
        pi.wy[w,y,a] <- g[w,y,a]/sum(g[w,y,])
      }
    }
  }
  for (i in 1:nfish) {
    age[i] ~ dcat(pi.wy[week[i],year[i],1:A])
    length[i] ~ dnorm(mu[age[i]],tau[age[i]])
  }
}
```


**APPENDIX F: DIDSON CONFIGURATION FOR KENAI
RIVER CHINOOK SONAR STUDY, 2007**

Appendix F1.-DIDSON configuration for Kenai River Chinook Sonar Study, 2007.

Dual-frequency identification sonars (DIDSONs) operate at 2 discrete frequencies: a higher frequency that produces higher resolution images, and a lower frequency that can detect targets at further ranges but at a reduced image resolution. The long-range model (DIDSON-LR) used in this study was operated in high frequency mode (1.2 MHz) to achieve maximum image resolution. Additionally the DIDSON-LR was fitted with an ultra high-resolution lens to further enhance the image resolution of the -LR system (DIDSON-LR+HRL). The high-resolution lens increases the image resolution by approximately a factor of two over the standard lens.

Overall nominal beam dimensions for a DIDSON-LR without a high-resolution lens are approximately 29° in the horizontal axis and 14° in the vertical axis. At 1.2 MHz, the 29° horizontal axis is a radial array of 48 beams that are nominally 0.54° wide and spaced across the array at ~ 0.60° intervals. The larger aperture of the high-resolution lens reduces the width of the individual beams of the standard lens and spreads them across a narrower field-of-view. Consequently, with the addition of the high-resolution lens, the overall nominal beam dimensions of the DIDSON-LR are reduced to approximately 15° in the horizontal axis and 3° in the vertical axis and the 48 individual beams are reduced to ~0.3° wide and spaced across the array at ~0.3° intervals (Appendix F2). The combined concentration of horizontal and vertical beam widths also increases the returned signal from a given target by 10 dB.

The resolution of a DIDSON image is defined in terms of down-range and cross-range resolution where cross-range resolution refers to the width and down-range resolution refers to the height of the individual pixels that make up the DIDSON image (Appendix F3). Each image pixel in a DIDSON frame has (x, y) rectangular coordinates that are mapped back to a beam and sample number defined by polar coordinates. The pixel height defines the down-range resolution and the pixel width defines the cross-range resolution of the image. Appendix F3 shows that image pixels are sometimes broken down into smaller screen pixels (e.g. pixels immediately to the right of the enlarged pixels), an artifact of conversions between rectangular and polar coordinates.

“Window Length”, i.e., the range interval sampled by the sonar, controls the down-range resolution of the DIDSON image. Because the DIDSON image is composed of 512 samples (pixels) in range, images with shorter window lengths are better resolved (i.e., down-range resolution = window length/512). Window length can be set to 2.5 m, 5.0 m, 10.0 m, or 20.0 m for the DIDSON-LR+HRL at 1.2 MHz. For this study, window length was set at 10 m, a compromise which allowed a reasonable distance to be covered while still operating in high frequency mode for optimal resolution. The down-range resolution (or pixel height) for a 10 m window length is 2 cm (1,000 cm/512).

The cross-range resolution is primarily determined by the individual beam spacing and beam width, both of which are ~0.3° for the DIDSON LR+HRL at 1.2 MHz (Appendix F2). Targets at closer range are better resolved because the individual beam widths and corresponding image pixels increase with range following the formula:

$$X = 2R \tan(\theta/2) \tag{1}$$

where

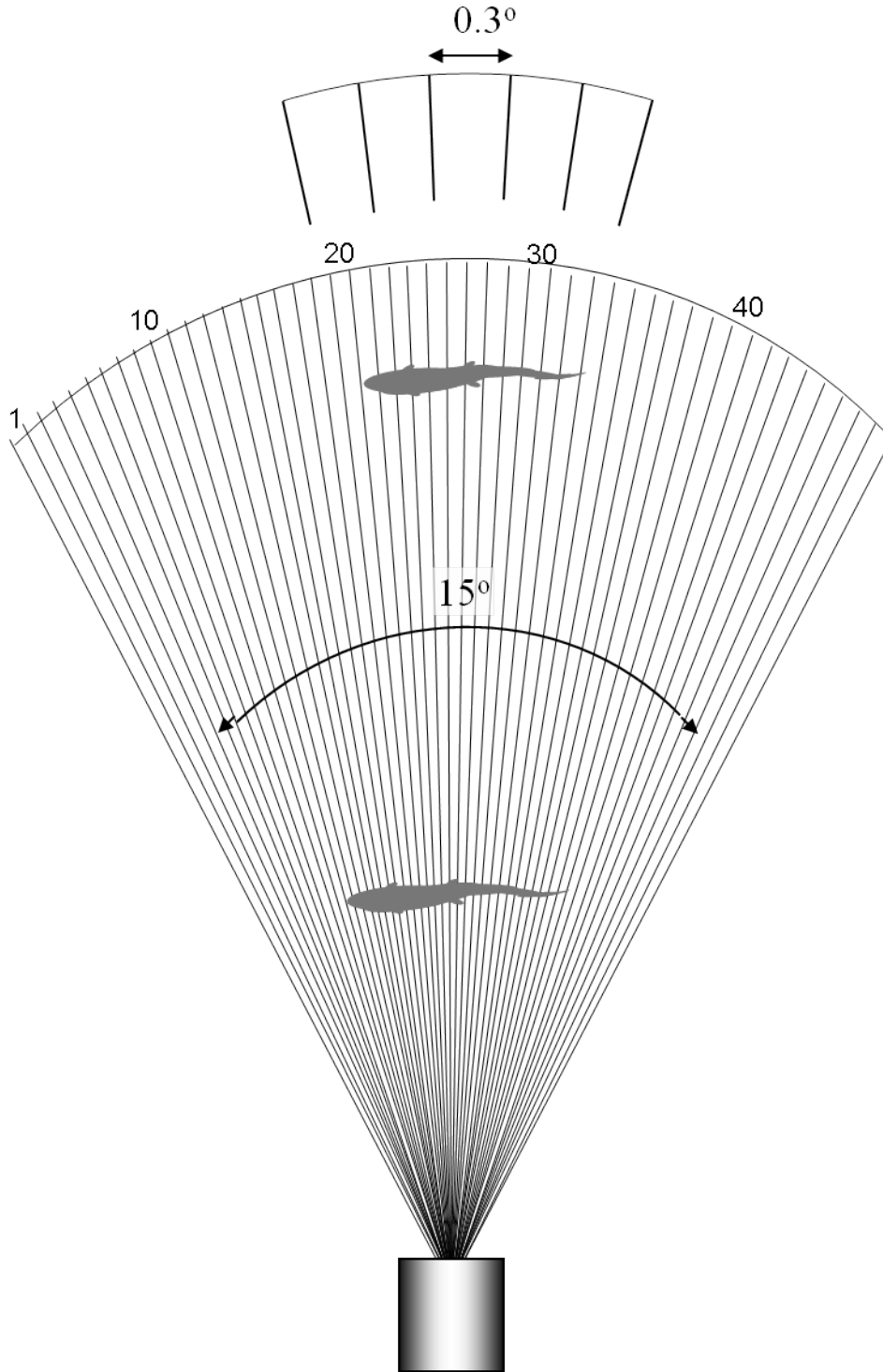
X = Width of the individual beam or “image pixel” in meters,

R = Range of interest in meters, and

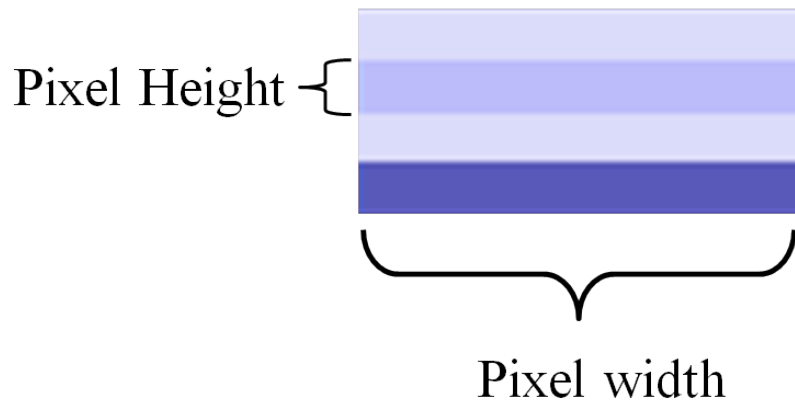
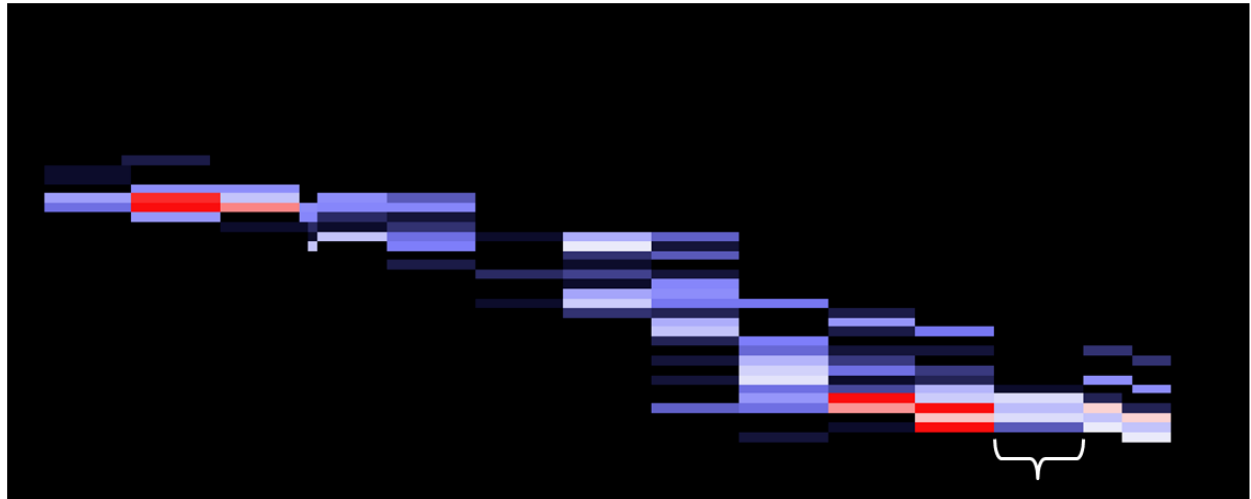
θ = Individual beam angle in degrees (approximately 0.3°).

The transmit power of the DIDSON sonar is fixed and the maximum receiver gain (-40 dB) was used during all data collection. The autofocus feature was enabled so that the sonar automatically set the lens focus to the mid-range of the selected display window (e.g. for a window length of 10 m that started at 5 m, the focus range would be 15 m–[5 m/2]). The image smoothing feature was disabled.

Appendix F2.—Diagram showing the horizontal plane of a DIDSON-LR sonar with a high resolution lens (DIDSON-LR+HRL). The overall horizontal beam width of 15° is comprised of 48 sub-beams with approximately 0.3° beam widths. Note that because the beam widths grow wider with range, fish at close range are better resolved than fish at far range (Adapted from Burwen et al. 2007).



Appendix F3.—Enlargement of a DIDSON video of a tethered Chinook salmon showing the individual pixels that comprise the image. Each image pixel in a DIDSON frame has (x, y) rectangular coordinates that are mapped back to a beam and sample number defined by polar coordinates range (Adapted from Burwen et al. 2010).



**APPENDIX G: DAILY PROPORTION OF UPSTREAM AND
DOWNSTREAM MOVING FILTERED TARGETS FOR THE
EARLY AND LATE RUNS, KENAI RIVER, 2007**

Appendix G1.—Daily proportion of upstream and downstream moving filtered targets for the early run, Kenai River, 2007.

Date	Downstream count	Upstream count	Daily total	% Downstream	% Upstream
20 May	9	18	27	33%	67%
21 May	15	60	75	20%	80%
22 May	6	66	72	8%	92%
23 May	15	51	66	23%	77%
24 May	6	91	97	6%	94%
25 May	9	88	97	9%	91%
26 May	6	72	78	8%	92%
27 May	9	81	90	10%	90%
28 May	3	117	120	3%	98%
29 May	0	144	144	0%	100%
30 May	9	164	173	5%	95%
31 May	3	252	255	1%	99%
1 June	9	225	234	4%	96%
2 June	3	186	189	2%	98%
3 June	3	277	280	1%	99%
4 June	6	303	309	2%	98%
5 June	3	519	522	1%	99%
6 June	9	605	614	1%	99%
7 June	6	996	1,002	1%	99%
8 June	3	1,146	1,149	0%	100%
9 June	6	731	737	1%	99%
10 June	0	647	647	0%	100%
11 June	12	488	500	2%	98%
12 June	18	724	742	2%	98%
13 June	6	716	722	1%	99%
14 June	11	666	677	2%	98%
15 June	24	698	722	3%	97%
16 June	36	494	530	7%	93%
17 June	18	470	488	4%	96%
18 June	12	270	282	4%	96%
19 June	15	486	501	3%	97%
20 June	3	282	285	1%	99%
21 June	12	283	295	4%	96%
22 June	18	320	338	5%	95%
23 June	0	485	485	0%	100%
24 June	4	276	280	1%	99%
25 June	6	195	201	3%	97%
26 June	9	250	259	3%	97%
27 June	9	320	329	3%	97%
28 June	25	641	666	4%	96%
29 June	24	434	458	5%	95%
30 June	6	567	573	1%	99%
Total	406	15,904	16,310	2%	98%

Appendix G2.–Daily proportion of upstream and downstream moving filtered targets for the late run, Kenai River, 2007.

Date	Downstream count	Upstream count	Daily total	% Downstream	% Upstream
1 July	12	609	621	2%	98%
2 July	15	401	416	4%	96%
3 July	8	450	458	2%	98%
4 July	15	501	516	3%	97%
5 July	16	506	522	3%	97%
6 July	24	510	534	4%	96%
7 July	8	578	586	1%	99%
8 July	27	1,051	1,078	3%	97%
9 July	27	601	628	4%	96%
10 July	10	500	510	2%	98%
11 July	30	927	957	3%	97%
12 July	24	710	734	3%	97%
13 July	30	527	557	5%	95%
14 July	42	1,037	1,079	4%	96%
15 July	51	1,282	1,333	4%	96%
16 July	90	667	757	12%	88%
17 July	72	776	848	8%	92%
18 July	39	1,729	1,768	2%	98%
19 July	46	1,754	1,800	3%	97%
20 July	29	2,153	2,182	1%	99%
21 July	25	1,677	1,702	1%	99%
22 July	63	2,751	2,814	2%	98%
23 July	132	1,901	2,033	6%	94%
24 July	76	3,008	3,084	2%	98%
25 July	59	3,490	3,549	2%	98%
26 July	73	2,659	2,732	3%	97%
27 July	65	3,357	3,422	2%	98%
28 July	55	1,779	1,834	3%	97%
29 July	28	859	887	3%	97%
30 July	63	922	985	6%	94%
31 July	51	1,340	1,391	4%	96%
1 August	29	866	895	3%	97%
2 August	24	330	354	7%	93%
3 August	25	397	422	6%	94%
4 August	37	374	411	9%	91%
Total	1,420	42,979	44,399	3%	97%

**APPENDIX H: AVERAGE VERTICAL ANGLE OF
FILTERED TARGETS BY TIDE STAGE, RUN, BANK, AND
DIRECTION OF TRAVEL (UPSTREAM OR
DOWNSTREAM) FOR THE EARLY AND LATE RUNS,
KENAI RIVER, 2007**

Appendix H1.—Average vertical angle of filtered targets by tide stage and direction of travel (upstream or downstream) for the early run, Kenai River, 2007.

Tide Stage / Fish Orientation	Average Vertical Angle	Standard Deviation	Sample Size
<i>Left Bank</i>			
<u>Falling</u>			
Downstream	-0.56	0.35	12
Upstream	-0.56	0.36	2,088
Tide Stage Total	-0.56	0.36	2,100
<u>Low</u>			
Downstream	-0.29	0.58	10
Upstream	-0.60	0.34	920
Tide Stage Total	-0.60	0.34	930
<u>Rising</u>			
Downstream	-0.30	0.55	19
Upstream	-0.28	0.45	467
Tide Stage Total	-0.28	0.45	486
Left Bank Total	-0.53	0.38	3,516
<i>Right Bank</i>			
<u>Falling</u>			
Downstream	-0.14	0.33	53
Upstream	-0.10	0.28	1,266
Tide Stage Total	-0.10	0.28	1,319
<u>Low</u>			
Downstream	-0.03	0.33	12
Upstream	-0.10	0.24	314
Tide Stage Total	-0.10	0.24	326
<u>Rising</u>			
Downstream	0.09	0.28	35
Upstream	0.00	0.44	419
Tide Stage Total	-0.01	0.43	454
Right Bank Total	-0.08	0.32	2,099

Appendix H2.–Average vertical angle of filtered targets by tide stage and direction of travel (upstream or downstream) for the late run, Kenai River, 2007.

Tide Stage /Fish Orientation	Average Vertical Angle	Standard Deviation	Sample Size
<i>Left Bank</i>			
<u>Falling</u>			
Downstream	-0.31	0.40	103
Upstream	-0.45	0.30	5,224
Tide Stage Total	-0.45	0.30	5,327
<u>Low</u>			
Downstream	-0.29	0.36	33
Upstream	-0.47	0.28	993
Tide Stage Total	-0.46	0.28	1,026
<u>Rising</u>			
Downstream	-0.11	0.55	78
Upstream	-0.17	0.49	2,045
Tide Stage Total	-0.17	0.49	2,123
Left Bank Total	-0.38	0.38	8,476
<i>Right Bank</i>			
<u>Falling</u>			
Downstream	-0.07	0.32	193
Upstream	-0.15	0.29	6,523
Tide Stage Total	-0.15	0.29	6,716
<u>Low</u>			
Downstream	-0.10	0.33	53
Upstream	-0.28	0.27	1,526
Tide Stage Total	-0.28	0.27	1,579
<u>Rising</u>			
Downstream	0.09	0.39	185
Upstream	-0.03	0.34	5,784
Tide Stage Total	-0.02	0.35	5,969
Right Bank Total	-0.11	0.32	14,264

**APPENDIX I: HISTORIC PASSAGE BY YEAR AND DATE
(1987–2007)**

Appendix II.—Kenai River early-run Chinook salmon sonar passage estimates, 1987–2007.

Date/Year	1987 ^a	1988	1989	1990	1991	1992	1993	1994	1995	1996
7 May										
8 May										
9 May										
10 May										
11 May										
12 May										
13 May										
14 May										
15 May										
16 May		188	180	78	30	54	64	238	98	60
17 May		415	319	57	12	48	85	342	99	91
18 May		259	264	93	65	88	91	260	78	63
19 May		260	180	136	55	40	66	302	149	96
20 May		406	147	93	68	78	69	369	228	177
21 May		184	245	69	51	90	165	327	465	165
22 May		182	164	75	111	108	117	246	265	156
23 May		231	186	63	66	150	160	212	286	159
24 May		288	279	51	66	126	141	303	265	159
25 May		351	300	76	57	79	150	170	198	153
26 May		393	270	70	81	93	168	150	189	240
27 May		387	419	87	81	66	150	267	165	204
28 May		483	357	61	78	78	361	258	159	330
29 May		713	269	221	51	45	538	347	222	512
30 May		333	164	154	51	111	388	321	351	348
31 May		501	157	175	69	114	266	369	282	474
1 June		556	258	153	150	106	187	321	357	603
2 June		545	194	294	240	107	412	266	369	741
3 June		598	233	225	362	232	324	298	549	873
4 June	1,059	755	246	178	177	190	255	304	693	1,051
5 June	552	782	280	192	316	166	276	351	429	943
6 June	1,495	493	384	156	296	319	327	198	807	741
7 June	1,145	506	545	304	215	515	198	384	843	773
8 June	602	771	890	414	243	375	297	306	999	918
9 June	1,024	569	912	339	444	486	378	462	789	1,140
10 June	985	333	913	272	275	264	453	432	876	684
11 June	1,004	320	710	453	334	234	549	423	774	882
12 June	1,044	302	577	568	400	394	600	329	417	864
13 June	2,168	188	599	445	369	236	951	376	492	1,071
14 June	1,297	289	458	330	268	174	811	514	691	1,111
15 June	975	510	335	658	441	312	407	306	636	1,116
16 June	786	808	397	485	615	239	616	453	648	420
17 June	612	535	514	267	330	339	567	315	750	495
18 June	783	533	464	238	493	320	606	435	808	697
19 June	771	200	295	331	437	390	422	636	419	657
20 June	682	175	498	369	314	548	504	402	594	315
21 June	517	373	520	257	457	372	621	570	438	351
22 June	487	312	614	267	433	297	399	366	375	396
23 June	529	375	547	240	396	213	607	550	178	401
24 June	303	674	564	322	251	337	720	696	450	573
25 June	564	582	374	258	235	362	808	734	429	684
26 June	731	436	369	322	261	330	1,051	597	334	504
27 June	452	549	309	231	340	291	1,158	639	946	228
28 June	587	827	425	240	327	253	798	681	696	303
29 June	371	495	376	208	258	121	728	929	984	234
30 June	388	915	292	193	270	197	660	649	615	351
Total	21,913^a	20,880	17,992	10,768	10,939	10,087	19,669	18,403	21,884	23,505

-continued-

